Magnetic Interactions in Molecular Materials

Thesis by:

Seth Adrian Miller

in Partial Fulfillment of the Requirements
for the Degree of
Doctor of Philosophy

California Institute of Technology
Pasadena, California

1999
(Submitted September 1, 1998)

Acknowledgments

Well, I have been at this for a while now, and I have built up a lot of debts to people who deserve thanks now that the end is here. First and foremost, of course, is my advisor Dennis Dougherty. I especially appreciate his liberal arts approach towards science, where every field is open to inquiry and I have been free to pursue my own interests and ideas. He has taught by example how to approach problems, and that the most interesting questions are often the most basic ones that everyone has assumed they understand better than they perhaps do. And finally, after a long effort, he has taught me how to focus on a single problem in a world full of really cool and wonderful distractions.

Then there is the Dougherty group, who have taught me all the things I need to know about grinding out the physical part of science. On the magnet side, I want to thank Dr. Kraig Anderson, who taught me a little about magnetism, something about synthesis, and a lot about the appropriate application of a colorful metaphor - his presence in lab is sorely missed. Jeff Clites is another who has always been a good source of chemical advice and the world's quickest retorts. Jesse Lin has been a living textbook, and his synthetic advice is greatly appreciated. Larry Henling and Dr. Mike Day have been extremely understanding and helpful in putting me at the front of the line to get that elusive last bit of data. Finally, Josh Maurer is acting less and less like the younger student lately, and in addition to enjoying his company I have learned a lot too.

The rest of the group can be forgiven for being on other projects and deserve some recognition as well. Dr. Scott Silverman's willingness to engage in pun wars (much to the dismay of everyone else) is appreciated and missed. Jen Ma has been a good friend and should consider moving to the Bay Area so we can still hang out. Dr. Sarah Ngola is now several thousand miles away, and mark my words she will have to put up with a visit eventually - just give me a few years to save for the plane ticket. Justin Gallivan is one of the silliest people alive, though he hides it well, and I will miss goofing off with him. I have appreciated Marcus Sarofim's good humor and large garage for storing my excess stuff. Dr. Pam England is wonder of nature, and that is a very good thing - I have really enjoyed her company and look forward to being able to enjoy it more in the future. Gabriel Brandt is a great source of obscure facts and, well, you can't help but admire someone who can use the work 'praxis' in a sentence without pausing.

That brings up the final thing about the Dougherty group: our constant discussions about politics and philosophy have been an inspiration. It is rare to find a group of people willing to talk about the evolution of consciousness or the origin of life as easily as about their work. This is a group who thinks of science as a whole, not just about their part, and I will keep that attitude towards my work with me always.

Ok, enough about the group. There are other people in this world too. Among chemists, I want to thank Will Greenberg and Brian Hudson, who were good roommates and friends during my time here. I wish there were

many more people in the world like them. Rob Rossi says he is cynical, but why is he always smiling? Marc Unger has been a lot of fun to talk science, science fiction, and society with over the years. Cindy Parrish has also been a good source of advice and a good, smiling person to vent to when life gets a little frustrating. Bruce Heitbrink, who I have seen too little of lately, is also a really cool person who will be missed. Nita Rudra and Silja Omarsdattir aren't chemists, which is a point in their favor, and even better they have been great friends, which is the most important thing of all.

Finally, I have to acknowledge my wife Cassandra. She has given up a lot of her own wants in order to be here, in smoggy, paved LA, with me while we did this graduate school adventure. I don't think there are words that can convey how much her sacrifices, her patience, and her understanding have meant to me. Even with gestures and facial expressions, I still have trouble getting the idea across. Suffice it to say that I really appreciate her presence here with me, and soon it will be her turn to drag me along somewhere too. And I will love it.

Abstract

A series of nitronylnitroxide and imino nitroxide radicals have been made that incorporate the benzene-hexafluorobenzene macromolecular synthon. These systems were designed to self-assemble into a crystal lattice in such a way that a ferromagnetic interaction is propagated. Sixteen systems, representing a potential total of thirty-two radicals, were investigated. One system was obtained with a stacking that should propagate a ferromagnetic interaction. This system, however, also contains a strong antiferromagnetic pathway, and its magnetic properties are unusual and still incompletely understood.

A molecule containing two dicyanoquinonediimine units linked *meta* through a benzene was synthesized. It was found to be a ground state triplet, as expected. Several metal complexes were synthesized, and the molecule was found to interact ferromagnetically with nickel. Crystals of these systems could not be obtained.

Two polymers based on the poly(arenemethide) conducting backbone were synthesized. At least one of these polymers was found to be unstable on doping. Neither system conducts.

TABLE OF CONTENTS

LIST OF FIGURES

LIST OF SCHEMES

LIST OF TABLES

LIST OF STRUCTURES

Chapter One : Magnetism and Conductivity in Organic Materials and Metal Complexes

Magnets and conductors of electricity are typically thought of as existing only in the realm of inorganic materials. Refrigerator magnets, for example, are rectangles of magnetite, Fe_3O_4, a brittle, opaque ceramic that is dug out of the earth, its properties intact. Conductivity is a property usually reserved for the elements, such as copper, aluminum, or, at its most unusual graphite, the stablest phase of pure carbon.

In the last thirty years, however, attention has turned to more sophisticated materials, made partially or wholly out of organic compounds, that can also exhibit these properties.[1] These materials come not out of nature, but out of the synthetic laboratories in academia and industry. The properties of these materials are often wholly different from their inorganic cousins, and can include transperancy, light weight, and solubulity in organic solvents or water. Some can also be recast as thin films, a crucial quality for many industrial applications.

Chemists are fascinated by such materials for reasons of basic science as well as industry. It is impossible to transmute the properties of metals, but it is possible to subtly modify the structure of an organic compound, and by doing so gently mold the properties of the final material. Such nudging can optimize a material for a particular application. It can also fill in our

understanding of magnetism and conductivity, providing surprising new structures and properties that test the true extent of our knowledge of solid state physics.

The materials discussed in this thesis are in no way intended to become component parts in a technology of the near future. Instead, each investigates an area where the understanding is shallow, with the hope that raising the level of knowledge will lead to new research, and perhaps to new materials that can become incorporated in everyday life.[2]

The subjects of magnetism and conductivity are specific manifestations of the interactions of electrons in 3-D materials. This introduction will start by overviewing magnetism, then go on to discuss conductivity and the relationship between the two properties. It will also briefly look at the physical methods used to characterize the properties of such materials. This discussion will provide a reference point from which the design principles and the results of the next three chapters can be interpreted.

What is magnetism?

The phenonemon of bulk magnetism, the spontaneous magnetic behavior most obviously recognized in materials such as magnetite, has been known for perhaps 4500 years in China.[3] Its first technological application was in the compass. This obviously important innovation has encouraged scholars since that time to wrestle with the question of how magnetism works. These efforts were doomed to failure, however, for in the last century

we have recognized that spontaneous, bulk magnetism is strictly quantum mechanical in nature, and cannot be properly explained without an understanding of electron spin.[4]

Ferromagnetism results from the parallel alignment of electron spins in a solid.[5] Each spin represents a very small magnetic moment. The additive effect of aligning all the spins throughout a material results in a macroscopic moment, most noticeable for interacting with other macroscopic moments, such as those in a paper clip or refrigerator door. Usually, though, electrons do not align in this manner, and there are several possibilities for how they can behave. These possible behaviors are outlined in Figure 1.1, and described below.

Paramagnetism: This is the most common behavior for compounds with unpaired electron spin. In this case, each individual electron spin is completely unaffected by its neighbors. The spins of a bulk material will align in the presence of a magnetic field, but because each spin has a magnetic moment of such small magnitude, that alignment is weak. In practice, temperatures near absolute zero, accompanied by magnetic fields of 5 to 10 Tesla, are required to completely align the spins in a paramagnetic sample, and those spins will relax to a random distribution as soon as the field is removed.

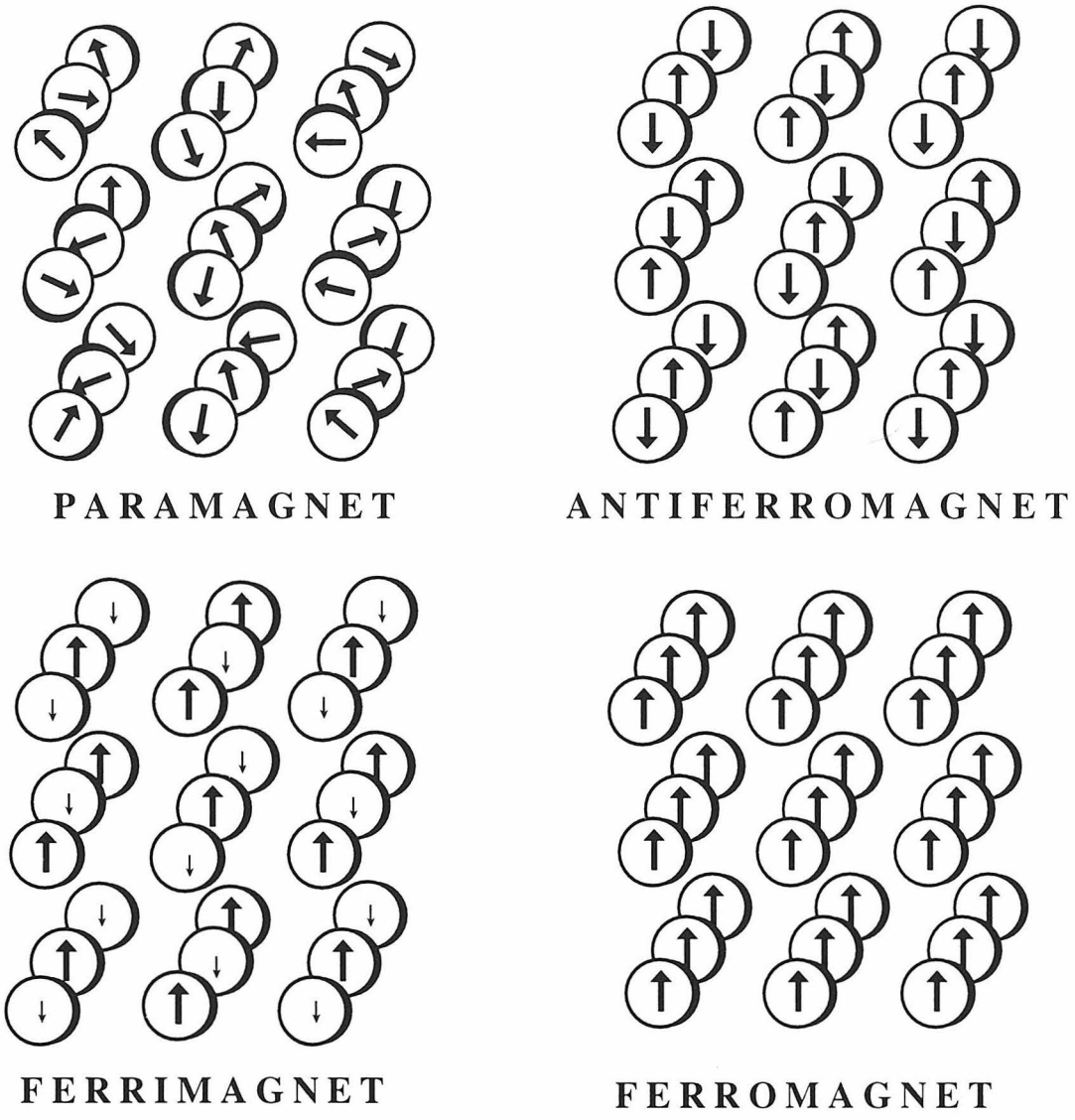

Figure 1.1 - The four principle classes of magnetism.

Antiferromagnetism: This is the other major behavior of compounds with unpaired spin. In this system, each spin pairs with its neighbor, and the result is a solid with no net magnetic moment, and which responds to a magnetic field as a diamagnet. The act of pairing is, in fact, analagous to the process of bonding, and if electrons can form such a pair they will. The energy

necessary to break this pairing is often so weak, that most systems with antiferromagnetic ground states behave as paramagnets - systems with uninteracting spins - except at extremely low temperatures.

Ferrimagnetism: Ferrimagnetism is a rarer behavior, in which the antiferromagnetic interactions between spins of different magnitudes result in a net moment. Magnetite is a ferrimagnet: S=5/2 Fe(III) atoms alternate in space with S=2 Fe(II) atoms and interact antiferromagnetically with them. The result is that each pair yields net S=1/2, and all the moments are aligned. A ferrimagnet maintains its alignment in the absence of an externally applied field.

Ferromagnetism: In true bulk ferromagnetism, all the spins in a solid are aligned. Two nearby spins can only align ferromagnetically if there is zero quantum mechanical overlap between the spin-containing orbitals. In such a case, there is no opportunity for a bond, even a weak bond, to form. Alignment of the spins, which correlates their motions and minimizes electron-electron repulsion, is thus the more stable state. A ferromagnet also has a net magnetic moment in the absence of an applied field.

Spin interactions in organic materials

In order to think about building a magnet out of molecular components, we must first obtain an understanding of how spins interact in molecules. For conjugated organic compounds, Ovchinnikov has proposed the 'star-nonstar' rule[6], which has been astonishingly successful in predicting the ground states of organic radicals. This rule applies to all alternant hydrocarbons, with no known exceptions.

According to this model, all the atoms in a molecule are alternately labelled with stars or without (nonstars), such that all starred atoms are adjacent only to nonstarred atoms (Figure 1.2). The number by which stars exceed nonstars is the number of aligned spins in the system, and this number multiplied by 1/2 (the spin of an electron) gives the molecule's spin state. (By convention, stars always outnumber nonstars.) As shown in the figure, *m*-xylylene and TMM are thus S=1 molecules, and *p*-xylylene and butadiene have a singlet (S=0) ground state.

As stated above, a ferromagnetic interaction can only occur if the unpaired electrons have zero quantum mechanical overlap, and the star-nonstar rule turns out to be an easy structural mnemonic for predicting this condition. The two degenerate orbitals of *m*-xylylene are non-overlapping, but significantly coextensive in space (Figure 1.3), and the radicals are thus aligned.

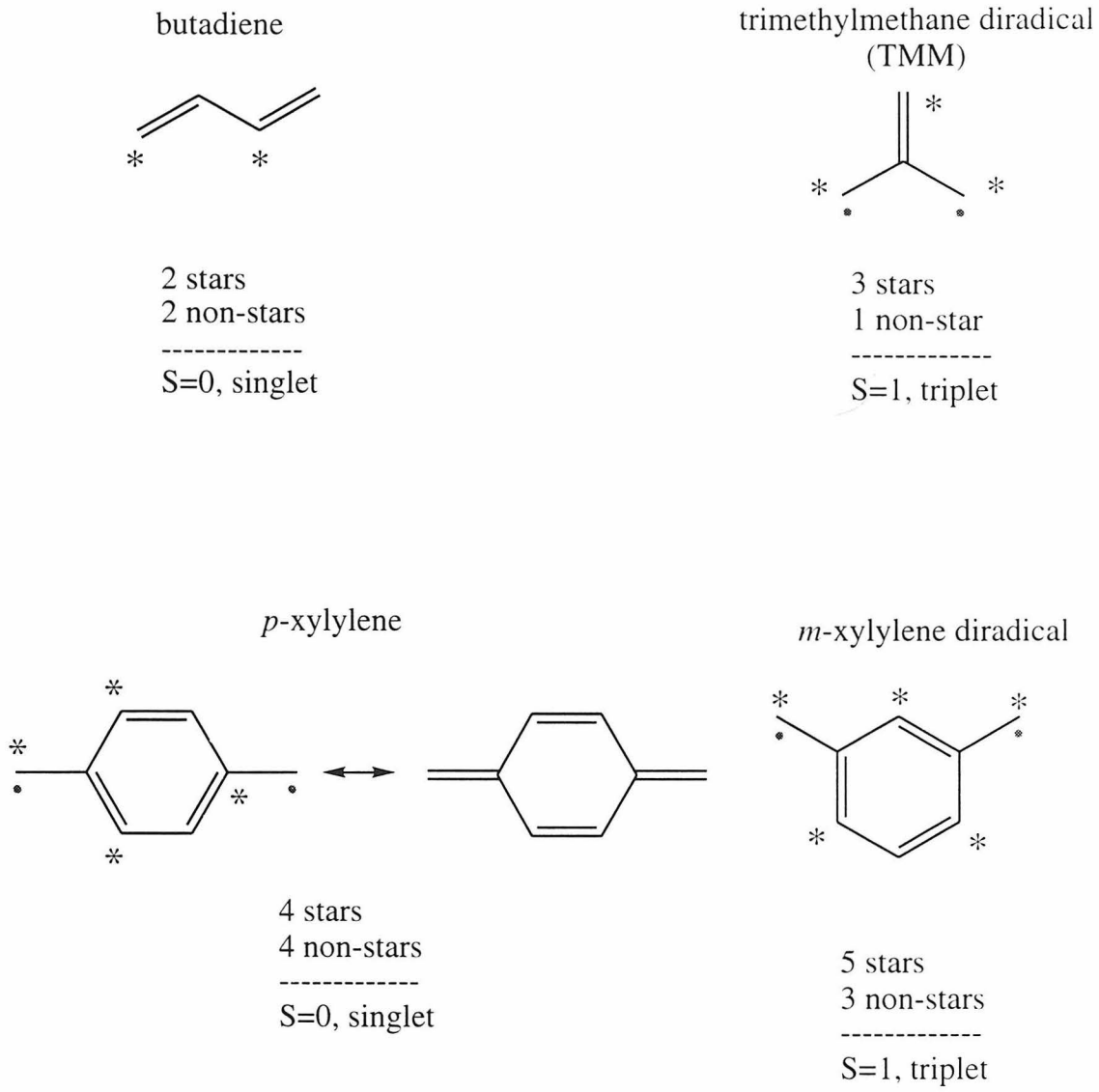

Figure 1.2 - The star-nonstar model

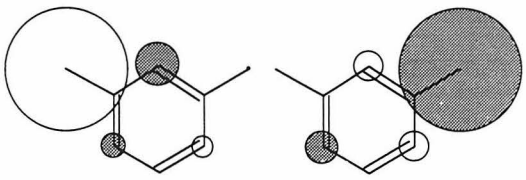

Figure 1.3 - Two degenerate HOMOs of *m*-xylylene have zero quantum mechanical overlap but significant physical overlap.[7]

The star-nonstar analysis holds true for molecules and materials far more complex than these simple model systems, where calculation of the HOMO is not possible. The oligomers and polymers obtained by elaboration on these motifs are shown in Figure 1.4 and behave as expected. As a result, the topological connection of unpaired spin bridged*meta* through a benzene can be considered a robust *ferromagnetic coupling unit*: if spin density is present at the α and α′ positions of *m*-xylylene derivatives, one can be sure that those spins are aligned.

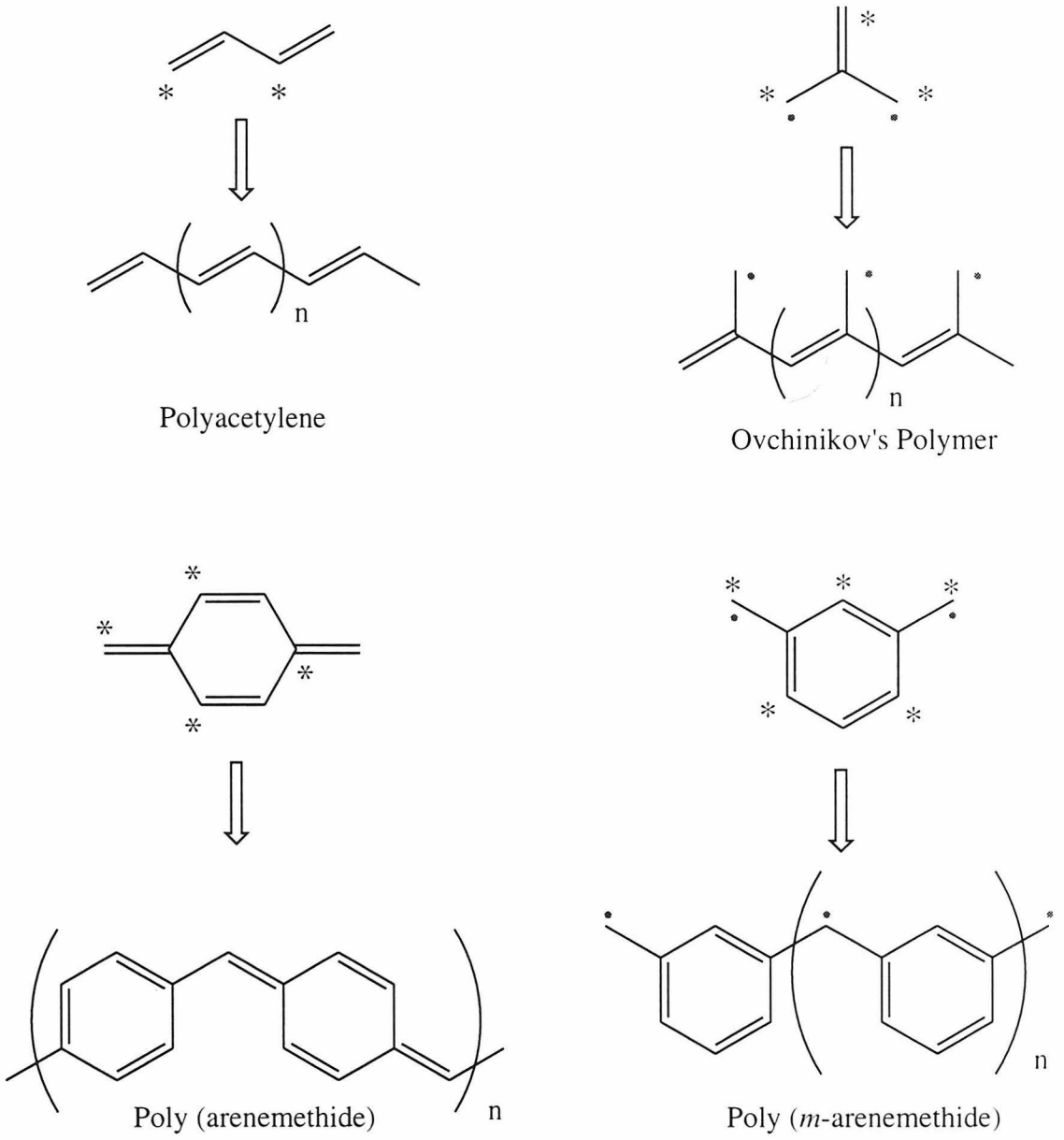

Figure 1.4 - Oligomers and polymers derived from elaboration of the model systems in Figure 1.2 display magnetic behavior predicted by the star-nonstar model. Poly(acetylene) is known to be non-magnetic, and poly(arenemethide) is discussed in Chapter 4. Oligomers of poly(*m*-arenemethide) have been made[8] and display the expected high-spin behavior.

Spin interactions between organics and metals

Metals are a more standard source of unpaired electrons than organic radicals, and they are the spin source for all technologically important magnets today. The direct interaction of spins on more than one metal atom can be mediated by their ligand sphere, and most recently a family of compounds using cyano ligands (and structurally similar to Prussian Blue) have been shown to be ferromagnets as high as 315K.[9] The spin density present on molecular and atomic orbitals falls off quickly with space, however, and only the smallest ligands can strongly communicate spin information from one metal to the next. These small ligands are by nature the least open to modification with organic chemistry.

One way to ensure a stronger communication of spin information in a metal-ligand system is to make the ligand itself a radical. In this case, the ligand spin density may be physically close to the metal, and a strong interaction is expected. Indeed, the magnetic interaction between nickel metal and a semiquoinone ligand (Figure 1.5) is strong even at room temperature.[10]

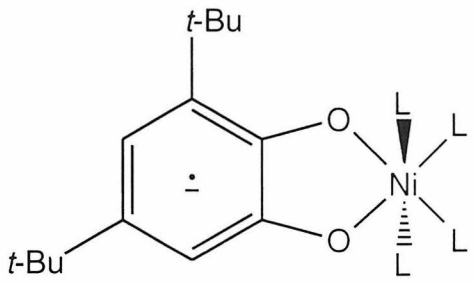

Figure 1.5 - The interaction between a semiquinone radical and nickel metal, shown above, is ferromagnetic at room temperature.

The nature of the interaction between a metal and a ligand-based radical is again predicted by examining the quantum-mechanical overlap

between the orbitals containing the two spins (Figure 1.6). Assuming the ligand radical is contained in a π orbital, if it encounters spin density in a d_π metal orbital, it will have positive overlap, and an antiferromagnetic (weak bonding) interaction will predominate. If the ligand radical physically overlaps with spin density in only d_σ orbitals, the two spins have zero quantum mechanical overlap, and the spins are ferromagnetically aligned. In the case where a metal has density in both d_σ and d_π orbitals, the antiferromagnetic interaction always predominates.

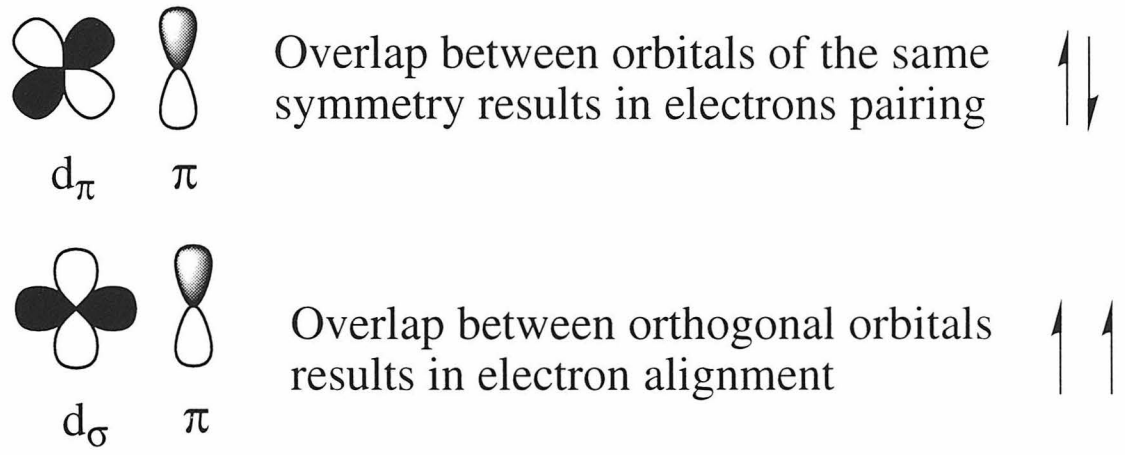

Figure 1.6 - Quantum mechanical overlap between ligand and metal spins results in an antiferromagnetic interaction. If the ligand and metal spins are in orthogonal orbitals, but there is still physical overlap, a ferromagnetic interaction results.

Measuring the magnetic properties of materials

Technology now exists to allow very subtle measurements on very small amounts of bulk material. The most important device in the material scientist's repetoire is the Superconducting Quantum Interference Device, or

SQUID. In a SQUID magnetometer, a small amount (5 to 200mg) of bulk material is loaded into a capsule or hollowed tube, and the sample is passed up and down through the coils of a Josephson junction. The magnetization is measured as a function of the current passing through the coils, which is itself affected by the net alignment of the bulk material. Application of an external magnetic field to the system partially aligns spins in the bulk sample, and the extent of alignment is an indicator of the spin state of the system.

There are two major experiments which provide details of the possible magnetic states that a paramagnetic material can inhabit in between diamagnetism (S=0) and ferromagnetism (S=∞). The first is a *variable field experiment*, in which the temperature is held constant at some low value (1.9K for the experiments discussed in the following chapters) and the magnetization of the material is recorded as a function of field.

Paramagnets are comprised of many, independently acting magnetic moments (spins), whose sizes are described by their S values. These magnets tend to align with an applied field, and larger moments (with larger S) tend to align more quickly with the field than smaller moments, whose weak interactions are more strongly influenced by thermal noise. The result is a characteristic saturation, or Brillouin curve, as shown in Figure 1.7. Experimental data can be fit to the theoretical curve in order to determine the spin state of the bulk sample.

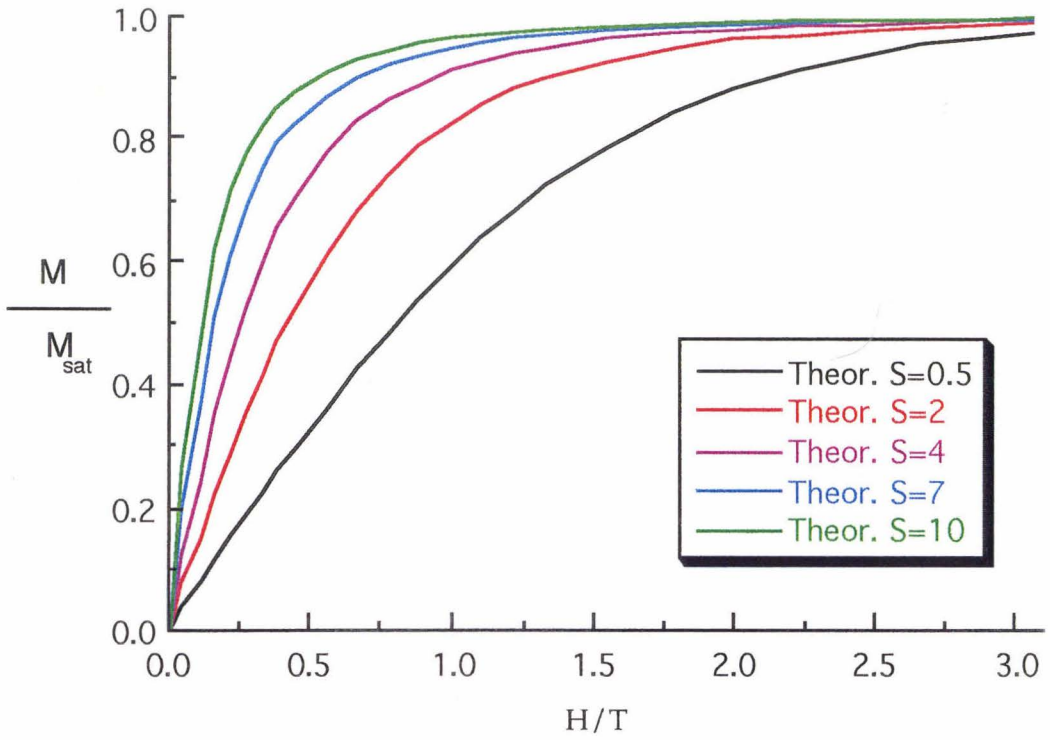

Figure 1.7 - Saturation curve for idealized paramagnets, with magnetization on the y axis and field on the x. Systems with larger S values saturate much more quickly in response to an applied field.

In a *variable temperature experiment,* the field is held constant below the value at which saturation effects become evident (for experiments in the following chapters, this value is 2000 gauss), and the temperature is varied. As the temperature is lowered from room temperature toward absolute zero, the ground state is no longer overwhelmed by thermal noise, and the magnetic moment of the material will go up for a ferromagnet and down for an antiferromagnet. Typical plots are shown in Figure 1.8.

Molecular orbital theory and band structure of conjugated polymers

Magnetism in organic systems is understood by applying simple rules that turn out to predict the important results of more sophisticated molecular orbital theory. Magnetic systems are *cross-conjugated*: there is no possible resonance form that can pair the two radicals that are connected; for instance, *meta* through a benzene. A standard conjugated organic backbone is not magnetic, but has the possibility of becoming conductive.[1b]

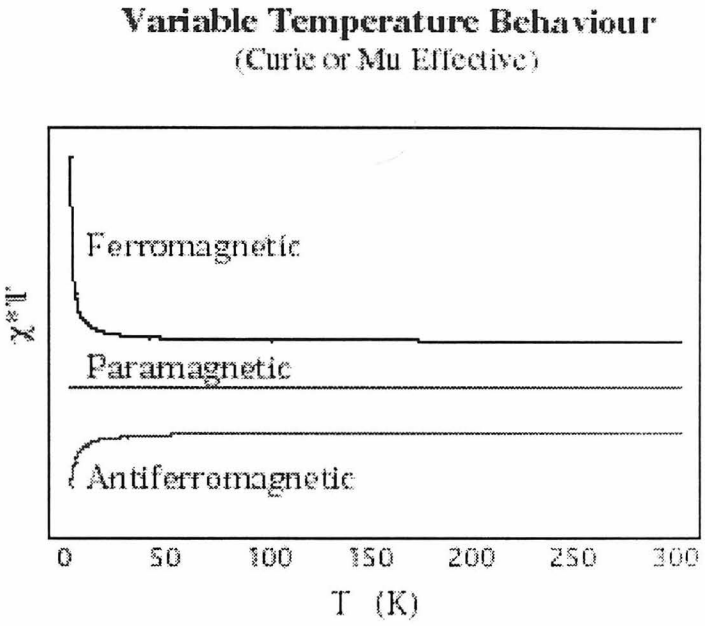

Figure 1.8 - Idealized variable temperature plots for a material with ferromagnetic, antiferromagnetic, or paramagnetic interactions predominating at low temperature.

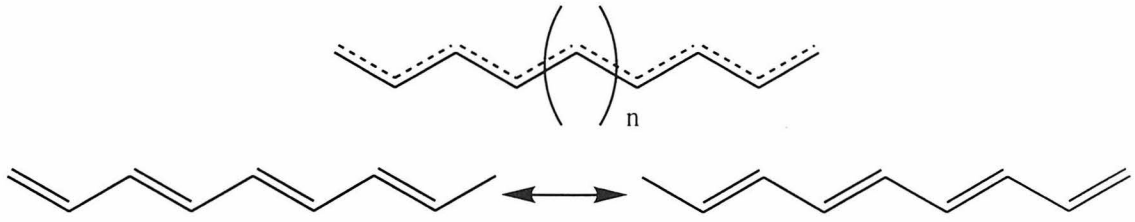

Figure 1.9 - Idealized polyacetylene exists as a resonance between two structures, as shown above.

The prototype conducting polymer is polyacetylene, a conjugated polymer most simply thought of as one sp^2 carbon repeated ad infinitum. Its molecular orbital can be approximated by examining the orbitals of conjugated ring systems, as shown in Figure 1.10. Benzene has six orbitals: three bonding and three antibonding. Circular dodecahexene has twelve orbitals: five bonding, five antibonding, and two non-bonding, the levels more densely packed than those of benzene. An infinite circle, as a model for linear polyacetylene, has orbitals packed infinitely densely throughout its energy spectrum.

Such a dense packing of orbitals is referred to as a 'band.' In this case it is helpful to think of the orbitals as forming two bands, one filled (corresponding to the HOMO) and one empty (corresponding to the LUMO.) The lower (HOMO) band is called the valence band, and the upper (LUMO) is called the conduction band. The midpoint between the two is called the Fermi level.

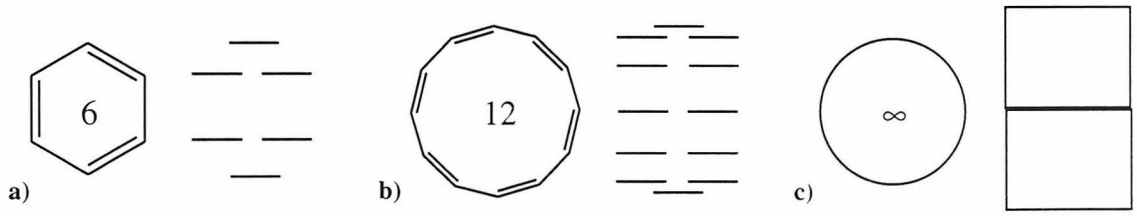

Figure 1.10 - a) The molecular orbital structure of benzene. b) The molecular orbital structure of a circular conjugated dodecahexene. c) The molecular structure of an infinite circle is too fine to describe, and it is drawn as a pair of bonding and antibonding bands of orbital density. The lower band is called the valence band, the upper the conduction band, and their interface the Fermi level.

In this simple treatment of polyacetylene there is an exact degeneracy between the valence and conduction bands. However, a molecule that has partial occupation of degenerate orbitals is prone to a Jahn-Teller distortion, known in solid state physics as a Peierls distortion. In this distortion, the fully delocalized representation of polyacetylene distorts into an alternating bond conformation with bonds of length 1.38 and 1.43Å[11], as shown in Figure 1.11. (For reference, a C-C single bond is 1.54Å and a C=C double bond is 1.35Å.) This opens up a band gap in the structure between the valence and conduction bands, destroying the degeneracy.

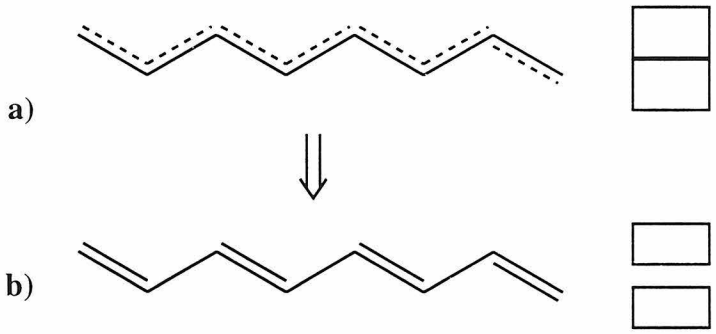

Figure 1.11 - A Peierls distortion in polyacetylene, taking the structure from a) to b), opens up a gap in its band structure.

Conduction, semiconduction, and doping

If there is an exact degeneracy between the valence and conduction bands, it takes no energy to promote an electron, creating a hole in the valence band and an electron in the conduction band. If there is a gap between the valence and conduction bands, then the material may be doped

to make it conduct: p-doping rips out an electron from the valence band, creating a hole; n-doping adds an electron to the conduction band. Most conjugated polymers are semiconducting or insulating in their pristine states. Doping can give them metallic conductivity.

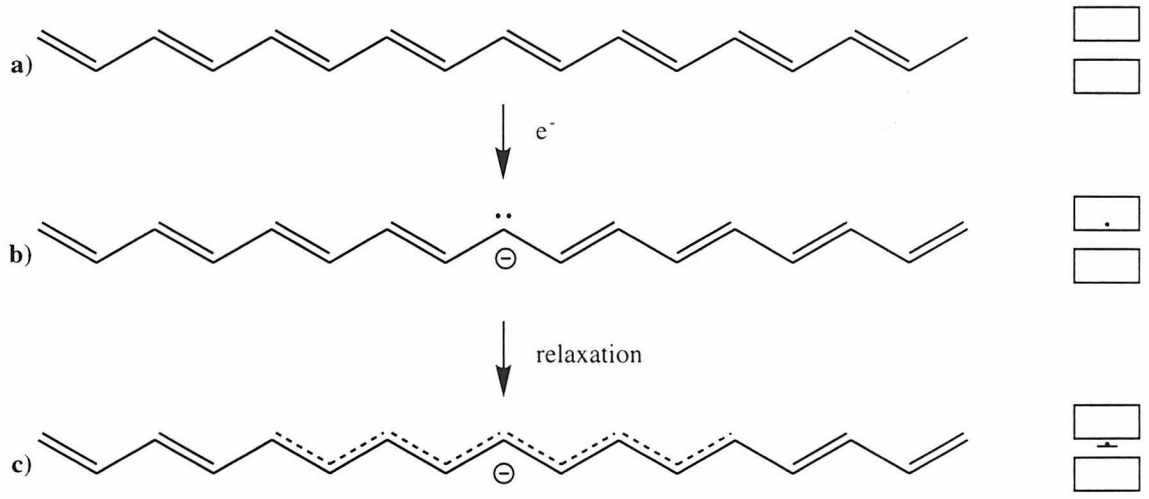

Figure 1.12 - A conducting polymer (a) is n-doped (b), adding an electron to the conduction band. The structure of the polymer relaxes slightly (c), and a new state is formed just below the conducton band. Electrons in these states are easily promoted to the conduction band, where they may more freely travel throughout the material.

If one applies a bias across the metal, the electrons are attracted to the positive electrode and the holes to the negative electrode. In a doped material, the electrons or holes can wander substantially from their original counterions. In polyacetylene, for example, 85% of charge is contained in 15 CH units around the dopant. Conductivity (σ) scales with the number of free carriers; $\sigma = ne\mu$, where n=carriers per unit volume and μ=carrier mobility. A small amount of dopant will give a large increase in carrier number and

therefore conduction. The conductivity of polyacetylene, 10^{-5} $(\Omega\ cm)^{-1}$ in the pristine state, rises 3 orders of magnitude upon doping with 1% AsF_5 and 7 orders of magnitude with 5% AsF_5, with a maximum conductivity on the order of 10^6 $(\Omega\ cm)^{-1}$ (depending on the dopant and the polymer morphology), roughly equivalent to that of copper.[12] This effect is not due solely to increasing the number of carriers. As the carrier density increases, the barrier preventing an electron from migrating from one counterion to the next becomes smaller and smaller. This is reflected as an increase in the mobility of the material. Past a certain level, though, increased doping decreases the carrier mobility, in part through degradation of the material, decreasing conductivity.

The basic rule in designing a conducting polymer is thus to create a conjugated topology, then dope it.

Hopping, twisting, and mobility

It has been assumed in the above analysis that the individual polymer strands are infinitely long. In practice this is not true, and, in order to get from cathode to anode, electrons must hop from strand to strand through the material.

It is hopping that eventually controls the conductivity of real materials. Electrons (or holes), trapped in an individual strand, must come into close contact with a doped segment of a neighboring strand in order to move

through the material. Increasing the length of a real polymer strand up to a certain point increases the conductivity of a material. The strand then has physically greater contact with its neighbors and thus a greater opportunity for the electron to find an optimal hopping site. The effect is most pronounced in small strands, and, beyond a certain point (>60 double bonds in polyacetylene[13]), increasing the length of the strands has a diminished effect. The conductivity in these systems is limited by the material's nanostructural morphology. The most conductive samples of polyacetylene have their polymer strands aligned, minimizing the distance between strands and thus the barrier to hopping.[12]

Twisting the conducting backbone similarly disrupts the material's conductivity. Simple derivatives of poly(acetylene), such as poly(phenylacetylene) are not conductive because the steric bulk of the phenyl groups causes considerable twisting to the backbone.[14] Electrons and holes cannot travel past these twists, and must hop from strand to strand to conduct.

The mobility of electrons is thus restricted by morphology. Doping will still increase the conductivity of a polymer, and in practice, conductivities of up to 10^{-2} $(\Omega\ cm)^{-1}$ can be acheived solely by hopping.[1b] Improvements beyond that limit require the presence of a conducting backbone.

Measuring conductivity

The most consistant measurements of conductivity are made with a four-point probe on a thin-film sample of material. A voltage is applied between the two outermost points, causing current to flow through the conducting material. The interface between the metallic probe and the conducting polymer may not be ohmic, and there may be a turn-on voltage associated with getting current to flow. As a result, measuring the voltage between the two inner probes affords a more accurate characterization of the material, and resistance can be solved for based on the geometry of the probes and the thickness of the material.[15]

Thin films of the material suitable for such experiments can be made by spin-coating or simple evaporation. Spin-coating affords more homogenous samples and is thus the preferred method. Samples are dissolved in a suitably volatile solvent and dropped slowly onto a rapidly spinning glass slide. Polymer is deposited on the slide as it spins, giving a coating of roughly uniform thickness. Thickness can be measured by profillometry or elipsometry, and for the experiments described below is usually on the order of 100nm.

Evaporation of several drops of polymer solution provides rougher, thicker coatings on the order of 1μm.

---

[1] a) for a review of magnetism, see Kahn, O.; *Molecular Magnetism*, VCH Publisher, Inc., New York, **1993**. b) for a comprehensive review of conducting

organic polymers and their physics see Skotheim , T.A., ed.; *Handbook of Conducting Polymers, Vol. 1 and 2,* Marcel Dekker, Inc., New York, 1986.

[1] Chien, J.C.W.; *Polyacetylene: Chemistry, Physics, and Materials Science,* Academic Press, Orlando, Florida, **1984**, p. 115

[2] Dougherty, D.A.; *Accounts of Chemical Research*, **1991**, *23*, 88

[3] Mattis, D.C.l *The Theory of Magnetism I*; 2nd ed., Spinger-Verlag, New York, **1988**, *17*, p295

[4] for a detailed discussion see Andersen, K.A.; Ph.D. Thesis, California Institute of Technology, **1996**, pp.121-158

[5] Carlin, R.L.; *Magnetochemistry,* Springer-Verlag, New York, **1986**, p.112.

[6] Ovchinikov, A.A.; *Theo. Chim. Acta*, **1978**, *47*, 297

[7] Orbital pictures calculated using HMO-Plus 2.0.2 by Allan Wissner, Wyeth-Ayerst Research, Lederle Laboratories, Pearl River, NY

[8] Itoh, K.; *Chemical Physics Letters*, **1987**, *1*, 235.

[9] Ferlay, S.; Mallah, T.; Ouahes, R.; Veillet, P.; Verdaguer, M.;*Nature*, **1995**, *378* , 701

[10] Benelli, C.; Dei, A.; Getteschi, D.; Pardi, L.; *Inorganic Chemistry*, **1988**, *27*, 2831

[11] Chien, J.C.W.; *Polyacetylene: Chemistry, Physics, and Materials Science,* Academic Press, Orlando, Florida, **1984**, p. 115

[12] Basescu, N.; Lie, Z.-X.; Moses, D.; Heeger, A.J.; Naarmann, H.; Theophilou, N.; *Nature*, **1987**, *327*, 403.

[13] Park, L.Y.; Ofer, D.; Gardner, T.J.; Schrock, R.R.; Wrighton, M.S.; *Chemistry of Materials*, **1992**, *4*, 1388

[14] Chien, J.C.W.; *Polyacetylene: Chemistry, Physics, and Materials Science*, Academic Press, Orlando, Florida, **1984**, p. 544

[15] Mayer, J.W.; *Electronic Materials in Science: For Integrated Circuits in Si and GaAs*, MacMillan Publishing Co., New York, **1990**, p. 34.

Chapter Two : Towards the crystal engineering of an organic ferromagnet

Macromolecular synthesis and crystal engineering: Problem and Scope

Macromolecular synthesis refers in general to attempts to acheive geometrical order between one or more molecules using non-covalent forces. Crystal engineering is one subfield of macromolecular synthesis, in which the emphasis is placed on rationally ordering molecules in the crystal lattice. Achievement of such ordering could yield materials with an impressive array of physical properties, including non-linear optical activity, catalytic function, high electron or hole mobility, and ferromagnetism.[1]

Currently, the art of macromolecular synthesis is still in its formative stages. For the organic chemist, it is probably best thought of as analagous to conventional covalent synthesis, as outlined by Lehn[2]. In conventional synthesis, as described by Corey[3], one conceptually breaks down the target molecule into its synthons, the more accessible building blocks which, when combined, form the target. The synthons are generalizable from reaction to reaction, and they form the welds with which a wide variety of substituents can be linked together. Covalent reactions tend not to convert 100% of the starting materials to product, and that inefficiency is reported as the yield of

the final product; the rest of the material reacts to generate unintended side-products.

In macromolecular synthesis, molecules are brought together non-covalently instead of covalently. In this case, the synthon is still the functionality of a molecule that serves to link it, with itself or other molecules, in an ordered fashion. The most basic synthon is perhaps the ion pair, where positive and negative ions tend to aggregate near each other, both in solution and in the solid state. A dramatic example of this has been recently shown by Tour et al.[4], who assembled cationic fullerene derivatives on an anionic DNA backbone.

Many other synthons are available, and a nearly exhaustive list appears in a review by Desiraju[5] and is reproduced in Table 2.1.

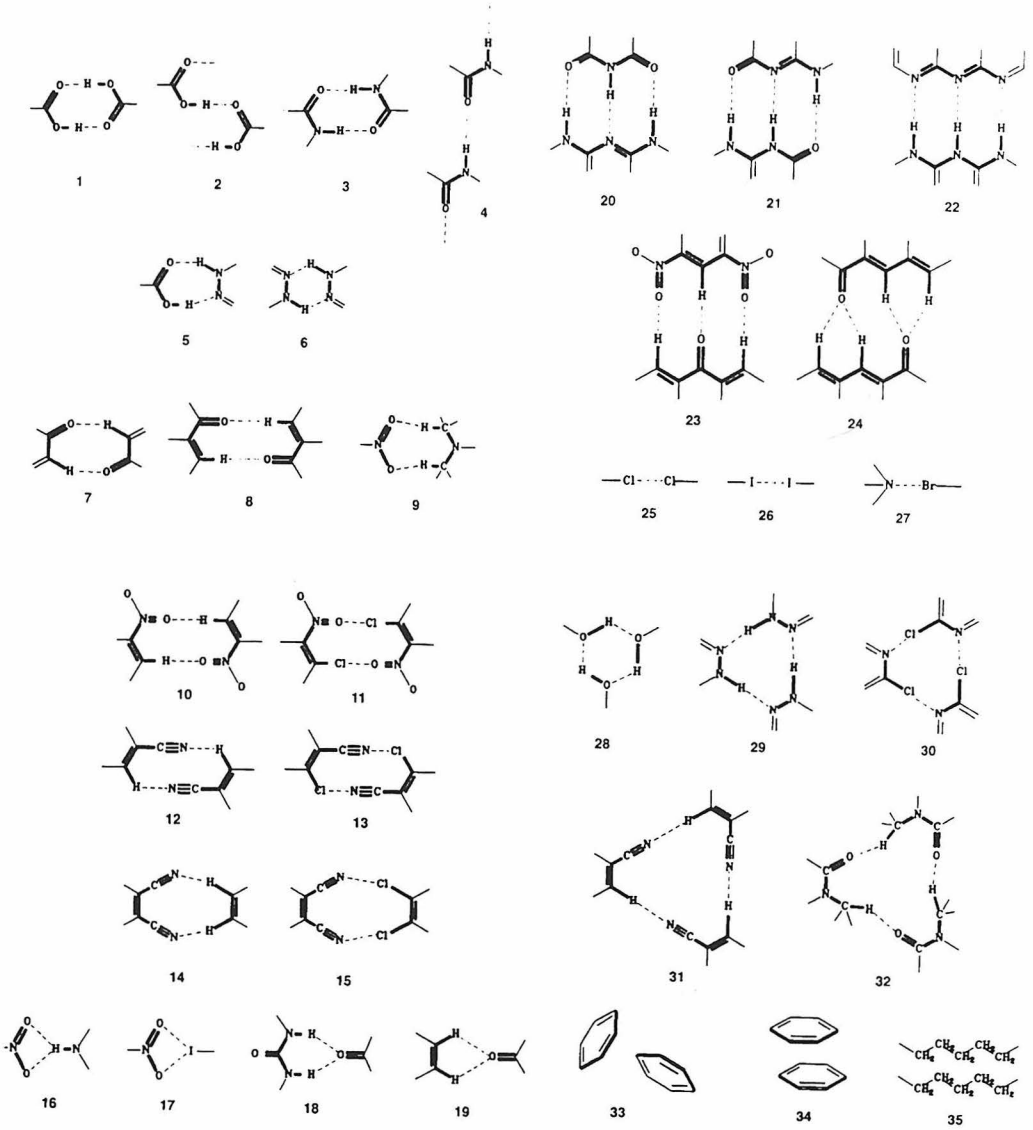

Table 2.1 - A sampling of 36 synthons that have been seen in crystal structures. From reference 5.

Crystal Engineering Design Parameters

One synthon that nicely illustrates the promise and pitfalls of crystal engineering is the carboxylic acid group, which can form strong hydrogen-bonded dimers. For example, carboxylic acids tends to form dimers in the

solid state, following synthon **1** from Table 2.1. Indeed, in about 85% of the small molecules examined by Desiraju[5], carboxylic acid groups tend to form these dimers. However, in the other 15%, an alternative ordering scheme predominated. One possibility is sython **2**, in which the carboxylic acid groups formed polymeric ribbons, though this is by no means the only alternative. This success rate can be thought of as analagous to the yield of conventional synthesis: instead of the conventional synthon directing 85% of the molecules to form the desired products, a macromolecular synthon may direct all the molecules to form the desired structure about 85% of the time.

A further limitation of this synthon in particular is that its reliance on hydrogen bonding eliminates the possibility of incorporating many other functional groups into the eventual crystal. Amines, for instance, will deprotonate the acids to form ion pairs. Alcohols, thiols, and other heteroatom-containing functional groups may also participate in hydrogen bonding, disrupting the intended network of carboxylic acid dimers. It is thus important to generate a large library of possible synthons that may be used to guide the assembly of a given structure for a given application.

In general, the packing of molecules into a crystal is determined by the priorities in the list below[6]:

1) **Maximize crystal density.** van der Waals forces, though weak, occur throughout the volume of the crystal and account for most of the enthalpy of crystal packing. Organic crystals tend

to have between 60-77% of their volume encompassed within the van der Waals radii of the component molecules. Any attempts to reduce the crystal density below this range usually result in the inclusion of solvent molecules in what would otherwise be voids. This general principle is also known as Kitaigorodskii's Principle of Close Packing, and is illustrated in Scheme 2.1[6]. Large molecules that cannot pack in a crystal lattice without significant void space will often collapse to glasses, which are an interesting phenomenon in their own right.[7]

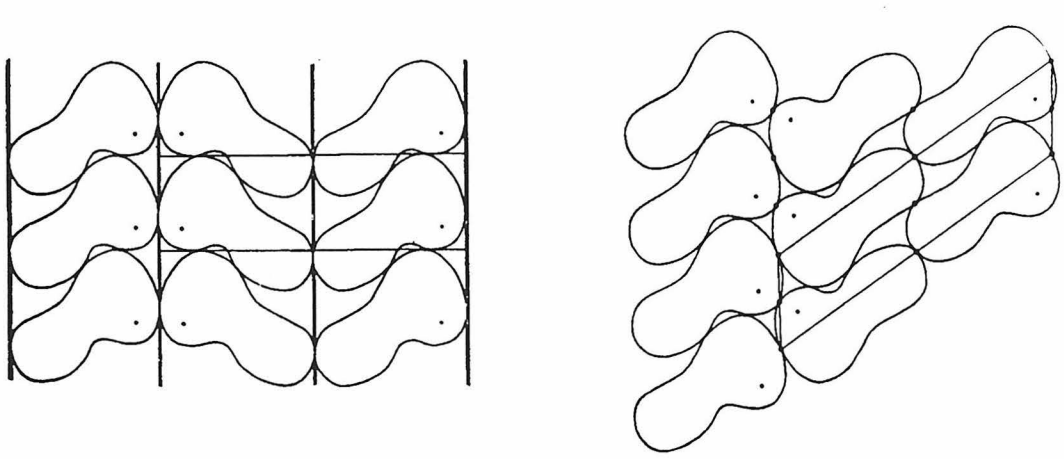

Scheme 2.1 - Molecules, which tend to have asymmetric shapes, prefer to pack in a way that maxmizes intermolecular contacts (right) over other methods (left).

2) **Satisfy H-bond donors and acceptors and any other special synthons.** When present, hydrogen bonds tend to dominate other special interactions because they are highly directional, and thus most sensitive to small perturbations in geometry. The

presence of multiple interactions of this type can make a crystal less dense. As an example, ice, which fulfills all of its possible hydrogen bonds, is less dense than water. Other synthons take advantage of specific electrostatic interactions or specifically favorable van der Waals contacts, as shown in Table 2.1.

3) **Minimize electrostatic energy.** Once the synthons have been satisfied, weaker electrostatic effects guide the crystal into its final structure. In the crystal, bond dipoles are much more imporant than molecular dipoles because the molecules pack too closely to be affected by unperturbed total dipoles. When two possible structures have nearly the same packing density, this would be the force that determines the lowest energy structure.

It should be noted that the carboxylic acid dimer, and in fact all of the synthons listed in the review by Desiraju, order molecules in one dimension only. The problem of ordering molecules precisely in three dimensions is far beyond the scope of current technology, and is likely impossible using only small molecules as the synthons.[8,9] There are many combinations of weak forces that potentially fall within less than a kilocalorie/mol range in energy difference, and it is not possible to computationally access such subtle interactions. Furthermore, crystallization is a kinetically controlled process where the slow step is the formation of a crystal nucleus, and there is no

guarantee that the true thermodynamic mimimum structure will be the experimental one. As a result, crystals often have several polymorphs, the supramolecular equivalent of isomers. Even at a single temperature, many possible structures may coexist as metastable states.

While polymorphism may prevent arbitrary control over the three dimensional structure of a crystal, several applications are potentially accessible using the limited set of tools currently available. One such application is the organization of organic radicals to form a ferromagnet, as discussed below.

An approach to organic ferromagnetism using crystal engineering

As discussed in chapter 1, spin is distributed across a π system in a spin-polarized fashion. If two organic radicals could be made to stack face-to-face, with regions of spin α on one molecule most closely positioned to regions of spin β on another, the antiferromagnetic interaction between those regions would align the spins on the two molecules.

This strategy has been tested in a model system by Izuoka et. al.[10] The cyclophane biscarbene, shown in Figure 2.1, can be generated at liquid nitrogen temperatures in a MeTHF matrix. This 'pseudo-ortho' system is predicted to couple ferromagnetically, and it does, with an astoundingly high J_{eff}=-3.5K. The 'pseudo-meta' system gives a ground state singlet, again as predicted by theory.

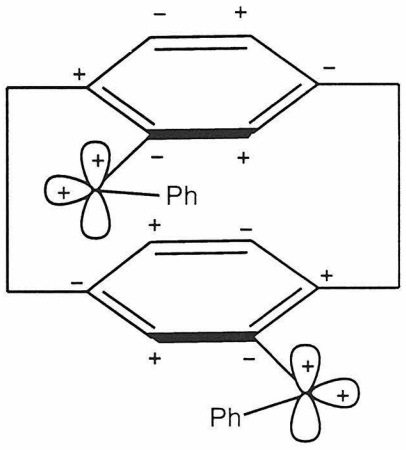

Figure 2.1 - In the above 'pseudo-ortho' cyclophane tetraradical, + spin density on the upper ring is physically closest to - spin density on the lower ring. As a result, the radicals are aligned, and the system has a quintet ground state with J_{eff}=-3.5 kcal/mol

This type of stacking has also been seen in a non-covalently constrained system, the galvinoxyl radical. At temperatures above 85K the radical serendipitously crystallizes into a structure where regions of spin α and spin β align as described above, and weak ferromagnetic interactions are seen between the radicals.[11] Below

85K the crystal undergoes a phase transition, and the molecule adopts an antiferromagnetic ground state.[11]

There are two significant problems associated with achieving bulk ferromagnetic order using this strategy. First, one-dimensional ordering of spins is necessary but not sufficient for achieving bulk ferromagnetism. Each 1-D system can potentially order antiferromagnetically to its neighbors, resulting in a bulk cancellation of magnetic dipoles.

Second, and more subtly, magnetic ordering by this mechanism requires tolerances at the sub-angstrom level. Though the sign of this spin may alternate from atom to atom, the magnitude does not. Atoms contributing to the spin-containing molecular orbital of a molecule contain the vast majority of spin density on the molecule, where the neighboring atoms are just polarized away from zero spin. This is illustrated for TMM in Figure 2.2. As a result, the interactions that favor antiferromagnetic order are much stronger than those that favor ferromagnetic order, and a slight slippage from the idealized geometry will result in a bulk antiferromagnet.

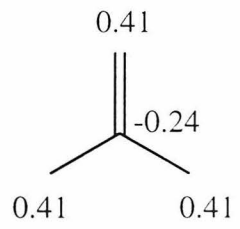

Figure 2.2 - The spin density of TMM, as approximated from EPR data.[12]

In some sense, then, building a ferromagnet by this pathway is the ultimate test of the guiding ability of a supramolecular synthon. Realistically, though, realization of a bulk ferromagnet in this way requires not only excellent design, but also a good dose of luck.

The benzene-hexafluorobenzene synthon

π stacking, generally discussed as the face-to-face stacking between aromatics, is an unfortunate misnomer; most aromatic systems are electron rich, and thus mutually repel. The π stacks that have been seen are usually slipped, allowing the electrostatically positive hydrogen of one ring to lie over the electron rich face of another, as shown in Figure 2.3. The face-to-face stacking seen in more extended systems is usually driven by van der Waals interactions, rather than elctrostatics[13].

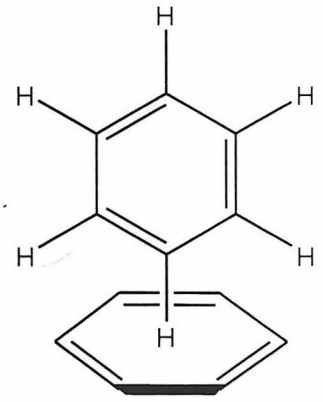

Figure 2.3 - A typical T-shaped interaction between two aromatic rings places the electron-poor hydrogen atom from one ring directly in the electron-rich face of the other.

Benzene and hexofluorobenzene have long been known to associate face-to-face, and the two liquids (benzene mp=5.5°, and hexafluorobenzene mp=4°) mix 1:1 to form a solid (mp=27) at room temperature.[14] The solid consists of stacks containing benzene and hexaflurobenzene, alternating in a 1-D chain (Scheme 2.2a).

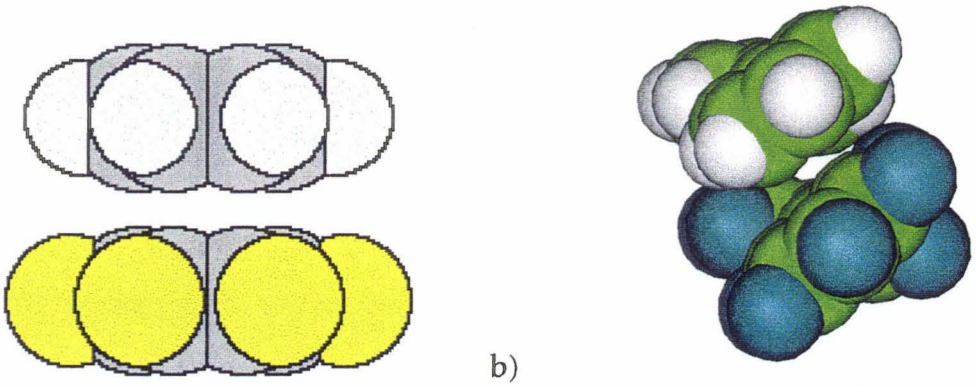

a) b)

Scheme 2.2 - a) Mixing benzene and hexafluorobenzene leads to a face-to-face, mixed stack. The rings are separated by 3.6Å. b) Mixed systems involving biphenyls (this picture produced from data in the Cambridge Crystallographic Database) also form alternating stacks. In this case, the molecules are sterically forbidden from assuming a complete face-to-face configuration.

This favorable interaction is a result of complementary electrostatics and sterics: the face of the benzene is electrostatically negative, with electrostatically positive hydrogen atoms ringing it. The face of hexafluorobenzene is electrostatically positive, with electrostatically negative fluorines ringing it. By coincidence, the magnitudes of the two quadrupoles are nearly identical, as are the molecular sizes. Stacking face-to-face thus allows both favorable electrostatics and close-packing. In addition to the above system, fluorinated biphenyls have also been shown to stack as predicted by this simple electrostatic picture, though the twist in the biphenyl unit prevents complete overlap of the aromatic faces (Scheme 2.2b).

This synthon has recently been used by others at Caltech in order to organize molecules to react in the solid state.[15,16] Diphenyl- and di(pentafluro-phenyl)diacetylenes form a mixed crystal in the predicted way

and can be photopolymerized. Similarly, 1-pentaflourophenyl-4-phenyldiacetylene itself crystallizes in the familliar face-to-face fashion and also photopolymerizes.[15] It should be noted that for each system the rings are not stacked precisely atop each other, since other forces involved in crystal packing conspire to move them slightly from this conceptually simplest orientation. Similar work has been done dimerizing double-bonded systems using this synthon.[16]

The project

This project aims to use the benzene-hexafluorobenzene synthon to organize the stacking of organic radicals. In this case the macromolecular target, a magnet, is analagous to the natural product target of conventional synthesis. Magnetism is well-enough understood to allow one to design a magnetic structure on paper, but the field of molecular magnetism is still young, so each new material represents a significant addition to the field. The magnetic properties of a crystal can be nondestructively and easily measured on 10-milligram scale samples of material, and the magnetic properties depend entirely upon the three-dimensional structure of the crystal formed.

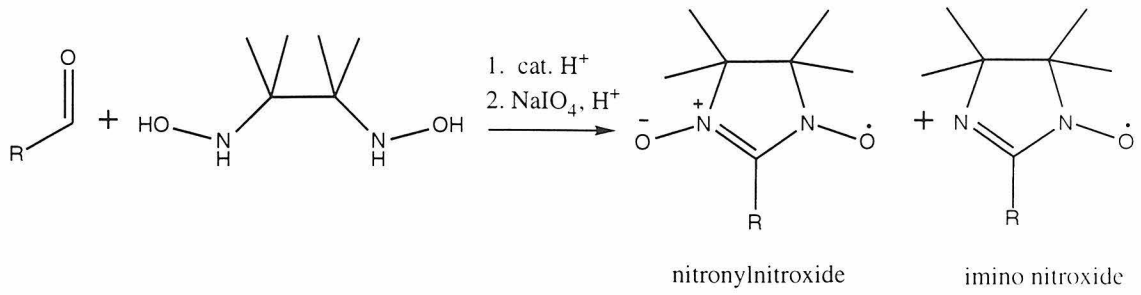

Scheme 2.3 - Synthesis of a nitronylnitroxide and nitroxide

The organic radical of choice for this experiment is the nitronylnitroxide. These radicals are air and water stable, highly colored, and can be chromatographed. There exists a considerable literature studying the magnetism of a variety of species[17], and the radical 4-nitrophenyl-nitronylnitroxide was the first known all-organic ferromagnet.[18] Nitronylnitroxides are easily synthesized in two steps from the corresponding aldehyde[19] (Scheme 2.3). Most important for this study, the spin-containing system is in direct conjugation with any variety of aromatic substituents, and spin-polarization across these substituents has been used to explain the magnetic behavior of several derivatives.[20] Finally, the synthesis of nitronylnitroxides yields the related imino nitroxide as a side-product, allowing two radicals to be created for each synthesis undertaken. This factor is an important advantage, given the anticipated need for a large number of trials to afford the desired product. Initial experiments focused on the better-studied nitronylnitroxdes.

The nitronylnitroxide unit, while polar, lacks any other specific macromolecular directing group that might interfere with the dominance of

the desired benzene-hexafluorobenzene synthon. This is the first system tested with the benzene-hexafluorobenzene synthon that is not entirely planar, as the methyl groups from the nitronylnitroxide protrude above and below the plane of the synthon. The van der Waals radius of a t-butyl group is similar to the breadth of a phenyl ring (3.30Å vs 2.92Å), so this system is expected to accomodate the perturbation.

Results and Discussion

Initial Attempts: Phenyl and Pentafluorophenyl nitronylnitroxide mixed system

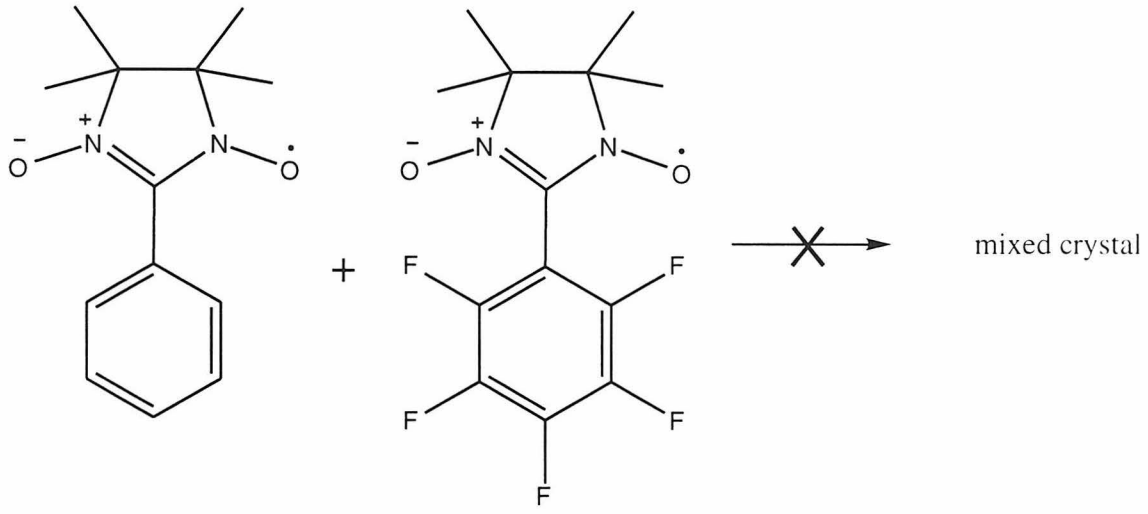

Scheme 2.4 - A simple mixed crystal system did not form as anticipated

The most logical place to start such research is to synthesize the phenyl[19] and pentafluorophenyl[21] nitronylnitroxide and attempt to form a 1:1 crystal. The two nitronylnitroxides were mixed (Scheme 2.4), and crystal growth was attempted in ether and ethyl acetate both by cooling and by slow evaporation. Under neither condition was a mixed crystal formed, as evidenced by observation of the original melting regimes, both using a traditional melting point aparatus and differential scanning calorimetry.

There are three possible reasons for this failure. The first is that the nitronylnitroxide group is expected to be considerably electron withdrawing, and thus the phenyl-nitronylnitroxide system may not be electron rich enough to make an intermolecular interaction favorable for formation of the mixed crystal. The second interpretation is that the nitronylnitroxide unit sterically prevents complete overlap of the rings, also reducing the strength of the interaction. Finally, the optimum geometry of packing for the two monomers may simply be denser than the best geometry for a mixed crystal.

Additional systems were designed to include both the fluorinated and non-fluorinated rings in a single molecule in order to minimize such ambiguities.

Biphenyl nitronylnitroxides

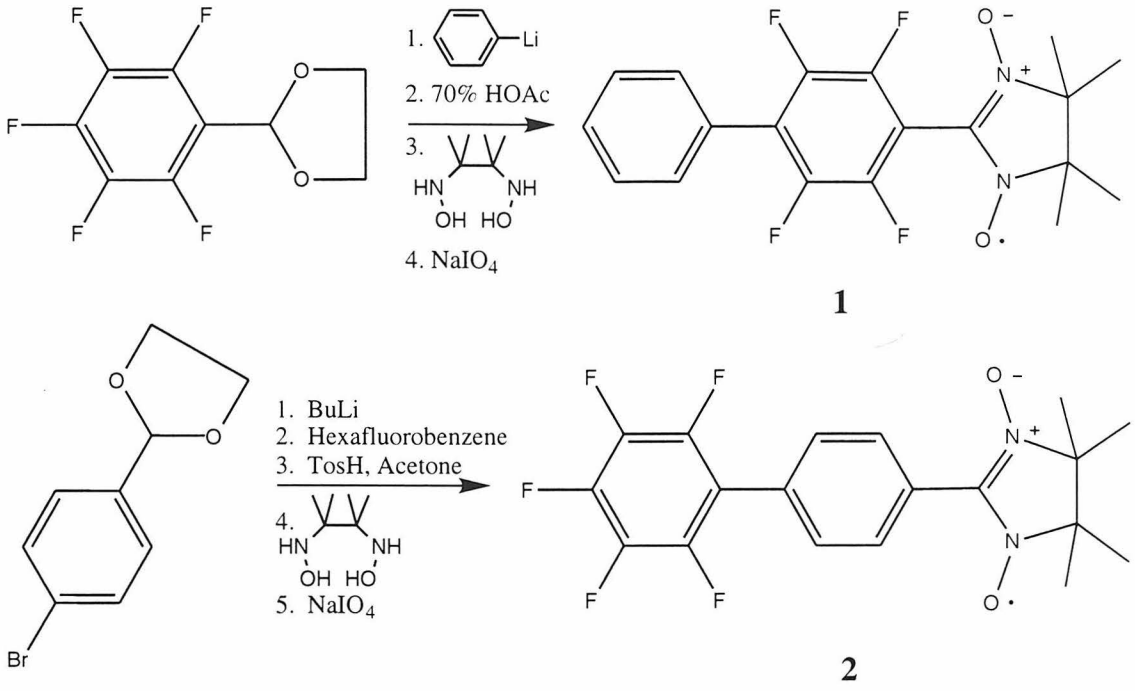

Scheme 2.5 - Synthesis of biphneyl nitronylnitroxides

The blue nitronylnitroxide (**1**) was synthesized according to Scheme 2.5, characterized magnetically, and structurally determined by x-ray crystallography. The *para-* isomer was the major product of the synthesis; the *meta-* isomer could be isolated in <10% yield when chromatographed as the ethylene glycol-protected aldehyde. The magnetic data of (**1**), showing an antiferromagnetic downturn at low termperature, is fairly standard for nitronylnitroxides, and is shown in Figure 2.4. The weak antiferromagnetism is probably dominated by very long, 6.18Å O-O contacts between nitronylnitroxide units.

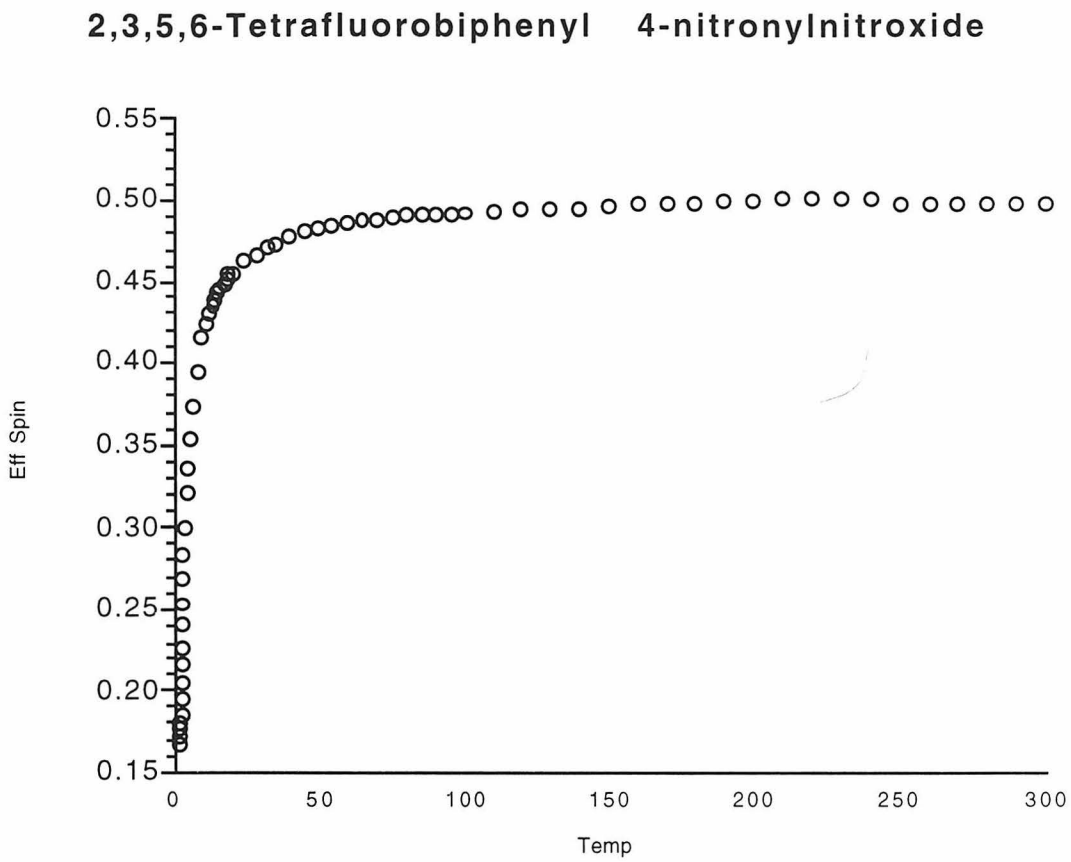

Figure 2.4 - Variable temperature data[22] for (1) shows S=1/2 behavior at high temperature with antiferromagnetic interactions predominating at low temperature. The variable temperature data for (2) is similar.

The synthon did not dominate the ordering of the molecule in the crystal, as shown in Structure 2.1. Ring twist between the phenyl units and the tetrafluorophenyl is 44°, and that between the tetrafluorophenyl and the nitronylnitroxide is 58°. (The five-membered ring of the nitronylnitroxide is itselft puckered out of planarity in order to stagger its four methyl groups, so all dihedrals involving this ring are listed as the average of the two possibilities.) The molecules stack in a staggered 1-D column with nitronylnitroxide units lying atop pheynyl rings and the tetrafluorophenyl rings tilted out of the plane. The C-F bonds from adjacent molecules point in opposite directions, and the structure may be stabilized in part by this favorable opposition of local dipoles.

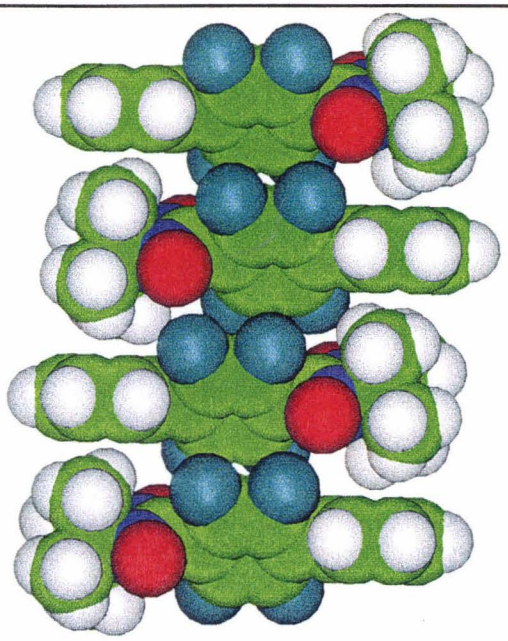

Structure 2.1 - Structure of a biphenyl nitronylnitroxide. This cutaway shows one of the 1-D stacks along the a axis.

The fault in this system is thought to be the twist between the phenyl rings preventing stacking as predicted by the synthon. Because **2** also contains this ring twist, no x-ray characterization was attempted. The next system eliminates this twisting.

Diphenylacetylene-nitronylnitroxide

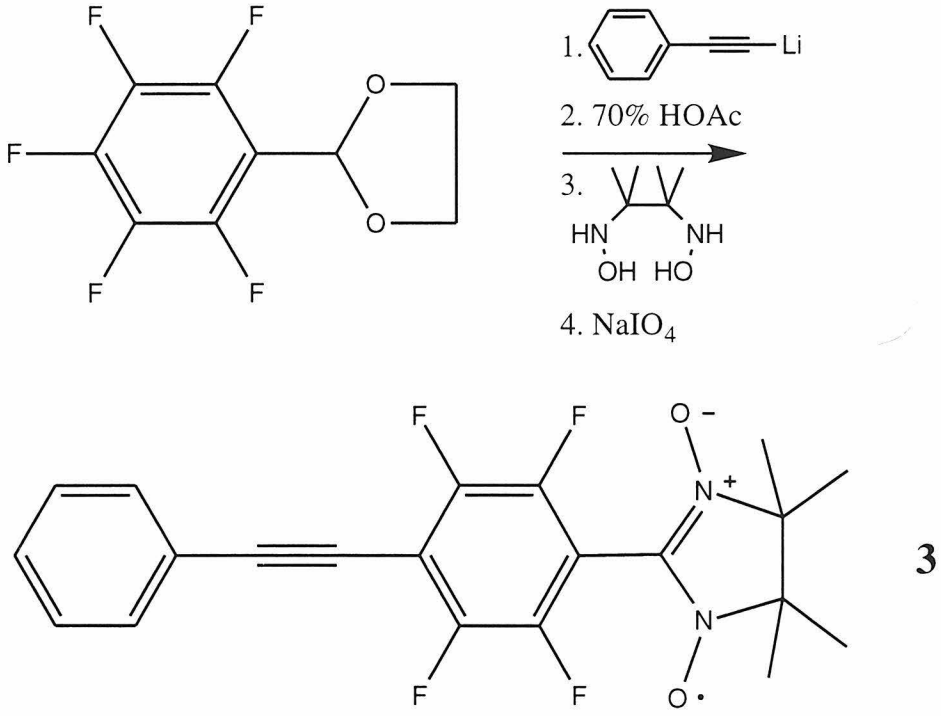

3

Scheme 2.6 - Synthesis of a diphenylacetylene nitronylnitroxide

Nitronylnitroxide (**3**), a purple compound synthesized according to Scheme 2.6, was also a weak antiferromagnet (Figure 2.5). Analysis of the x-ray structure (Structure 2.2) shows that the synthon now behaves at least partially as intended. It dimerizes in a head-to-tail fashion with unfluorinated rings stacked on fluorinated rings. The radicals are prevented from forming infinite 1-D stacks by the twist of the nitronylnitroxide unit, approximately 60° out of the plane. This extreme twisting disrupts both the 1-D network and the delocalization of spin density out onto the aromatic synthons.

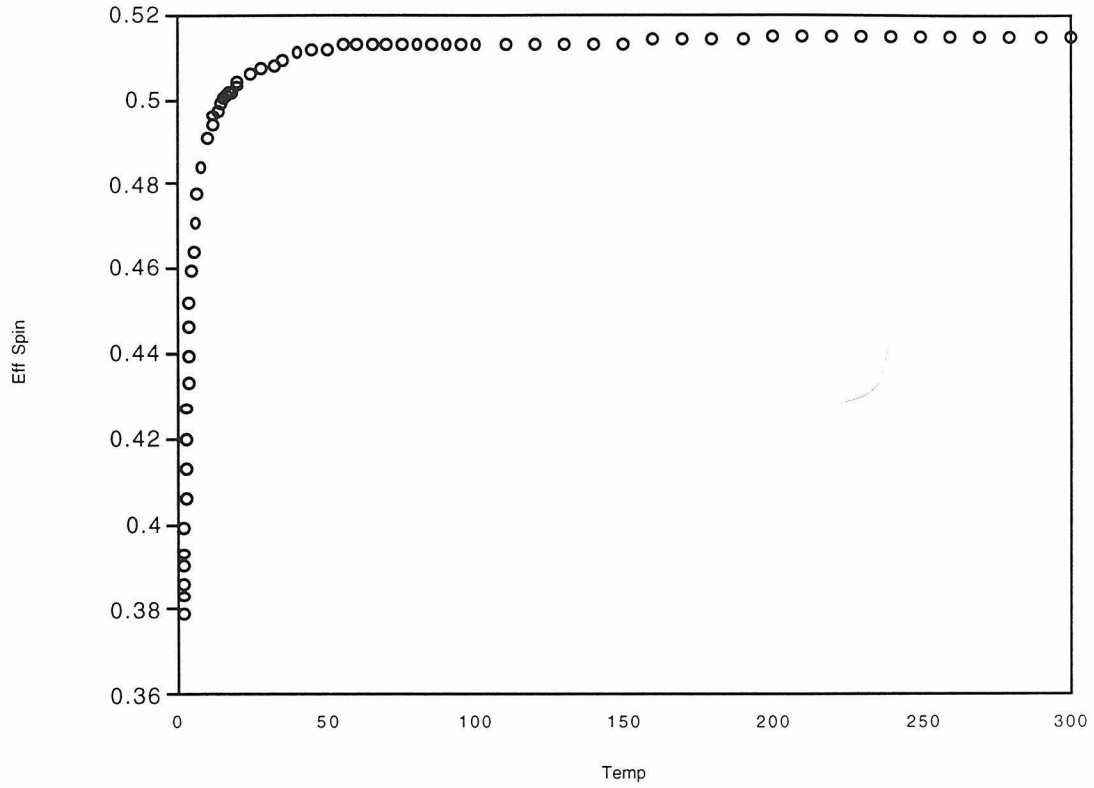

Figure 2.5 - Variable temperature plot[22] of 3 reveals weak antiferromagnetic behavior.

The steric bulk of the twisted nitronylnitroxide prevents the rings from lining up in a direct face-to-face fashion. In this case, atoms of the unfluorinated ring are often situated near the center of a carbon-carbon bond of its fluorinated partner. Because the antiferromagnetic interactions are much stronger than the ferromagnetic ones, this slippage will likely result in antiferromagnetic dimers. There is no need to invoke such an effect to explain the magnetic data; the weak downturn is consistant with nearest neighbor O-O contacts of 6.22Å.

This was a minor success. Future structures were designed with a planar spacer in between the synthons and the nitronylnitroxide unit in order to allow the entire molecule to remain in the same plane.

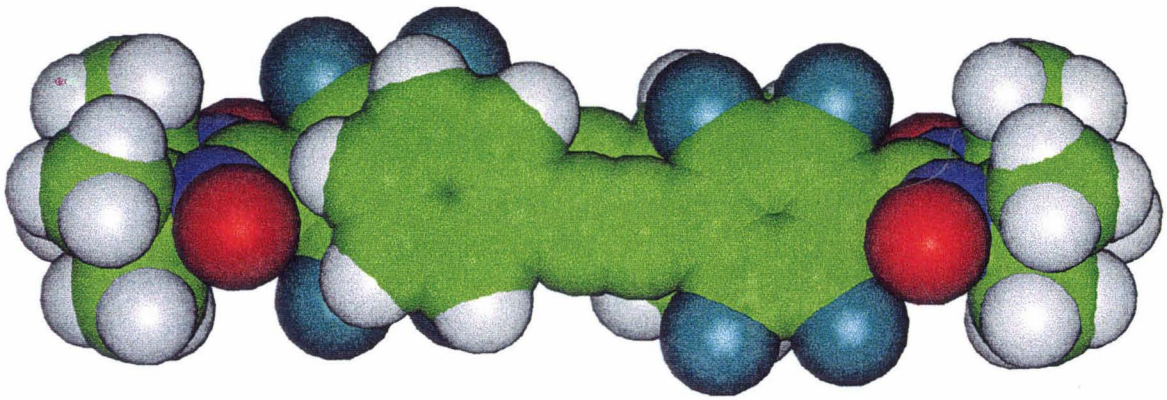

Structure 2.2 - Structure of an diphenylacetylene nitronylnitroxide looking directly down the b axis (other molecules removed for clarity). Face-to-face dimers form, but they do not precisely overlap.

Acetylenic and vinylic spacers between the synthon and the nitronylnitroxide

Acetylenic groups were the preferred target for spacers between the synthons and the radical because they would preserve the mirror symmetry of the molecule, and thus presumably lead to simpler, less disordered crystal structures. Several attempts were made to

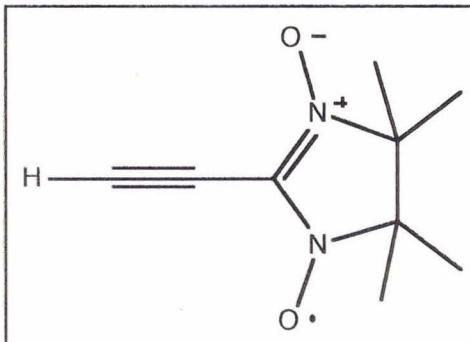

Figure 2.6 - Ethynylnitronylnitroxide

synthesize nitronylnitroxides with acetylenic groups directly attatched to the radical. The literature has one report of a successful synthesis of a red, unstable material thought to be the ethynylnitronylnitroxide shown in Figure 2.6[23]. Experiments designed to create nitronylnitroxide **4** (Scheme 2.7a) using standard oxidizing conditions resulted in a fleeting blue color (a color characteristic of previous nitronylnitroxide radicals) followed by decomposition. Oxidation with less than a stoichiometric amount of chloranil, followed immediately by chromatography, allowed isolation of a blue compound in extremely low yield. Magnetic characterization of the compound showed no moment at low temperature, and, given the small amount of sample isolated, it was not pursued further.

The fluorinated nitronylnitroxide **5** (Scheme 2.7b) was synthesized with the hopes that the electron-withdrawing nature of the fluorinated ring would make the acetylnic unit more stable to oxidation. Addition of the protected propargyl alcohol to hexafluorobenzene proceeds in low yield; the initial reaction activates the molecule for further additions, and the disubstituted products predominate. Oxidation by PCC affords the desired aldehyde.[24] Condensation with the bis(hydroxylamine) to make the nitronylnitroxide precursor was unsuccessful, however, and the radical could not be obtained.

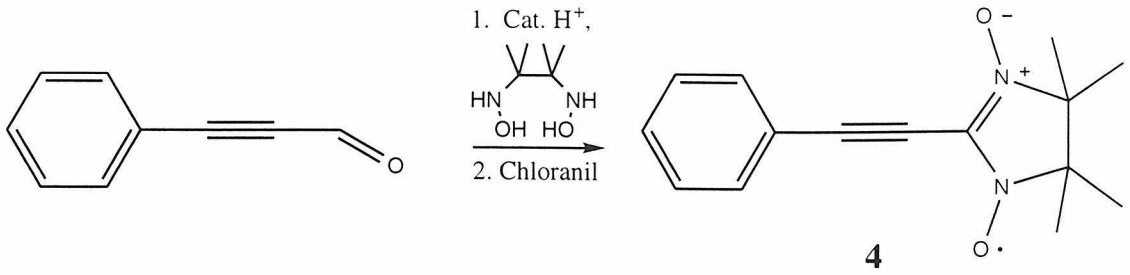

4

a)

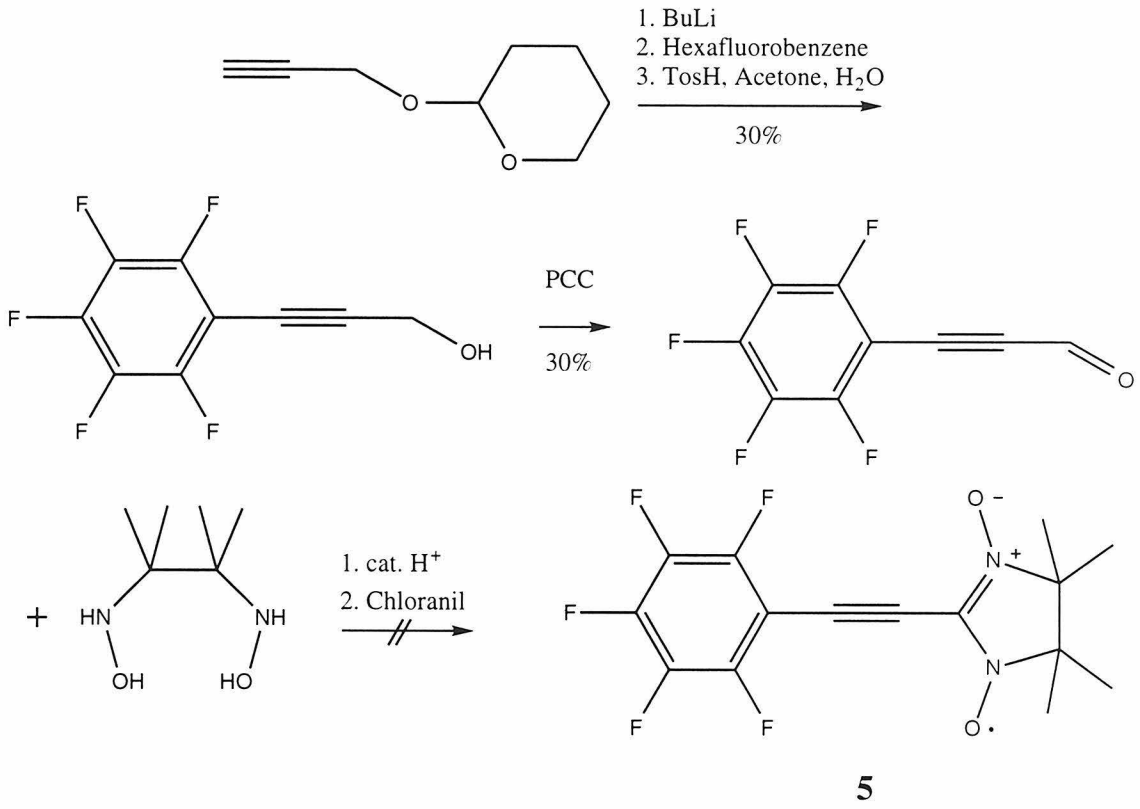

5

b)

Scheme 2.7 - a) Synthesis of phneylethylnylnitronylnitroxide; b) Synthesis of pentafluorophenylethynylnitronylnitroxide

Since vinylic spacers have been shown in the literature to be easily synthesized[25], the previously described strategies were repeated, with this group separating the synthon from the radical.

Phenyl-vinyl-nitronylnitroxide mixed with pentafluorophenyl-vinyl-nitronylnitroxide

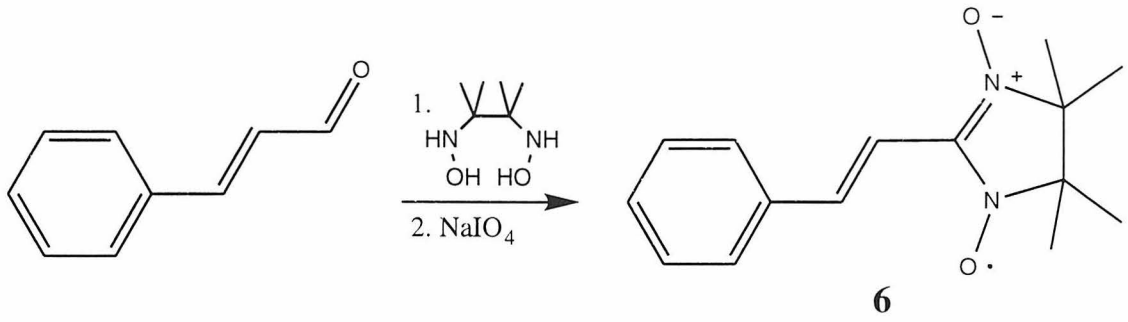

6

a)

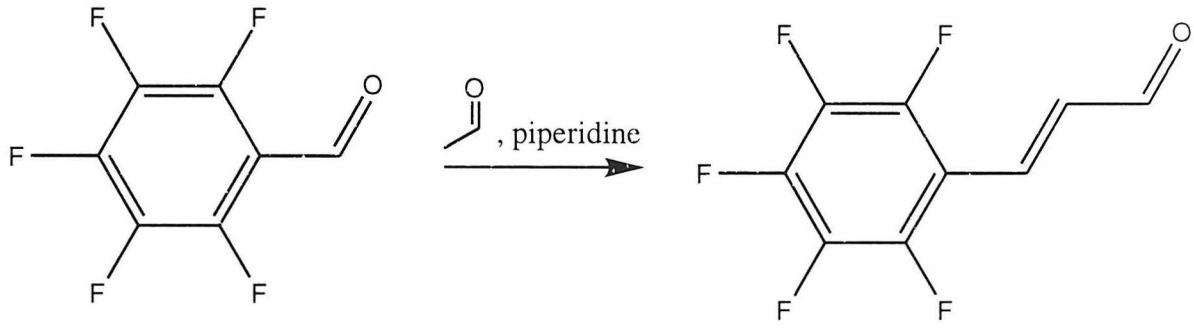

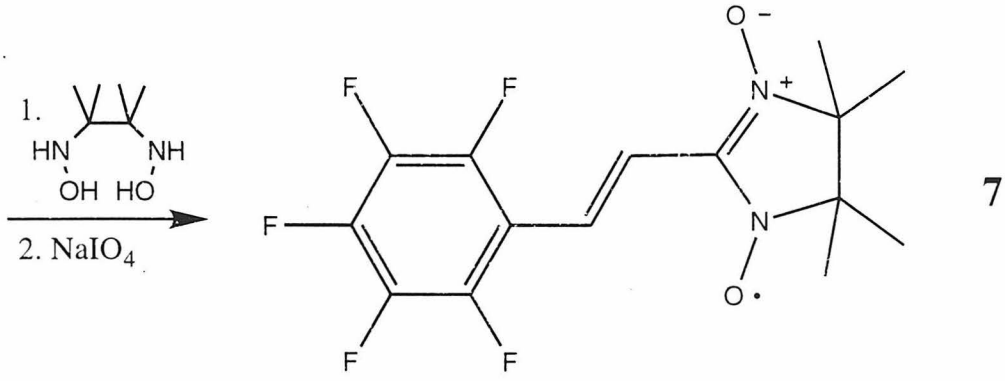

7

b)

Scheme 2.8 - Synthesis of vinylnitronylnitroxides: a) radical (6), cinnemaldehyde nitronylnitroxide. b) radical (7), pentafluorocinnemaldehyde nitronylnitroxide.

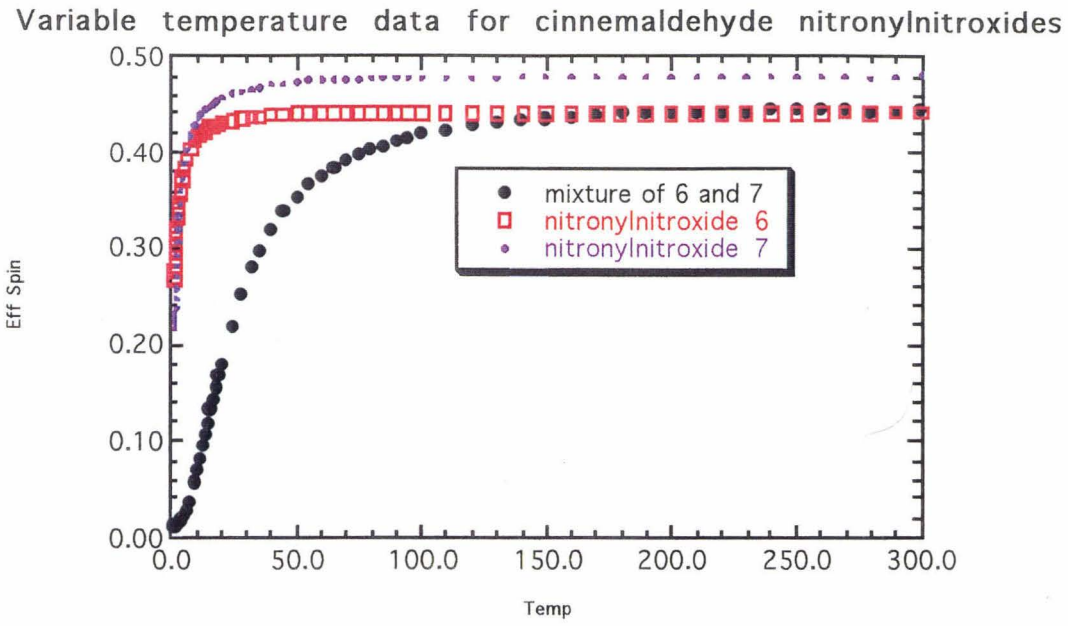

Figure 2.7 - Variable temperature SQUID measurements[22] from (6), (7), and the mixture of the two. Each is S=1/2 at room temperature; impurities in (6) lower the calculated value slightly. The antiferromagnetic interactions in the mixture are far stronger than in either of the two starting materials. This arises from an unusually short, 3.38Å distance between nitronylnitroxide oxygens.

Nitronylnitroxides 6 and 7 were isolated as green solids and magnetically characterized. A 1:1 mixture resulted in a solid with a dramatically stronger antiferromagnetic interaction than either starting material, as shown in Figure 2.7.

The mixed crystal, shown in Structure 2.3, is a disordered 38:62 mixture of 6:7. The radical 6 is unstable in solution and likely decomposed to give a supernatant liquid with components in this ratio. Crystallographic analysis of 7 shows that the structure is indeed different from that of the mixed crystal.

No analysis of the structure of **6** was made because of the instability of the material, and no further attempt was made to explore the ratios that might bound the stability of this mixed crystal phase.

The structure of this mixed system is not as would be predicted based on the synthon. Space-filling considerations overwhelm the predicted electronic ones, since the aromatic groups slide under the vinyllic groups instead of pairing. The strong antiferromagnetic interactions result from unusally close contact between nitronylnitroxide oxygens of 3.30Å. By comparison, the oxygen-oxygen distance in **6** is 4.75Å, and the interaction is as a result much weaker.

The variation in the electronics in this mixed system clearly favors a new crystal phase that is likely alternating for a true 1:1 ratio. However, the isosteric nature of the components allows one to easily fill the other's slot, and is a good recipe for disorder. It is possible that this concern may extend to other systems involving this synthon.

The vinyl group, however, performed as expected. The dihedral angle between the nitronylnitroxide and this spacer is 3°C, and that between the spacer and the fluorinated biphenyl also 3°C.

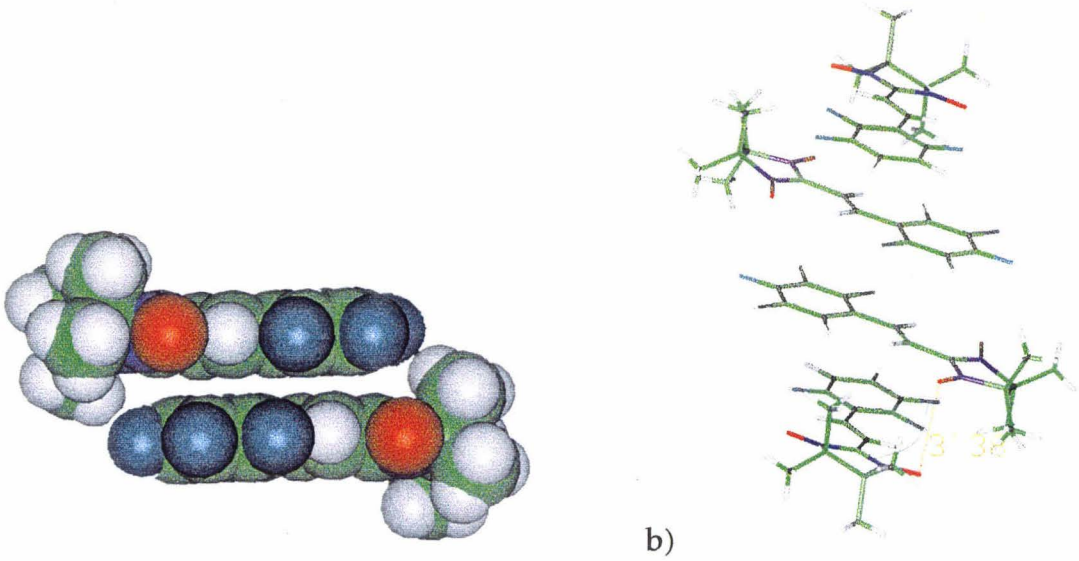

a) b)

Structure 2.3 - Disordered mixed crystal of phenylvinyl- and pentafluorophenylvinyl- nitronylnitroxides. The radicals (shown only as pentafluorophenyls here) stack face-to-face as dimers, shown in a). The oxygen atoms (red) on two perpendicular radicals are only 3.30Å apart.

Biphenyl-vinyl nitronylnitroxide

Nitronylnitroxide **8** (Scheme 2.9) was synthesized by expanding on the tetrafluorobiphenyl aldehyde used as a precursor to **1**. It was isolated as a green solid and displayed moderately strong antiferromagnetism (Figure 2.8). This strong coupling likely results from O-O close contacts of 3.66Å.

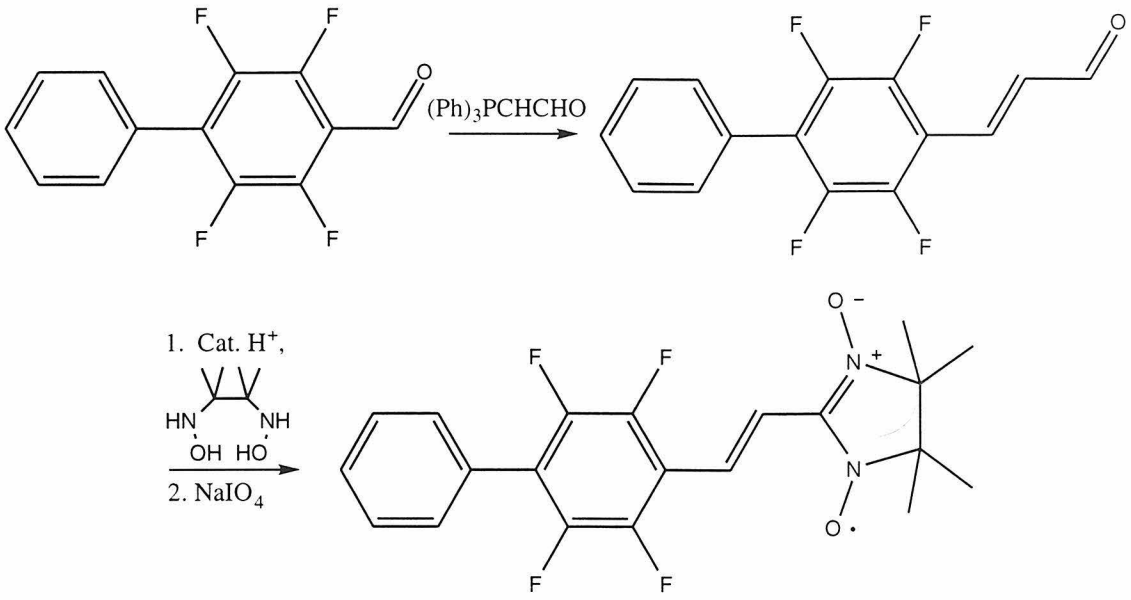

8

Scheme 2.9 - Synthesis of a biphenylvinyl nitronylnitroxide.

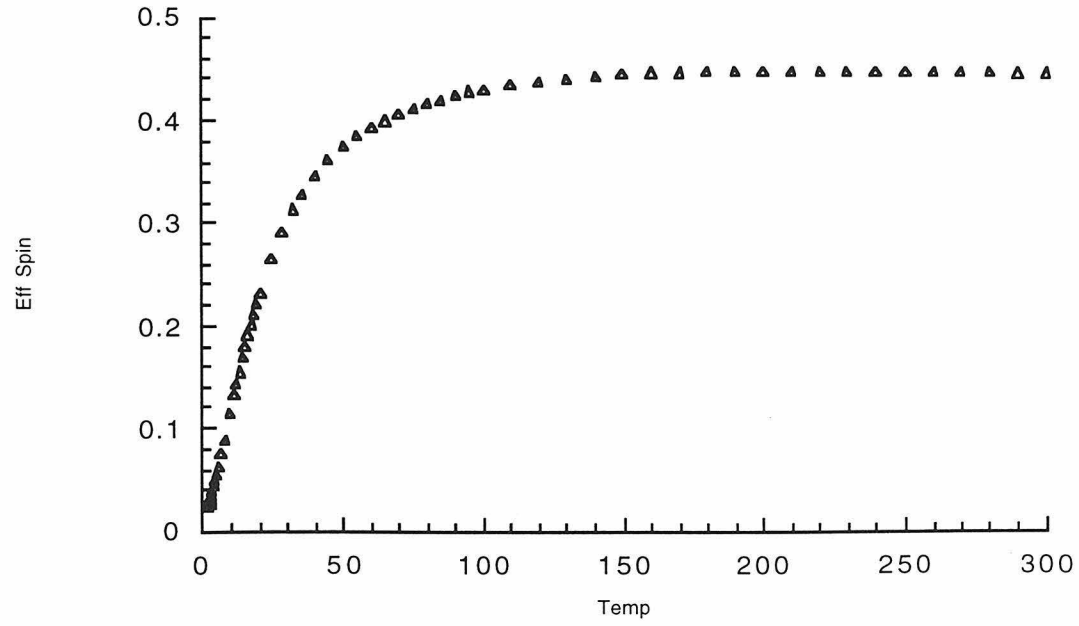

Figure 2.8 - Variable temperature plot[22] for nitronynitroxide 8.

The structure (Structure 2.4) shows no influence of the synthon, with crystal packing considerations dominating this system as they did in Structure 2.3 above. The nitronylnitroxide ring and vinyl spacer are essentially planar (1° dihedral), though the fluorinated ring is twisted 16° out of this plane. The two phenyl rings are twisted 45° from each other.

The structure shows 1-D stacks throughout, as shown in Structure 2.4. Unlike in other of the 1-D systems, the molecules in the stacks are not coplanar.

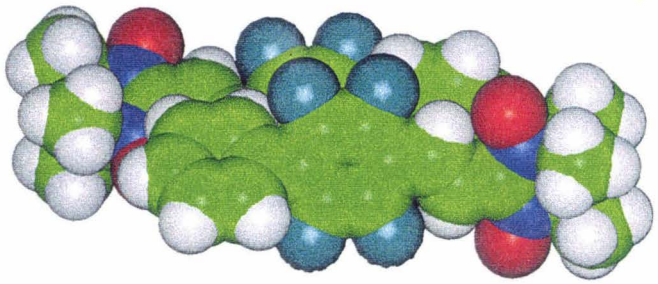

a)

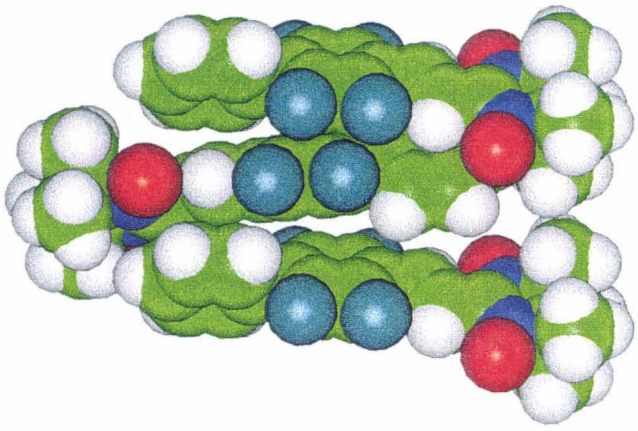

b)

Structure 2.4 - Structure of a biphenylvinyl nitronylnitroxide. a) The packing shows no influence of the synthon, with fluorinated rings slip-stacked over other fluorinated rings. b) The twisting of the rings causes the molecules to intercalate into stacks at odd angles.

The ring twist between the two phenyl rings is limiting the strength of the association of the synthons. Systems with acetylenic spacers between the phenyl rings dimerize at minimum in all the systems studied so far, but any perturbation seems to disrupt stacking in biphenyls. Biphenyls are thus rejected as potential synthons for this sytems.

Diphenylacetylene-vinyl-nitronylnitroxide (DVN)

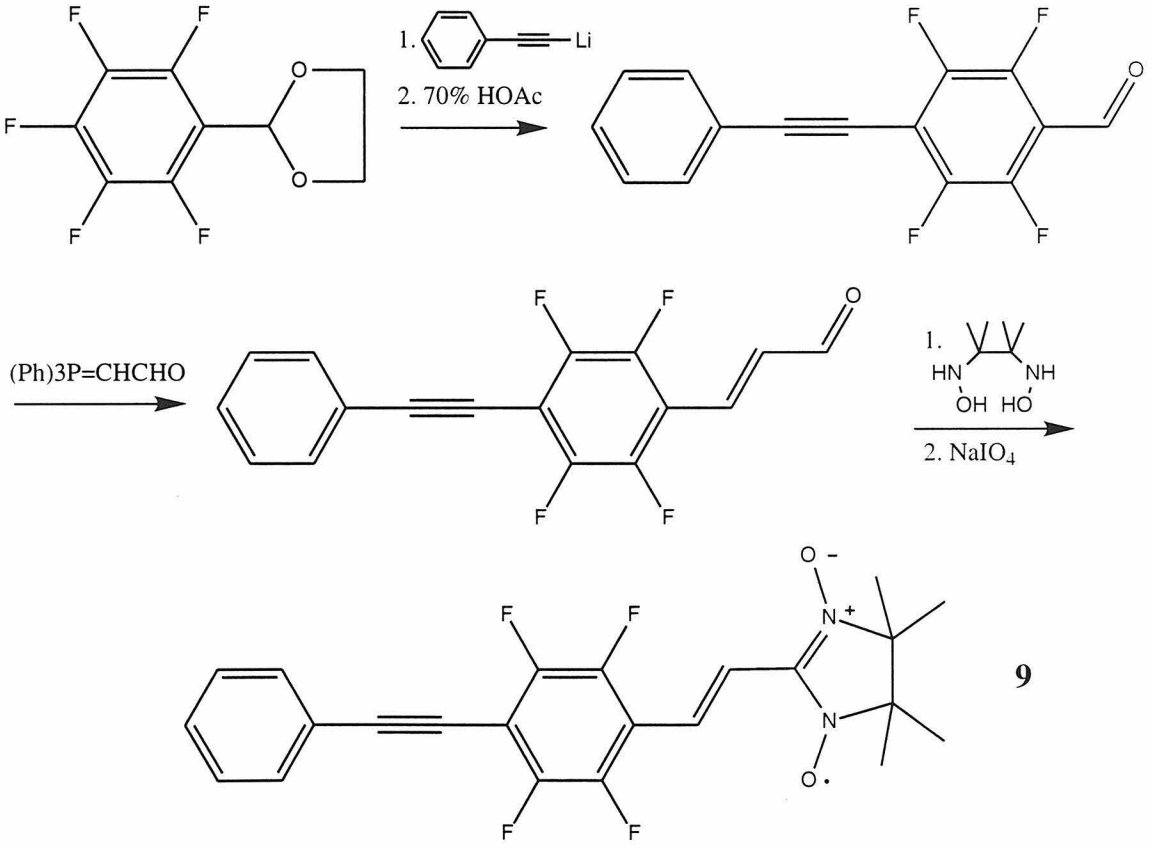

9

Scheme 2.10 - Synthesis of DVN (9)

The cinnemaldehyde precursor to nitronylnitroxide **9** was crystallized in order to examine the effects of this substituent on the directing ability of

the synthon. Previous investigations of 1-pentafluorophenyl-2-phenylacetylene had seen essentially face-to-face stacking.[15] Perturbation of this symmetry by addition of the cinnemaldehyde results in a structure where the rings are shifted by about one bond length relative to their predicted positions.

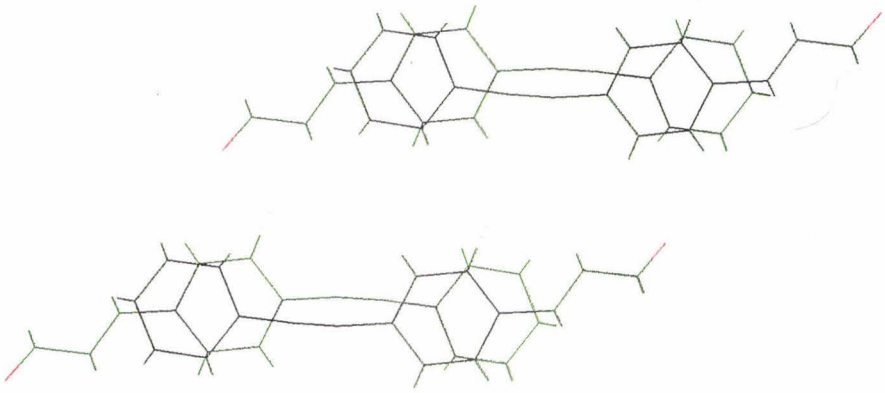

a)

b)

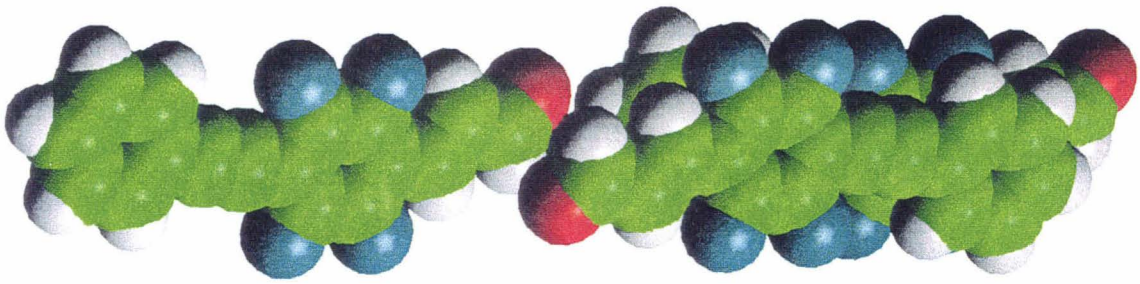

Figure 2.9 - 1-(1-Carboxyvinyl-2,3,5,6-tetrafluorophenyl)-2-phenylacetylene. a) The non-fluorinated rings are slipped slightly from their intended positions. b) The C-O bonds align in the crystal to oppose their dipoles.

This is not surprising given the nature of the interaction. The vinyl group, linked directly to an electron-withdrawing ring and an aldehyde, is expected to be electrostatically similar to the fluorinated ring. As a result, sliding the unfluorinated ring slightly atop it is not expected to have a large

energetic cost. This type of sliding interaction may be pernicious to a system such as this that requires direct alignment of the two rings.

Nitronylnitroxide **9** (Scheme 2.10) was isolated as a green solid. Because void space is anticipated underneath the vinyl groups for the target packing, the molecule was isolated by evaporation from fifteen different organic solvents, and three polymorphs were identified as determined by variations in melting point and magnetic behavior (shown in Figure 2.10). The highest melting polymorph was isolated from methylcyclohexane, methanol, acetone, toluene, benzene, DMF, and acetonitrile, and melted at 186°C. A polymorph melting at 163°C was isolated from chloroform, methylene chloride, and *cis*- and *trans*-dichloroethylene. The lowest melting polymorph, from THF, metled at 144°C, though some samples melted in a range from 144° to 163°C. The sample decomposed in nitromethane and acetic aid. The magnetic data of the two lower melting polymorphs is nearly identical, and they may represent the same crystal phase at low temperature. Based on the molecular weight calculated from an assumption of spin=0.5 behavior at room temperature in the variable temperature data, it did not appear that solvent was included in any of these systems.

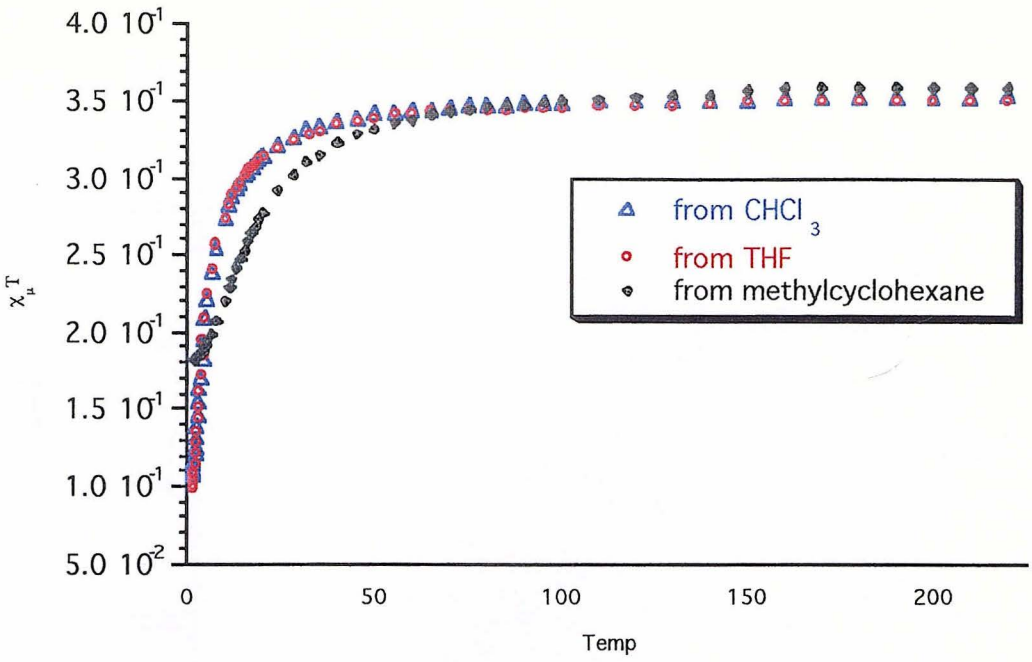

Figure 2.10 - Variable temperature data from 3 polymorphs of 9. The polymorph from methycyclohexane loses almost exactly half of its χT by 1.8K.

The magnetic data from the system isolated from methycyclohexane is extremely unusual. The variable temperature data levels off at $\chi_m T$=1.81 at 1.8K, almost exactly half its room temperature value of $\chi_m T$=3.59 (Figure 2.11). This could be explained by a system with two J's: one large J corresponding to the downturn and linking half of the radicals in the system, the other J near zero. In such a system, half of the radicals would be paired at low temperature, the other half still non-communicating; the net result would be a plot as seen.

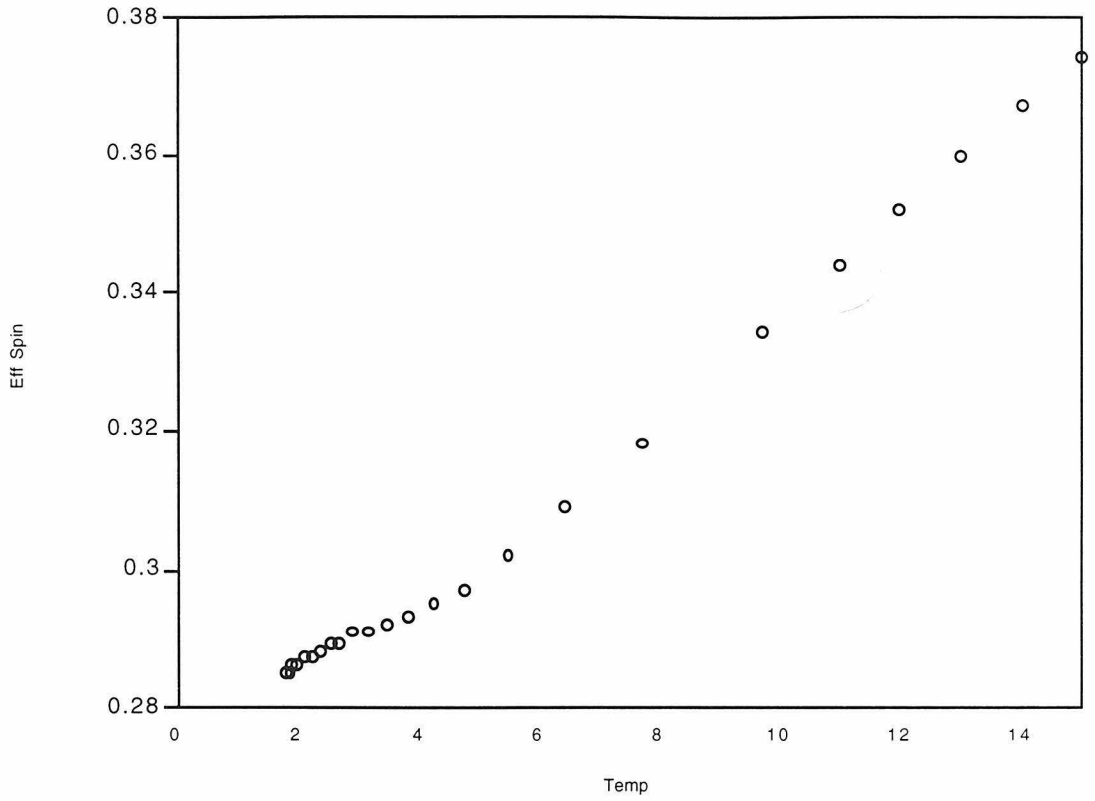

Figure 2.11 - At low temperatures, the methylcyclohexane-derived sample of nitronylnitroxide 9 shows an inflection, and approaches 1/2 the original value of $\chi_m T$. [22]

The saturation plot also behaves in a way not seen for other nitronylnitroxides. The Brouillan fit finds a high spin state, S=1.25, which may be indicative of ferromagnetic interactions between the monomers at low temperature. The material does not behave in an ideal fashion, however. There is a very large linear component to the data (represented as m3 in Figure 2.12 below) that it is indicitave of a linear chain Heisenberg antiferromagnet, and this is consistant with the variable temperature data. If

ferromagnetic interactions exist, they are competing with antiferromagnetic ones. Furthermore, at 5.5 Tesla, only 40% of the expected spin is seen; the rest is assumed to be antiferromagnetically coupled to its neighbors. This behavior complicates interpretation of the data, so that, while it is evocative of higher spin behavior, this cannot be rigorously concluded.

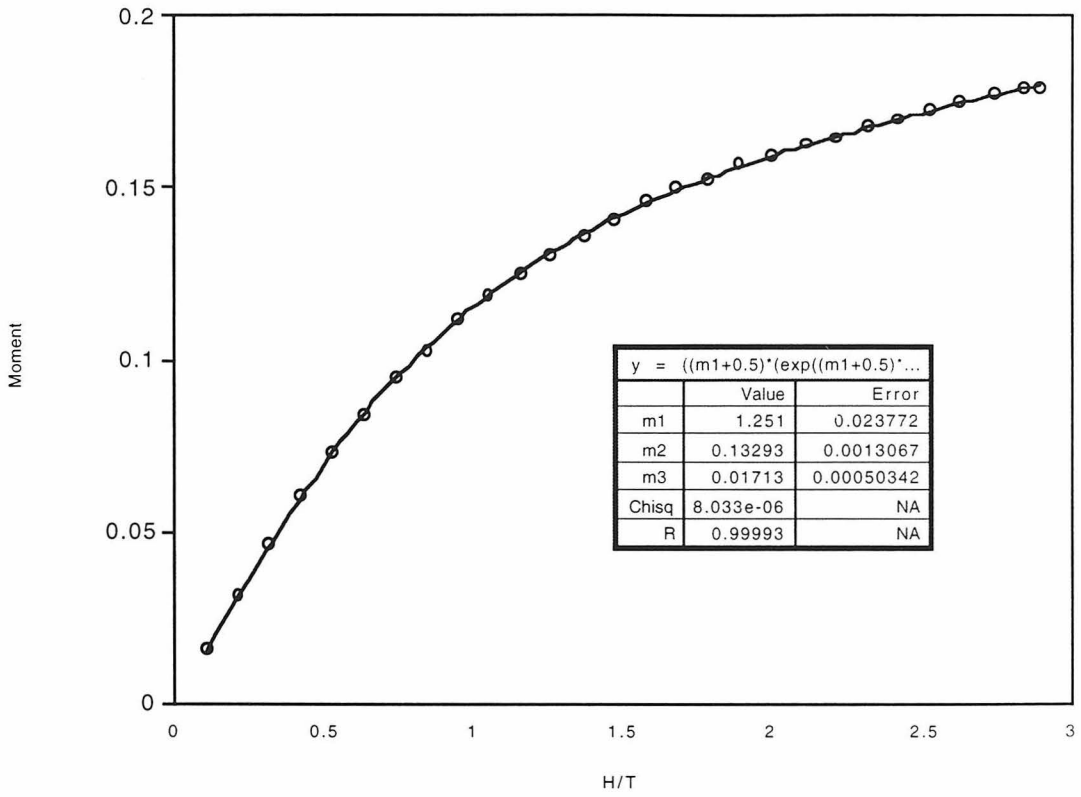

Figure 2.12 - A saturation curve for nitronylnitroxide 9, isolated from methylcyclohexane. The curve is fit to S=1.25. The other two polymorphs of 9 show a linear response to an applied field, indicative of a standard linear chain Heisenberg antiferromagnet.

The crystal structure of the methylcyclohexane system is shown below. There is considerable disorder about the vinyl group, which extends to the nitronylnitroxide oxygens and the two fluorines closest to the vinyl group (Structure 2.5). This complicates any interpretation of the magnetic data that relies on knowledge of the O-O nearest neighbor contacts. The shortest contacts in the solved structure are 3.75Å, and based on the thermal displacement parameters this should vary maximally by about eight tenths of an angstrom. There is very little disorder in the acetylene, the unfluorinated phenyl group, and the four methyls at the nitronylnitroxide.

The 1-D stacks that form do not follow the predicted associations for the synthon. Instead, the molecules are slipped slightly by the need to accomodate the disordered vinyl unit to form the intercalated structure, and no ferromagnetic interaction is promulgated by this pathway.

The extremely short, 3.58Å to 4.01Å (variable distances due to the disorder) intermolecular O-O distance that extends up the stack should couple the systems strongly antiferromagnetically. This is likely responsible for the turndown at relatively high temperatures.

Of equal interest, however, is an even shorter, 3.19Å to 3.34Å C-O contact that also extends up the 1-D stacks. Because the carbon atoms are polarized oppositely from the oxygens in nitronylnitroxide units, should result in a *ferromagnetic* interaction.

It is not clear whether the competition between these two forces is responsible for the unusual magnetic behavior, and further study will be required.

Finally, it should be emphasized that the structure below was solved at 85K, and may not represent the material in the 1-4K region that is under discussion.

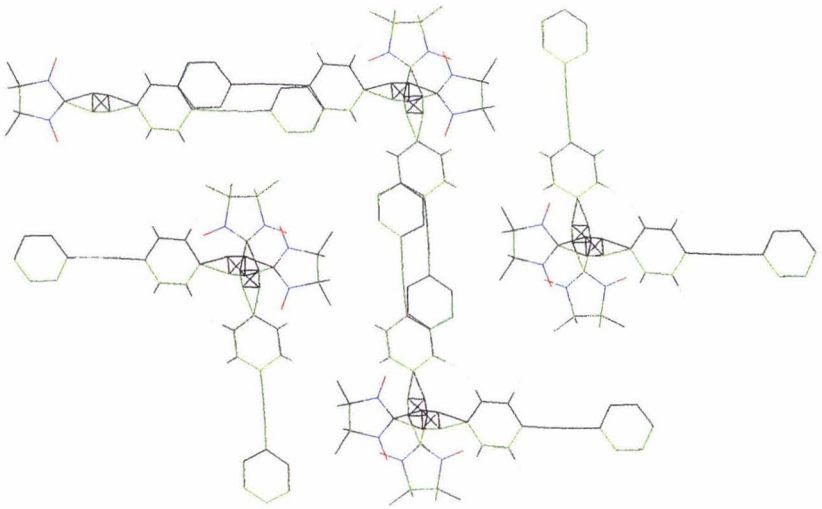

Structure 2.5 - Structure of nitronylnitroxide 9 from methylcyclohexane. The disordered molecules form slipped 1-D stacks that intercalate like Lincoln Logs™. The oxygens have close contacts at the intercalation sites (overlapping red atoms above) and can strongly antiferromagnetically couple.

Further efforts focused on derivatives of this system that might fill the space underneath the vinyl groups and allow for 1-D stacks.

Propyl DVN

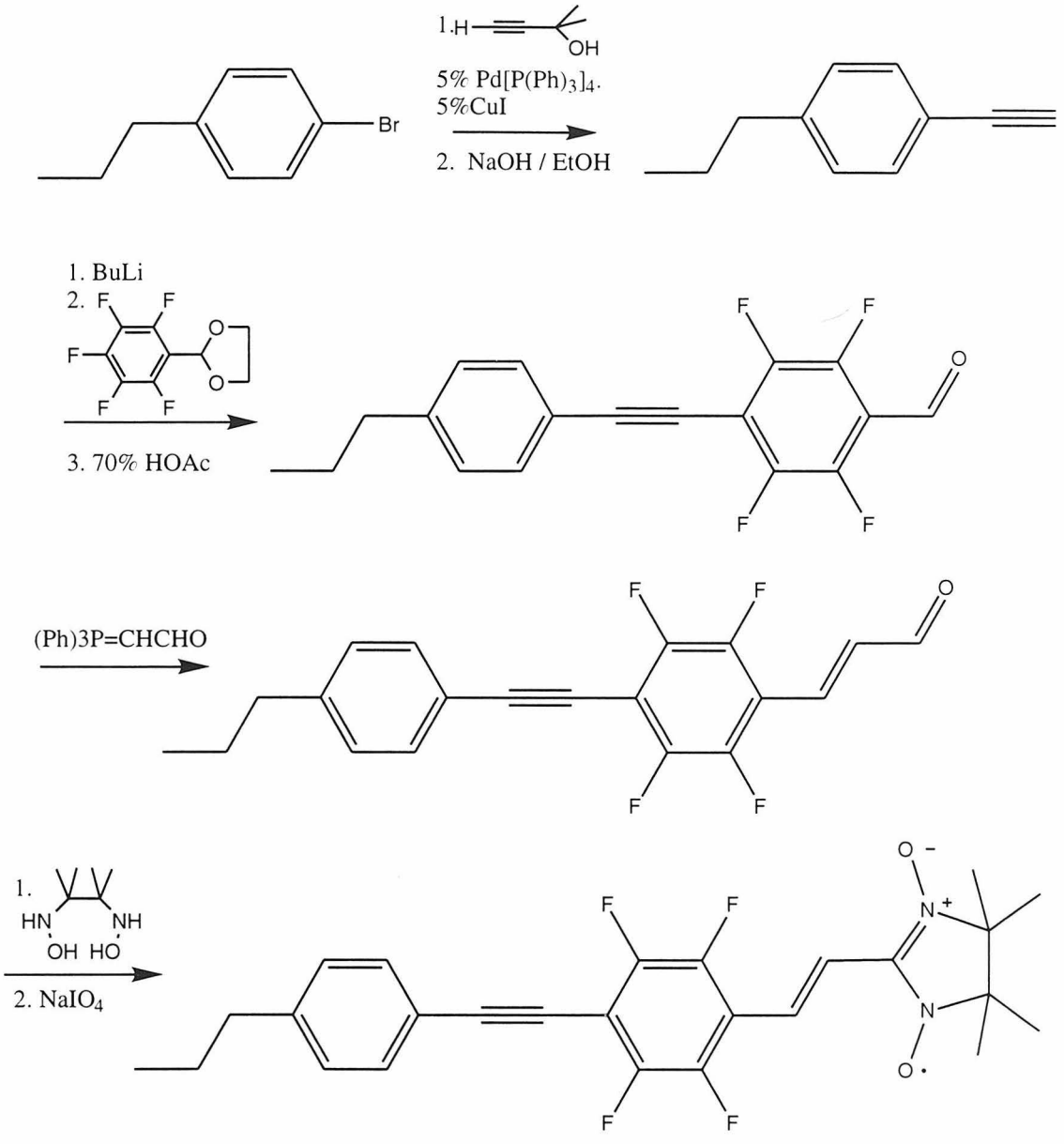

10

Scheme 2.11 - Synthsis of Propyl DVN

Nitronylnitroxide **10** was isolated as a green solid according to Scheme 2.11. This compound again displayed weak antiferromagnetism (Figure 2.7).

The crystal structure was disordered, with a phase transition near room temperature, complicating its solution. A CCD structure collected by Dr. Joe Ziller at Irvine was able to unambiguously confirm the molecule's identity, but reliable information on packing has not yet been determined.

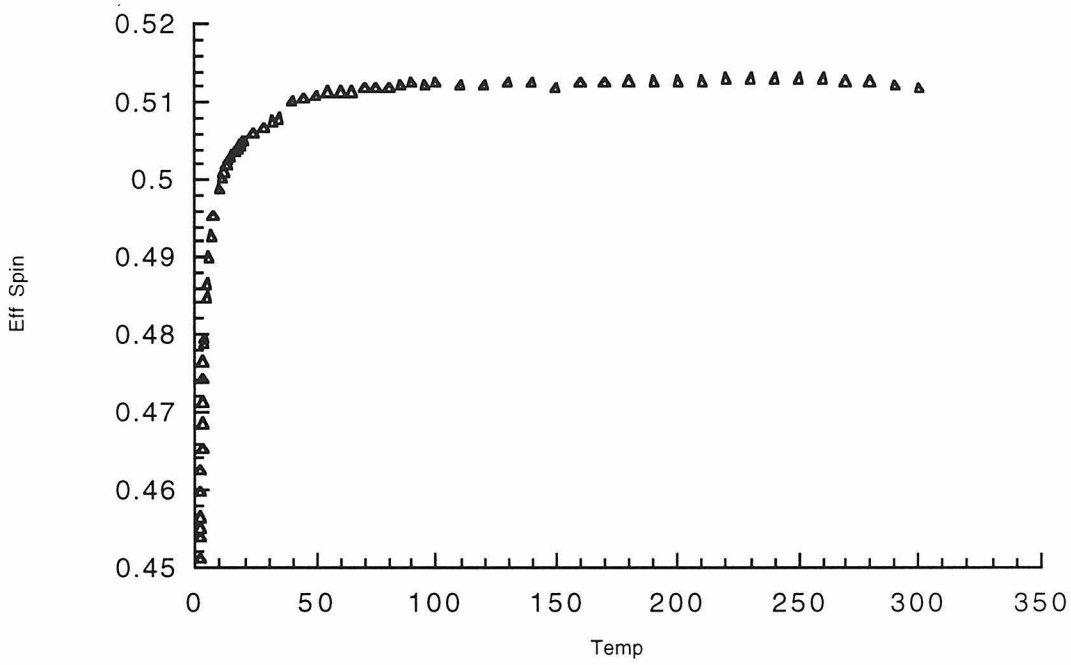

Figure 2.13 - Variable temperature data[22] for nitronylnitroxide 10.

A new synthetic strategy was developed in order to more quickly create DVN derivates that might crystallize as planned.

Convergent approach to DVNs

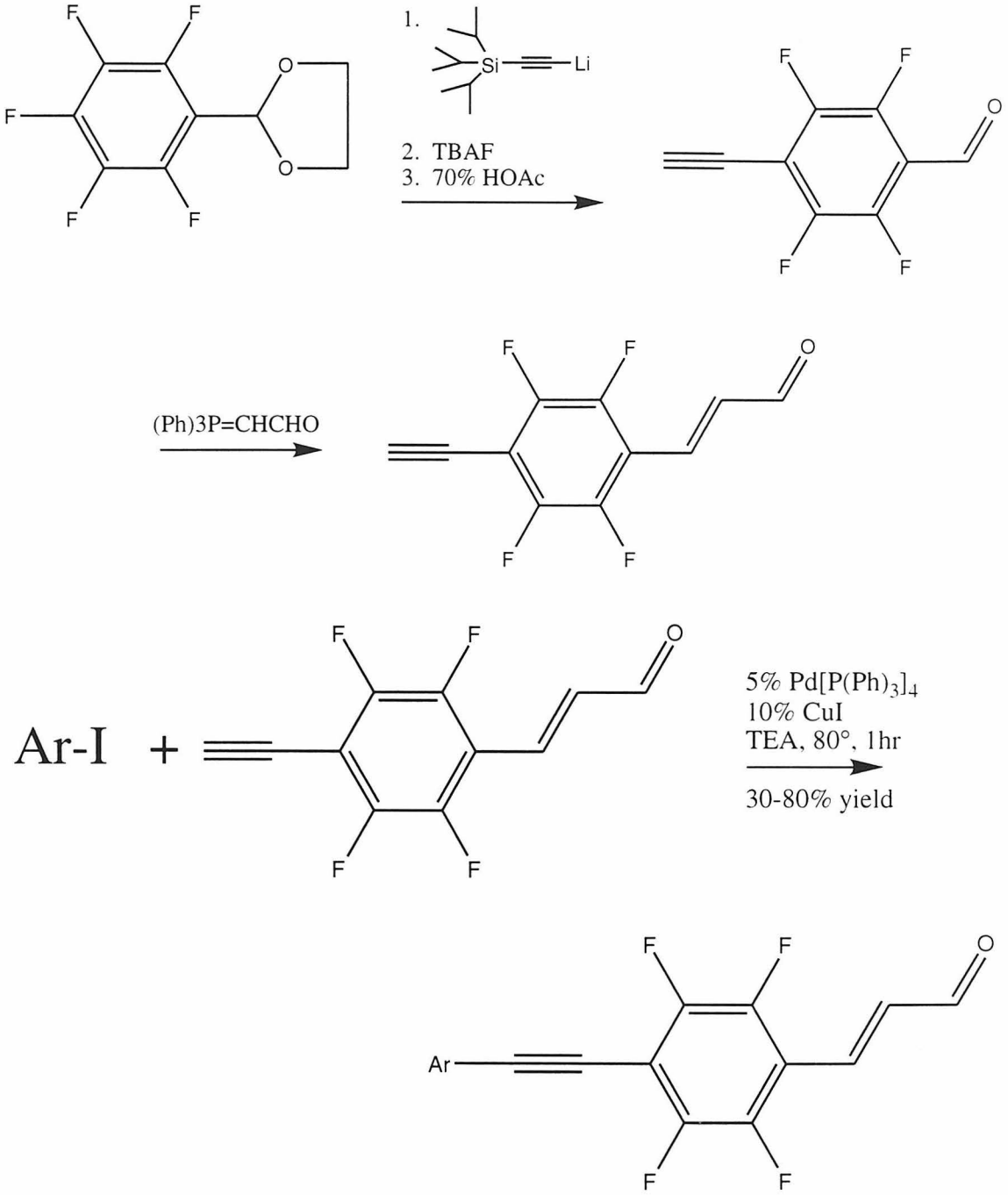

Scheme 2.12 - Synthesis of cinnamaldehydes by a convergent pathway

The approach shown in Scheme 2.12 allows for the quick formation of a variety of DVN derivatives from appropriate aryl iodides. Addition of TIPS-acetylene to protected pentafluorobenzaldehyde takes place in refluxing THF, and the product is partially deprotected by unreacted TIPS-acetyllithium to give bis(TIPS)acetylene as a biproduct. As a result, using 1.2 equivalents of TIPS-acetylene gives optimum yield of a mixture of protected and deprotected product. After workup, this crude material is dissolved in THF with several milliliters of water added and stirred for 10 minutes with TBAF to remove the remaining TIPS. This material is chromatographed, then the acetal is deprotected by heating to 90° in 70% HOAc for 24 hours. The pure material is then pumped on at 80 mtorr for 24 hours to remove any remaining TIPS-F and pentafluorobenzaldehyde that were not separated by chromatography. Condensation of this aldehyde to the cinnemaldehyde is straightforward, and the final product was purified by chromatography and stored frozen.

Higher yields of coupled product were obtained using 10% CuI instead of 5%, though this may be due to the small scale of the experiments - 5% CuI is typically less than 10mg, and this amount may adhere unreacting to the side of the flask. Aryl bromides would not couple by this pathway, and aryl triflates gave only very low (5%) yields. Six new cinnamaldehydes were synthesized by this route (Table 2.2):

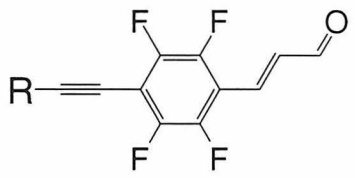

R	Cinnemaldehyde #
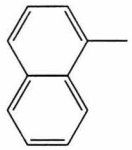	**11a**
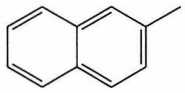	**12a**
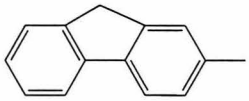	**13a**
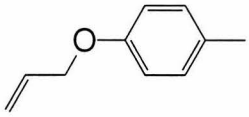	**14a**
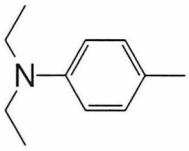	**15a**
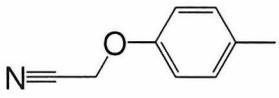	**16a**

Table 2.2 - Cinnemaldehydes synthesized through convergent route. Not all cinnemaldehydes were convertable to their nitronylnitroxides - see text below.

Radical **11** was isolated only as the imino nitroxide. It displays weak antiferromagnetic coupling (Figure 2.14). The crystal structure of the nitroxide shows 1-D stacks of radicals, slipped from their intended position

(Structure 2.6). The nearest intermolecular O-O distance is 4.45Å, which is consistant with the weak magnetic turndown.

Of interest in this structure is the 13° dihedral angle between the imino nitroxide and the vinyl spacer, with another 8° angle between the spacer and the fluorinated ring. A naphthyl group cannot slide completely under the five-membered radical ring as a result of this twisting, and there is a small amount of void space there. This is suprising, because it indicates that perhaps a substituent as small as a methyl group, rather than the propyl group or others tried, may be able to direct the synthon to the proper location. However, this dihedral twist is probably induced by crystal packing forces specific to this system, and it is not possible to ensure its presence in any other derivatives.

This arrangement does further validate the original design, as it demonstrates that the radicals can form 1-D stacks as planned. There is even some overlap between the napthyl and fluorinated rings, and this overlap should yield ferromagnetic order based on the star-nonstar rule. This effect is probably overwhelmed by other antiferromagnetic interactions.

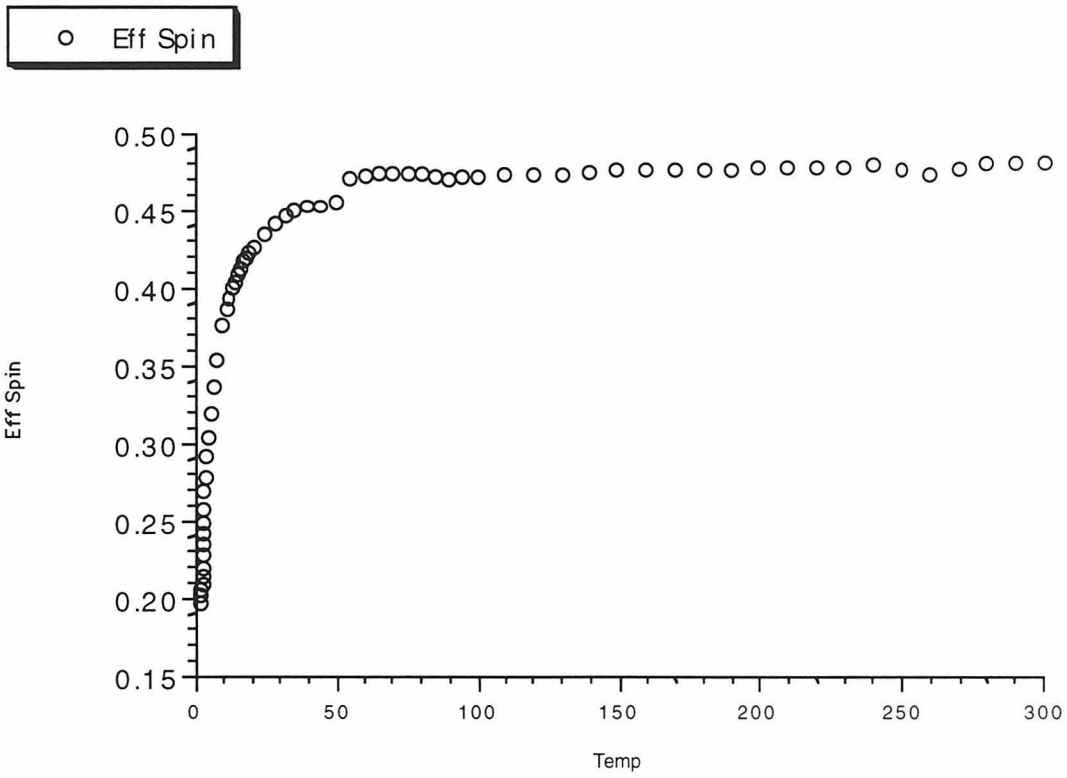

Figure 2.14 - Nitroxide (11) displays weak antiferromagnetic coupling. [22] **The discontinuity at about 50K is an instrumental error.**

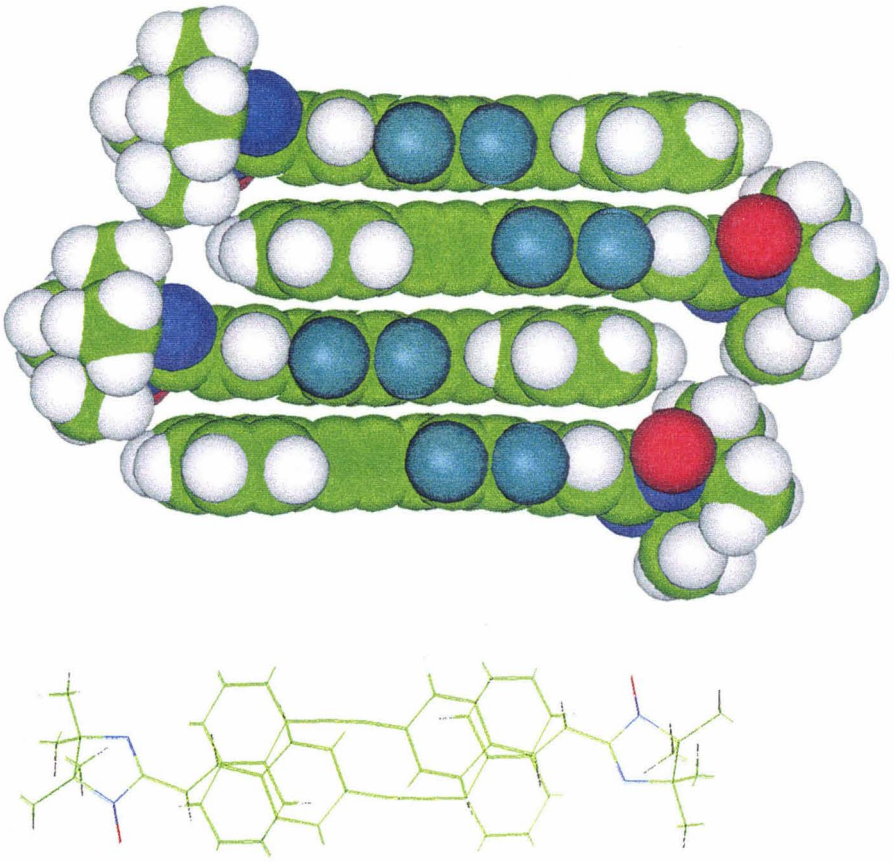

Structure 2.6 - Nitroxide (11)

Radical **12** was isolated both as the imino nitroxide and the nitronylnitroxide (as a minor product). Both systems displayed antiferromagnetic coupling.[22] Crystals suitable for data collection could not be grown from either system.

Radical **13** was also isolated as the imino nitroxide and the nitronylnitroxide, and both were antiferromagnetic.[22] Again, crystals suitable for data collection could not be grown.

Radical **14** was isolated as the imino nitroxide and nitronylnitroxide, and again, both were antiferromagnetic. The nitronylnitroxide displayed similar crystal habit to **10**. Attempts to obtain a low-temperature solution of the system failed because of a phase transition in the crystal just below room temperature. The high temperature structure is disordered and is still in the process of being refined.

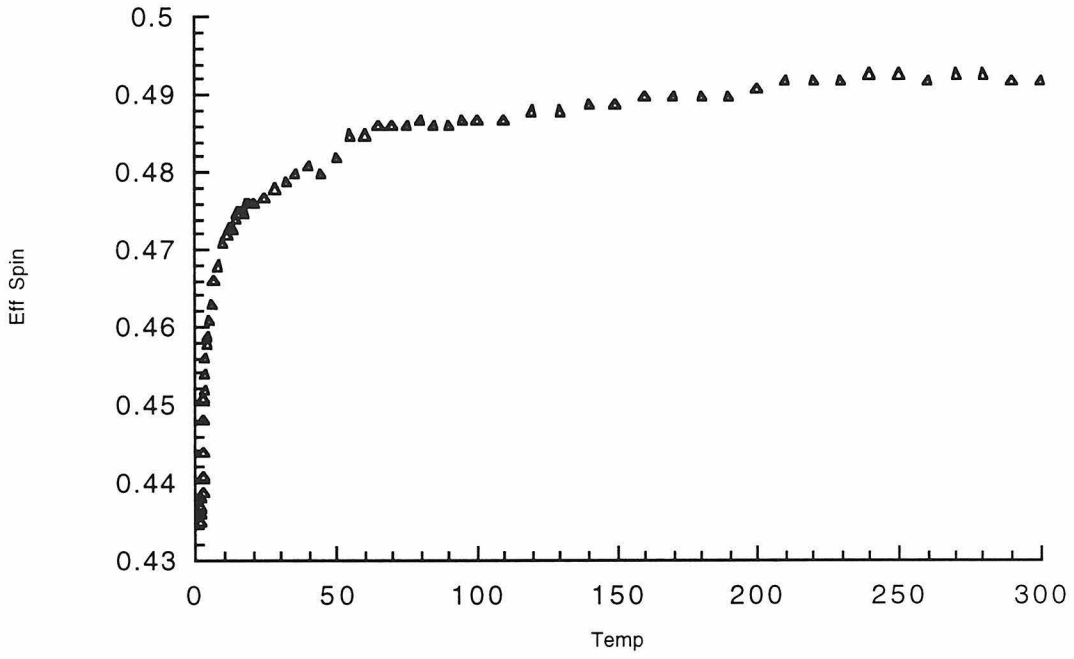

Figure 2.15 - Nitronylnitroxide (14) is weakly antiferromagnetic.

Radical **15** cannot be formed with $NaIO_4$, as it will oxidize the dimethyl aniline unit. PbO_2, another traditional oxidant for nitronylnitroxides, did not give product that could be isolated. Nickel peroxide, silver oxide, Fremy's

salt, and DDQ all lead to obvious decomposition of the product. Chloranil, which has a potential near that of PbO_2 and significantly lower than dimethylaniline was used as the oxidant. A solution of the nitronylnitroxide precursor and chloranil are stirred in chloroform solution for 45 minutes, then poured directly onto a silica column to separate the components. No green nitronylnitroxide was formed at any point in this reaction. No product could be isolated that corresponded to the red imino nitroxide

Cinnemaldehyde **15a** reacted with the hydroxylamine precursor at its cyano position as well as at the aldehyde, and could not be converted to the nitronylnitroxide.

Conclusions

The benzene-hexafluorobenzene macromolecular synthon was tested for its ability to align organic radicals, with the hope of creating an interesting magnetic material. The use of one interaction per molecule, or the use of biphenyls, failed to organize the systems in the desired structure.

Molecules containing two synthons separated by an acetylene successfully organized the molecules. These structures ranged from face-to-face dimers to slipped stacks of radicals in one dimension. The slippage was not predicted and seriously compromises attempts to organize radicals to form a magnet. The positioning of a fluorine atom over an aromatic ring, which should be electrostatically unfavorable, does not appear to significantly destabilize these structures. In one case, for nitronylnitroxide **9**, the slippage

was seredipidously beneficial, and produced a material that should couple ferromagnetically in 1-D stacks.

A vinyl group was used as a conjugated spacer to keep the nitronylnitroxide unit planar with its aromatic substituents. Disorder about this group complicated solution of the crystal structures. Disorder about the vinyl group, combined with disorder about flexible substituents elsewhere on the molecule, lead to systems that were isolable as large crystals but whose structures were not soluble.

Nitronylnitroxides were studied in depth for this work. Synthesis of imino nitroxides were attempted but, with one exception, these materials would not form large crystals for further study. The inability to form crystals of some of the nitronylnitroxides, particularly the 2-napthyl derivative, were especially disappointing. These materials often formed very long, very thin crystals, and this may be one drawback of trying to crystallize materials that form 1-D stacks.

The most interesting data came from nitronylnitroxide **9**, and this system is still not completely understood. Single crystal or very low temperature experiments may be necessary to test for the presence of ferromagnetic interactions.

Continuation of this project with more derivatives may yet yield a magnet. In particular, methyl-DVN, or derivatives of **12** seem promising candidates for elaboration.

Experimental Procedures

2,3-Bis(hydroxyamino)-2,3,-dimethylbutane (BHD) is obtained from the sulfuric acid salt (practical grade, purchased from Acros Organics). The salt (5.0g) is suspended in 10mL water and sonicated. Small scoops of anhydrous potassium carbonate are added and the solution stirred until the evolution of gas has ceased. Additional potassium carbonate is added until all the water is absorbed into a hard paste. The paste is extracted overnight with dichloromethane, and the dichloromethane is evaporated until only a few milliters remains. (Care must be taken at this step, because the product is volitile and will sublime into a rotory evaporator.) Petroleum ether is added to the dichloromethane solution and a white powder precipitates. This powder is collected by filtration (1.2g, yield may vary) and stored in a dessicator. The powder should be used as soon as possible after its synthesis.

General procedure for the synthesis of nitronylnitroxides and imino nitrixodes. The appropriate aldehyde or cinnemaldehyde is dissolved in chloroform and 1.5 equivalents BHD is added. The solution is refluxed for one hour and allowed to cool to room temperature, then added to a water solution of 1 equivalent $NaIO_4$ with several drops of acetic acid. About 5 mL of methanol is added to the biphasic system and it is stirred for 1 hour. A solution of sodium bicarbonate is used to quench the acetic acid, and the chloroform layer is separated out. Chromatography of this layer in

chloroform affords the imino nitroxide (red/orange or red/violet), which runs just above the nitronylnitroxide (blue, purple, or green). The radicals are usually recrystallized from methanol or methylcyclohexane. Yields range from 10-40% overall from the aldehyde.

1-carboxy-2,3,5,6-tetrafluorobiphenyl (1a) Pentafluorobenzaldehyde, ethylene glycol acetal (780mg, 3.25mmol), is dissolved in 10mL THF and cooled to -78°C. 1.8M phenyllithium (2mL, 3.6mmol) is added dropwise and the solution allowed to warm to room temperature and stirred for 2 hours. After a standard workup, the product can be recrystallized from ethyl acetate to yield 430mg (44%) product; more can be recovered from the mother liquor. The *meta*-isomer can be purified from the mother liquor by column chromatography in 10% ethyl acetate in hexanes. The acetal is deprotected by heating in 75% acetic acid at 90°C overnight to yield pure aldehyde. This can be further recrystallized from hexanes to yield a colorless solid, Mp=96-98. 300 MHz ^{1}H NMR, $CDCl_3$, δ =7.50, m, 5H; 10.34, s, 1H. 75 MHz ^{13}C, $CDCl_3$, δ = 129.2, 129.4, 130.5, 130.6, 183.0 ppm. GC/MS m/z 254 (M^+, 100), 224 (30), 206 (20).

Nitronylnitroxide (1) Mp=197-200. FTIR 3056 (w), 3002 (w), 2992 (w), 2940 (w), 1655 (m), 1576 (w), 1490 (vs), 1441 (vs), 1430 (vs), 1376 (s), 1300 (w), 1220 (w), 1175 (m), 1138 (m), 986 (s), 964 (m), 923 (w), 870 (w), 850 (w), 792 (m), 756 (m), 735 (m), 708 (m), 698 (m), 648 (m), 538 (m).

1-carboxy-8,9,10,11,12-pentafluorobiphenyl (2a) 4-Bromobenzaldehyde, ethylene glycol acetal (832 mg, 3.6 mmol) is dissolved in 50 mL of THF under argon and cooled to -78°C. 1.6M butyllithium (2.3 mL, 3.6 mmoL) is added and the system is stirred 30 minutes. Hexafluorobenzene (1.5mL, 13mmol) is added all at once and the solution is stirred 10 minutes at -78°C, then allowed to warm to room temperature and stirred for three hours. After the usual workup the crude material is refluxed in acetone with a trace amount of tosylic acid in order to deprotect the acetal. The resulting material is recrystallized from hexanes to yield 401mg (41%) product. Mp = 74-76°C. 300 MHz ^{1}H NMR, $CDCl_3$, δ = 7.61, d, 2H; 8.00, d, 2H; 10.08, s, 1H. 75 MHz ^{13}C, $CDCl_3$, δ = 129.6, 130.7, 131.1, 136.3, 191.2 ppm. GC/MS m/z 271 ($M-1^+$, 100), 243 (45), 224 (33), 193 (20).

Nitronylnitroxide (2) Mp = 164-165. FTIR KBr ν = 3099 (w), 3001 (m), 2941 (m), 1649 (w), 1518 (vs), 1497 (vs), 1450 (m), 1426 (m), 1390 (s), 1364 (vs), 1315 (s), 1263 (w), 12220 (m), 1165 (w), 1132 (m), 1064 (s), 991 (vs), 854 (s), 832 (m), 782 (w), 764 (w), 716 (w), 664 (w), 629 (w), 619 (w), 542 (m), 527 (w), 458 (w).

1-(1-carboxy-2,3,5,6-tetrafluorophenyl)-2-phenylacetylene (3a) Phenylacetylene (1.6mL, 14.5mmol) is dissolved in 15mL THF and cooled to -78°C. 1.6M butyllithium (9.0mL, 14.4mmol) is added and the system allowed to warm to room temperature. Pentafluorobenzaldehyde, ethylene glycol acetal (3.47g,

14.5mmol) is added all at once and the solution is stirred overnight. After a standard workup the crude material is dissolved in a minimum of 70% acetic acid and heated at 80°C overnight. Cooling the acetic acid solution yields crystals which are washed with water and dried in vacuo. 1.32g of product are collected (33% yield). Mp=125-126. 300 MHz ^{1}H NMR, $CDCl_3$, δ =7.44, m, 3H; 7.62, dd, 2H; 10.3, s, 1H. 75 MHz ^{13}C, $CDCl_3$, δ = 74.2, 77.0, 120.7, 128.4, 130.0, 131.9, 144.7 (m), 148.1 (m), 182.0 ppm. GC/MS m/z 278 (M^+, 100), 250 (20), 230 (14), 199 (10).

Nitronylnitroxide (3) Mp=197-200. FTIR KBr ν = 2926 (w), 2218 (w), 1654 (m), 1648 *m), 1491 (vs), 1426 (s), 1377 (s), 1174 (m), 1135 (w), 1071 (w), 988 (m), 964 (w), 929 (w), 870 (w), 758 (m), 708 (w), 689 (m), 575 (w), 539 (w).

Nitronylnitroxide (6) Mp=115-120.

Pentafluorocinnemaldehyde was synthsized following a literature procedure.[26] 300 MHz ^{1}H NMR, $CDCl_3$, δ = 6.87, dd, 1H; 7.43, d, 1H; 9.65, d, 1H. 75 MHz ^{13}C, $CDCl_3$, δ = 109.3 (m), 134.8, 135.7 (m), 139.0 (m), 140.1 (m), 143.4 (m), 146.8 (m), 192.9. GC/MS m/z 222 (M^+, 100), 203 (30), 194 (85), 174 (30), 143 (87), 123 (50).

Nitronylnitroxide (7) Mp=151-153. FTIR KBr ν = 3072 (w), 2995 (w), 2934 (w), 1523 (vs), 1493 (vs), 1452 (w), 1423 (m), 1377 (m), 1326 (w), 1281 (w), 1264 (w), 1214 (w), 1170 (w), 1138 (m), 1038 (w), 1012 (m), 1002 (m), 989 (m), 972 (m), 962 (m), 934 (w), 867 (w), 791 9w), 685 (w), 668 (w), 600 (w), 567 (w), 542 (m).

Mixed crystal of (6) and (7) Mp=115-117. FTIR KBr ν = 3089 (w), 3064 (w), 2989 (m), 1524 (vs), 1505 (vs), 1453 (m), 1426 (m), 1410 (m), 1388 (m), 1376 (s), 1324 (m), 1277 (m), 1266 (w), 1216 (s), 1036 (w), 1012 (m), 1002 (m), 976 (s), 962 (w), 936 (w), 866 (w), 750 (w), 687 (m), 598 (w), 568 (w), 541 (m), 506 (w).

1-Carboxyvinyl-8,9,10,11,12-pentafluorobiphenyl (8a) 1-Carboxy-8,9,10,11,12-pentafluorobiphenyl (1.0g, 4mmol) and formylmethylene triphenylphosphorane (1.2g, 4mmol) are dissolved in benzene and refluxed overnight under argon. The crude product is dry-loaded onto a column and chromatographed in 10% ethyl acetate in hexanes, then recrystallized from methylcyclohexane. 726mg (65%) of product were isolated. Mp = 108-112. 300 MHz ^{1}H NMR, $CDCl_3$, δ = 6.99, dd, 1H; 7.48, m, 5H; 7.52, d, 1H; 9.72, d, 1H 75 MHz ^{13}C, $CDCl_3$, δ = 112.7 (T), 122.5 (T), 126.4, 128.5, 129.4, 129.8, 134.8 (t), 135.9, 142.0 (), 143.4 (m), 145.3 (m), 146.8 (m), 193.3. GC/MS m/z 280 (M^+, 100). 261 (20), 252 (60), 232 (20), 201 (17).

Nitronylnitroxide (8) Mp=168-170. FTIR KBr ν = 3074 (w), 2993 (m), 2943 (m), 1483 (vs), 1463 (m), 1439 (s), 1428 (m), 1386 (m), 1373 (s), 1316 (m), 1279 (m), 1261 (m), 1213 (m), 1186 (w), 1170 (m), 1050 (m), 1030 (w), 978 (s), 969 (s), 921 (w), 873 (w), 848 (m), 794 (w), 772 (w), 754 (m), 732 (m), 698 (m), 648 (m), 592 (w), 541 (w), 496 (w).

1-(1-Carboxyvinyl-2,3,5,6-tetrafluorophenyl)-2-phenylacetylene (9a) 8a (1.65g, 5.9mmol) and formylmethylene triphenylphosphorane (1.2g, 4mmol) are dissolved in benzene and refluxed four hours under argon. The crude material is columned in 1:1 dichloromethane:hexanes to give 1.54g (86%). Mp = 144-146. 300 MHz ^{1}H NMR, $CDCl_3$, δ =6.97, dd, 1H; 7.40, m, 4H; 7.56, dd, 2H; 9.69, d, 1H. 75 MHz ^{13}C, $CDCl_3$, δ = 74.1, 77.0, 104.1, 113.7 (t), 121.0, 128.3, 129.8, 131.8, 135.0, 135.5, 143.0 (m), 144.6 (m), 146.2 (m), 148.2 (m), 193.1 ppm. GC/MS m/z 304 (M^+, 100), 276 (35), 256 (30).

Nitronylnitroxide (9) The melting points of product obtained from: THF = 144-146; $CHCl_3$ = 164-165; Methylcyclohexane = 184-186; FTIR KBr (identical for each polymorph) ν = 2990 (w), 2941 (w), 2221 (w), 1485 (vs), 1432 (m), 1421 (w), 1387 (w), 1374 (m), 1328 (m), 1290 (w), 1231 (w), 1208 (w), 1169 (w), 1137 (w), 1098 (w), 1068 (w), 1036 (w), 984 (m), 971 (m), 952 (w), 931 (w), 867 (w), 759 (m), 688 (m), 598 (w), 540 (w), 527 (w).

1-Ethynyl-4-propylbenzene 2-methyl-2-hydroxybutyne (1.5mL, 15.5mmol) and 4-propyl-bromobenzene (2mL, 12.9mmol) are dissolved in 20mL triethylamine, and tetrakis(triphenylphosphine) palladium(0) (750mg, 0.65mmol) and copper iodide (122mg, 0.65mmol) are added as solids. The system is refluxed four hours and afforded the standard workup. The residue is dry-loaded and chromatographed in 15% ethyl acetate in hexanes. 2.11 g of the protected product is isolated as a brown oil. This oil is boiled in 50mL isopropyl alcohol with potassium hydroxide (2.4g, 60mmol) for seven hours. After workup, 1.2g of product is isolated by running a silica plug in hexanes (64% total yield). 300 MHz ^{1}H NMR, $CDCl_3$, δ = 0.95, t, 3H; 1.65, m, 2H; 2.60, t, 2H; 3.05, s, 1H; 7.14, d, 2H; 7.43, d, 2H. 75 MHz ^{13}C, $CDCl_3$, δ = 13.5, 24.1, 37.7, 76.2, 83.6, 119.0, 128.2, 131.8, 143.4 ppm. GC/MS m/z 144 (M^+, 30), 115 (100), 89 (12), 63 (11).

1-(1-Carboxy-2,3,5,6-tetrafluorophenyl)-2-(4-propylphenyl)acetylene (10b) 1-Ethynyl-4-propylbenzene (1.1g, 7.7mmol) is dissolved in 20mL THF and cooled to -78°C. 1.6M Butyllithium (4.5mL, 7.2mmol) is added slowly and the solution turns orange. The solution is allowed to warm to room temperature and stir for 1 hour, then pentafluorobenzaldehyde, ethylene glycol acetal (1.8g, 7.4mmol) is added as a solid and the resulting solution is stirred overnight. After standard workup the residue is dissolved in a minimum of 70% acetic acid at 80°C and heated overnight. Crystals form upon cooling this solution and 864mg of product are collected (35% yield). 300 MHz ^{1}H NMR, $CDCl_3$, δ =

0.95, t, 3H; 1.65, m, 2H; 2.62, t, 2H; 7.20, d, 2H; 7.47, d, 2H; 10.23, s, 1H. 75 MHz ^{13}C, $CDCl_3$, δ = 13.4, 24.0, 37.8, 73.5 (t), 106.1 (t), 110.6 (t), 114.0 (t), 117.8, 128.5, 131.8, 144.5 (m), 145.4, 147.7 (m), 181.7 (m) ppm.

1-(1-Carboxyvinyl-2,3,5,6-tetrafluorophenyl)-2-(4-propylphenyl) acetylene (10a) **10b** (484mg, 1.5mmol) and formylmethylene triphenylphosphorane (1.2g, 4mmol) are dissolved in benzene and refluxed overnight under argon. The material is dry-loaded and chromatographed in 10% ethyl acetate in petroleum ether. 442mg of product (84%) is collected. Mp = 98-100. 300 MHz ^1H NMR, $CDCl_3$, δ = .93, t, 3H; 1.62, m, 2H; 2.60, t, 2H; 6.94, dd, 1H; 7.16, d, 2H; 7.40, s, 1H; 7.44, d, 2H; 9.66, d, 1H. 75 MHz ^{13}C, $CDCl_3$, δ = 13.4, 24.0, 37.8, 73.7 (t), 104.6, 106.6 (t), 113.4 (t), 128.5, 131.7, 134.9 (t), 135.5, 142.9 (m), 144.5 (m), 145.0, 146.2 (m), 147.9 (m), 193.1 ppm.

Nitronylnitroxide (10) Mp = 190-191. FTIR KBr ν = 2986 (w), 2960 (m), 2860 (w), 2216 (m), 138 (w), 1605 (w), 1560 (w), 1518 (w), 1490 (vs), 1452 (w), 1422 (w), 1376 (m), 1328 (m), 1274 (w), 1216 (m), 1168 (w), 1141 (m), 1098 (w), 1036 (w), 987 (s), 971 (m), 951 (w), 932 (w), 866 (w), 843 (w), 812 (m), 596 (w), 542 (m).

1-Carboxy-4-ethynyl-2,3,5,6-tetrafluorobenzene (11b) Triisopropylsilylacetylene (16.2mL, 72.2mmol) is dissolved in 200mL THF and cooled to -78°C. 1.6M Butyllithium in hexanes (50.7mL, 81.1mmol) is added over 30 minutes and

the solution is warmed to room temperature. Pentafluorobenzaldehyde, ethylene glycol acetal (19.5g, 81.1mmol) is added as a solid and the solution is refluxed for 5 hours and afforded a standard workup. The crude material is dissolved in 500mL of THF with 30mL water, and 110mL of 1.0M tetrabutylammonium fluoride in THF is added. The solution is stirred for 15 minutes, worked up, and the crude material is dry loaded and chromatographed in 10% ethyl acetate in petroleum ether. The acetal is isolated contaminated with some unreacted pentafluorobenzaldehyde acetal and triisopropylsilyl fluoride (TIPSF). This crude material is dissolved in 500 mL 70% acetic acid and heated for 36 hours at 80°C. The product is extracted in diethyl ether/hexanes, the organic layer is washed with sodium cabonate solution, dried with $MgSO_4$ and evaporated. The product is pumped on at 80mtorr for two days in the dark to remove the TIPSF and pentafluorobenzaldehyde impurities with minimal loss of the target material. 7.76g (53%) of white powder is isolated. 300 MHz ^1H NMR, $CDCl_3$, δ = 3.89, s, 1H; 10.27, s, 1H. 75 MHz ^{13}C, $CDCl_3$, δ = 93.4, 108.3 (m), 115.1 (m), 144.4 (m), 145.6 (m), 147.8 (m), 148.8 (m), 181.8. GC/MS m/z 202 (M+ 100), 173 (30), 123 (50).

1-Carboxyvinyl-4-ethynyl-2,3,5,6-tetrafluorobenzene (11c) 11b (5.82g, 29mmol) and formylmethylene triphenylphosphorane (8.76g, 29mmol) are dissolved in benzene and refluxed overnight under argon. The crude material is dry loaded onto a column and chromatographed in 10% ethyl acetate in

petroleum ether. A white powder (5.41g, 82%) is isolated and stored in a freezer until further use. 300 MHz ^{1}H NMR, $CDCl_3$, δ = 3.83, s, 1H; 6.81, dd, 1H; 7.37, d, 1H; 9.59, d, 1H. 75 MHz ^{13}C, $CDCl_3$, δ = 92.2, 104.6 (m), 114.6 (m), 134.9, 135.4 (m), 142.7 (m), 145.2 (m), 145.5 (m), 148.7 (m), 192.9. GC/MS m/z 228 (M^+, 100), 209 (26), 200 (94), 180 (31), 149 (27), 129 (27).

1-Carboxyvinyl-4-(1-naphthyl)ethynyl-2,3,5,6-tetrafluorobenzene (11a) **11c** (301mg, 1.32mmol) and 1-iodonaphthalene (335mg, 1.32mmol) are dissolved in 10mL triethylamine with heating and vigorous stirring. Tetrakistriphenylphosphine palladium(0) (85mg, 5.5%) and copper iodide (25mg, 13%) are immediately added and the solution is heated at 80°C for 1 hour. Over this time solid product crashes out and stirring may stop. The supernatant solution is decanted off and the remaining solid is boiled several times in chloroform with stirring to dissolve the product, and filtered to separate it from insoluble impurities. The soluble fractions are evaporated and recrystallized from boiling chloroform. 99.1mg (21%) of yellow powder, nearly insoluble in most organic solvents, is collected. Mp = 237-244. 300 MHz ^{1}H NMR, $CDCl_3$, δ = 6.22, s, 1H; 7.01, dd, 1H; 7.29, m, 2H; 7.49, m, 3H; 7.64, m, 2H; 9.73, d, 1H.

Nitroxide (11) Oxidation by the standard method afforded no nitronylnitroxide. The nitroxide could be crystallized from methanol. Mp =

174-177. FTIR KBr ν = 2982 (w), 2213 (w),. 1482 (vs), 1376 (w), 1341 (w), 1309 (w), 1263 (w), 1113 (w), 1041 (w), 978 (m), 940 (w), 800 (m), 772 (m), 668 (m), 610 (w), 580 (w), 564 (w).

1-Carboxyvinyl-4-(2-naphthyl)ethynyl-2,3,5,6-tetrafluorobenzene (12a) Using the method decribed for **11a** afforded **12a** in 77% yield. This product was poorly soluble in most solvents. Mp=215-220. 300 MHz ^{1}H NMR, $CDCl_3$, δ = 7.02, dd, 1H; 7.46, s, 1H; 7.54, m, 2H; 7.62, dd, 1H; 7.86, m, 3H; 8.16, s, 1H; 9.74, d, 1H.

Nitronylnitroxide 12 Mp = 187-189. FTIR KBr ν = 3061 (w), 2989 (w), 2934 (w), 2218 (m), 1484 (vs), 1459 (m), 1451 (w), 1438 (w), 1421 (w), 1387 (w), 1375 (m), 1324 (w), 1251 (w), 1216 (m), 1168 (w), 1138 (w), 990 (m), 970 (m), 860 (w), 817 (m), 748 (m), 690 (w), 668 (m), 541 (w), 474 (w).

1-Carboxyvinyl-4-(2-fluorenyl)ethynyl-2,3,5,6-tetrafluorobenzene (13a) 2-Iodofluorene was obtained via a literature procedure.[27] Using the method described for **11a** afforded **13a** in 60% yield. This product was poorly soluble in most solvents. Mp = 254-257. 300 MHz ^{1}H NMR, $CDCl_3$, δ = 3.98, s, 2H; 7.07, dd, 1H; 7.4-7.7, m, 5H; 7.83, m, 3H; 9.77, d, 1H.

Nitronylnitroxide 13 Mp = 205-208. FTIR KBr ν = 2989 (w), 2926 (w), 2211 (m), 1485 (vs), 1420 (m), 1384 (m), 1380 (m), 1327 (m), 1275 9w), 1213 (m), 1140 (m), 984 (m), 974 (m0, 823 (w), 767 (m), 730 (m).

1-Carboxyvinyl-4-(4-allyloxyphenyl)ethynyl-2,3,5,6-tetrafluorobenzene (14a) Synthesis of this aldehyde followed the method described for **11a**, except the solid was not recrystallized from chloroform. The material was purified by dry-loading a column and chromatographing the material in 10% ethyl acetate in petroleum ether, and obtained in 33% yield. Mp = 141-144. 300 MHz ^{1}H NMR, $CDCl_3$, δ =4.58, m, 2H; 5.39, m, 2H; 6.04, m, 1H; 6.92, d, 2H; 7.01, dd, 1H; 7.51, m, 3H; 9.73, d, 1H. 75 MHz ^{13}C, $CDCl_3$, δ = 68.6, 73.2 (m), 104.9 (m), 113.2, 114.7, 117.9, 132.3, 133.5, 134.9 (m), 135.9, 159.7, 193.3

Nitronylnitroxide 14 Mp = 183-184. FTIR KBr ν = 3074 (w), 2996 (w), 2927 (w), 2214 (m), 1648 (w), 1604 (s), 1518 (s), 1489 (vs), 1452 (w), 1433 (w), 1422 (w), 1375 (m), 1291 (w), 1259 (m), 1215 (w), 1172 (m), 1140 (w), 1097 (w), 985 (m) 971 (m), 951 (w), 931 (w), 913 (w), 866 (w), 831 (m), 600 (w), 560 (w), 540 (m).

1-Carboxyvinyl-4-(4-diethylaminophenyl)ethynyl-2,3,5,6-tetrafluorobenzene (15a) This material was obtained as a bright orange solid following the procedure for **14a** (28% yield). Mp = 164-172. 300 MHz ^{1}H NMR, $CDCl_3$, δ = 1.19, t, 6H, 3.39, q, 4H; 6.60, d, 2H; 6.96, dd, 1H; 7.39, d, 2H; 7.44, d, 1H, 9.68, d,

1H. 75 MHz ^{13}C, $CDCl_3$, δ = 12.2, 44.2, 65.8, 73.2 (m), 96.5, 100.7, 106.1, 112.0, (t), 133.3 (t), 133.4, 134.3 (t), 136.2, 142.9 (m), 144.2 (m), 146.4 (m), 147.6 (m), 148.3

1-Carboxyvinyl-4-(4-acetonitrylyloxy)ethynyl-2,3,5,6-tetrafluorobenzene (16a) This material was obtained following the procedure for **14a** (28% yield). 300 MHz ^1H NMR, $CDCl_3$, δ = 4.83, s, 2H; 7.02, m, 3H; 7.55, m, 3H; 9.75, d, 2H.

1-Carboxy-4-ethenyl-2,3,5,6-tetrafluorobenzene ß-Bromostyrene (mixture of isomers) (31.g, 17mmol) is dissolved in 100mL of freshly distilled THF and cooled to -100°C. 1.7M *t*-Butyllithium (20mL, 34 mmol) is added over two hours, and the solution is stirred an additional two hours. Pentafluorobenzalehyde, ethylene glycol acetal (4.1g, 17 mmol) is dissolved in 5 mL THF and added all at once. The solution is stirred two hours and allowed to warm to room temperature overnight. After a standard workup the crude material is dissolved in a minimum 70% acetic acid and heated at 80°C for 24 hours. The solid material that precipitates out upon cooling is predominately the *trans* isomer - the *cis* isomer eliminates bromide to form **3a**. This precipitate is recrystallized from methylcyclohexanes to give 1.57g product (28%). When reacted with DHB, no nitronylnitroxide precursor is formed. 300 MHz ^1H NMR, $CDCl_3$, δ = 7.10, d, 1H; 7.40, m, 3H; 7.59, m, 3H; 10.28, s, 1H. 75 MHz ^{13}C, $CDCl_3$, δ = 113.7, 128.0, 130.4, 132.7, 136.4, 141.2 (m), 183.0 ppm. GC/MS m/z 280 (M^+, 100), 259 (40), 232 (40), 201 (35).

Stilbene nitronylnitroxide Stilbene carboxaldehyde was purchased from Aldrich. Mp = 131-133. FTIR KBr ν = 3047 (w), 3029 (w), 2986 (m), 2939 (w), 1602 (m), 1499 (w), 1482 (w), 1449 (m), 1420 (w), 1391 (s), 363 (vs), 1333 (w), 1303 (m), 1216 (m), 1165 (m), 1130 (m), 972 (m), 865 (m), 824 (m), 757 (m), 7223 (m), 695 (m), 636 (w), 616 (m), 535 (m), 456 (w).

1-Carboxyvinyl-4-ethenyl-2,3,5,6-tetrafluorobenzene 1-Carboxy-4-ethenyl-2,3,5,6-tetrafluorobenzene (353mg, 1.26mmol) and formylmethylene triphenylphosphorane (400mg, 1.32mmol) are dissolved in benzene and refluxed four hours under argon. The crude product is chromatographed in chloroform and recrystallized from methylcyclohexanes to afford 281mg of product (73%). 300 MHz ^{1}H NMR, $CDCl_3$, δ = 7.00, m, 2H; 7.39, m, 3H; 7.54, m, 4H; 9.72, d, 1H. 75 MHz ^{13}C, $CDCl_3$, δ = 113.1; 127.0; 128.7; 129.2; 134.4 (t); 135.1; 136.2; 138.8 (t); 193.4. GC/MS m/z 306 (M^+, 100), 286 (20), 258 (25), 238 (25).

1-Carboxy-4-(4-phenyl)butadiynyl-2,3,5,6-tetrafluorobenzene 1-Trimethylsilyl-4-phenylbutadiyne[28] (644mg, 3.25mmol) is dissolved in 10mL of freshly distilled THF and cooled to -78°C. 2.15mL of 1.5M methyllithium-lithium bromide complex in diethyl ether is added dropwise and the solution is allowed to warm to room temperature and stir for 1 hour. Pentafluorobenzaldehyde, ethylene glycol acetal (780mg, 3.25mmol) is added and the solution is allowed to stir overnight. After standard workup the

crude material is columned in 10% ethyl acetate in petroleum ether. The pure material is dissolved in 70% acetic acid and heated 18 hours at 80°C, and recrystallized from methylcylcohexanes to yield 137mg (14%) product. This material could not be converted into the nitronylnitroxide. 300 MHz ^{1}H NMR, $CDCl_3$, δ = 7.39, m, 3H; 7.58, d, 2H; 10.30, s, 1H. GC/MS m/z 302 (M^+, 100), 274 (15), 254 (10), 223 (10).

---

[1] Buchanan, R.C.; Park, T.; *Materials Crystal Chemistry*, Marcel Dekker, Inc.; New York; **1997**

[2] Lehn, J.-M.; *Angewante Chemie*, **1988**, *100*, 91

[3] Corey, E.J.; *Chemical Society Review*, **1988**, *17*, 111

[4] by Cassell-AM Scrivens-WA Tour-JM ANGEW-CHEM v37 (11) : pp1528-1531

[5] Desiraju, G.R.; *Angevante Chemie International Edition*,**1995**, *34*, 2311

[6]Kitaigorodskii, A.I.; *Molecular Crystals and Molecules*, Academic Press, New York, **1973**

[7] by Oldham-WJ Lachicotte-RJ Bazan-GC J-AM-CHEM-S v120 (12) : pp2987-2988

[8] Dunitz, J,; Bernstein, J.; *Accounts of Chemical Research*, **1995**, *28*, 193

[9] Gavezzotti, A.; *Accounts of Chemical Research*; **1994**, *27*, 309

[10] Izuoka, A.; Murata, S.; Sugawara, T.; Iwamura, H.; *Journal of the American Chemical Society*, **1987**, *109*, 2631.

[11] Kinoshita, M.; *Japanese Journal of Applied Physics*, **1994**, *33*, 5718

[12] Dowd, P.; *Accounts of Chemical Research*, **1972**, *5*, 242

[13] Zhang, J.S.; Moore, J.S.; *Journal of the American Chemical Society*, **1992**, *114*, 9701

[14]Patrick, C.R.; Prosser, G.S.; *Nature*, **1966**, *187*, 1021

[15] Coates, G.W.; Dunn, A.R.; Henling, L.M.; Dougherty, D.A.; Grubbs, R.H.; *Angewante Chemie International Edition*, **1997**, *36*, 248

[16] Coates, G.W.; Dunn, A.R.; Henling, L.M.; Ziller, J.W.; Lobkovsky, E.B.; Grubbs, R.H.l *Journal of the American Chemical Society*, **1998**, *120*, 3641

[17] Kinoshita, M.; *Japanese Journal of Applied Physics*, **1994**, *33*, 5718

[18] Awaga, K.; Maruyama, Y.; *Chemical Physics Letters*, **1989**, *158*, 556

[19] Osiecki, J.H.; Ullman, E.F.; *Journal of the American Chemical Society*; **1968**, *90*, 1078

[20] Matsushita, M.M.; Izuoka, A.; Sugaware, T.; Kobayashi, T.; Wada, N.; Takeda, N.; Ishikawa, M.; *Journal of the American Chemical Society*; **???**

[21] Goldman, J.; Petersen, T.E.; Torssell, K.; *Tetrahedron*, **1973**, *29*, 3833

[22] The y-axis of these plots shows "Effective Spin" which can be calculated from $\chi_m T$ from the formula $\chi_m T = 0.5\ S(S+1)$, where S is effective spin. This assumes g=2.00, which should hold true for organic radicals. These plots most directly illustrate the spin=0.5 character of the materials at 300K. The downturn represents antiferromagnetic coupling of the materials, and should not be interpreted as spin<0.5, which is physically impossible.

[23] Dulog, L.; Kim, J.S.; *Makromolcular Chemie*; **1989**, *190*, 2609

[24] Barrow, I.; Pedler, A.E.; *Tetrahedron*, **1976**, *32*, 1829

[25] Wang, H.L.; Zhang, D.Q.; Wan, M.X.; Zhu, D.B.; *Solid State Communications*, **1993**, *85*, 685

[26] Ivanova, N.G.; Barkhosh, V.A.; Vorozhtosov, N.N., Jr.; *Zh.Obshch. Khim.*, **1969**, *39*, 1347

[27] Keumi, T.; Umeda, T.; Inoue, Y.; Kitajima, H.; *Bulletin of the Chemical Society of Japan*, **1989**, *62*, 89.

[28] Holmes, A.B.; Jennings-White, C.L.D.; Schulthess, A.H.; *Journal of the Chemical Society, Chemistry Communications*, **1979**, *1979*, 840.

Chapter Three : A *meta*-linked Dicyanoquinonediimine and Its Metal Complexes

Anion radicals as components in molecule-based conductors and magnets

Organic anion radicals, particularly TCNQ, TCNE, and DCNQI (Figure 3.1a), have been extensively studied as components in electronically interesting materials. The charge-transfer salt of TCNQ and TTF was found in 1973 to be conducting[1], and since then dozens of similar compounds have shown semiconducing, metallic, and even superconducting behavior.[2]

TCNQ and TCNE in particular have been important components in many of the molecule-based magnetic materials synthesized by Joel Miller and others.[3] In these materials, the charge transfer salts between a metallocene and an electron acceptor form alternating 1-D stacks, and several are bulk ferromagnets below 20K. As a result, nearly every possible charge transfer salt of these simple ions has been explored over the years. The number of

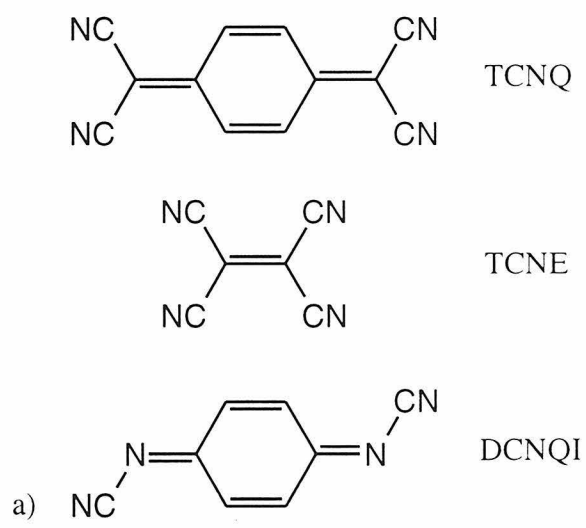

Figure 3.1 - a) Tetracyanoquinone (TCNQ), tetracyanoethylene (TCNE) and dicyanoquinonediimine (DCNQI).

permutations of this sort is limited, though, by the impossibility of making simple derivatives of TCNE and TCNQ. Substitution on the 6-membered ring of TCNQ distorts the cyano groups from planarity (and thus conjugation with the system)[4], and replacement of any of the cyano groups in either system drastically alters its electronic properties.

DCNQI is a more recently developed system[5] that is attractive because it has a similar oxidation potential to TCNQ and TCNE, and substitution to its rings can subtly change its electronic character.[6] The potential of simple DCNQI can be swung from +0.79V (4F-DNCQI) to +0.05 [4(Me)-DCNQI] vs Ag/AgCl, and can be tuned to any potential in between the two.[4] The cyano-imine functionality is sufficiently tolerant of steric bulk to allow such large groups as phenyls or *t*-butyl groups on the ring without loss of its electron affinity.

Metal complexes of cyanoquinones and quinonediimines

One additional advantage to working with these anion radicals is that they may ligate metals through their cyano moieties. Few such materials have been described in the literature. Of note, however, is the reaction of bis(benzene)vanadium with TCNE: in this, vanadium metal loses its coordination to benzene and binds instead to the cyano groups of TCNE. This reaction forms an amorphous powder that is a room temperature ferromagnet.[7] Unfortunately, this material has never been completely

characterized, and no other cyano-containing ligand produces a ferromagnet as the product of this reaction.

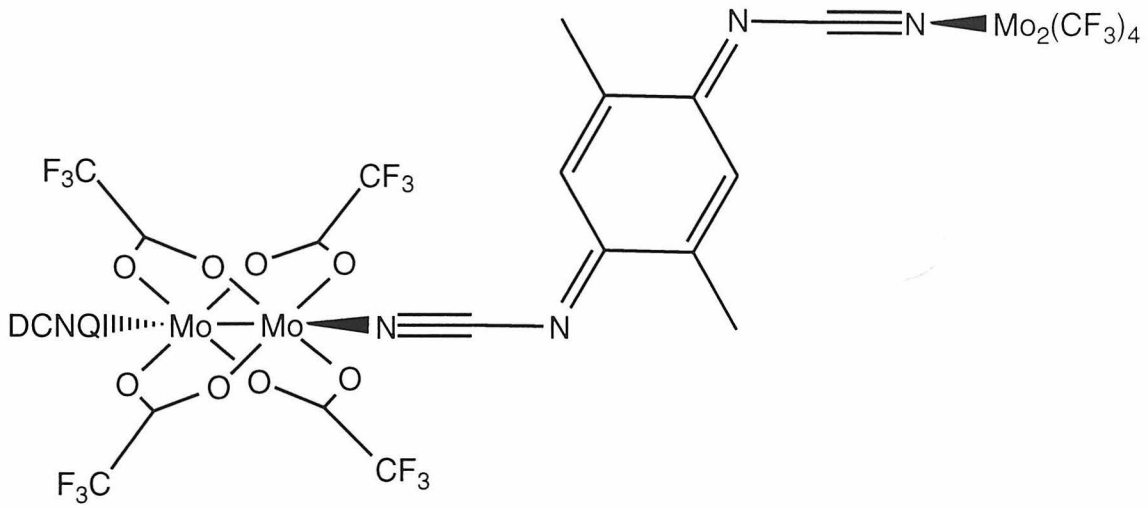

Figure 3.2 - A complex between $Mo_2(O_2CCF_3)_4$ and DCNQI.

Other materials containing a cyanoquinone include the complex between $Mo_2(O_2CCF_3)_4$ and DCNQI[8] (Figure 3.2) or TCNQ[9]. All of the published results so far have been with diamagnetic metals or diamagnetic dimers of TCNQ[10].

The copper salt of 2,5-dimethyldicyanoquinonediimine (DM-DNCQI), in particular, has been extensively studied, as it is a true metal over a large temperature range.[11] In this material, the copper atoms are of an intermediate oxidation state between Cu(I) and Cu(II). DCNQI anions ligate copper atoms with both its nitrile groups, and form 1-D stacks in the process. Conduction occurs along these 1-D stacks. This is an encouraging result from the perspective of using DCNQIs as the basis of molecular magnetic materials,

as it shows that there can be tight coupling between the orbitals of the ligand and those of a metal.

Despite the many derivatives of DCNQI that have been made[12], no one has yet examined the case of multiple quinone units connected to form a higher spin system. This project has synthesized the first such molecules and examined their metal complexes.

Results and Discussion

The target molecule for examination, MBDCNQI, is shown in Figure 3.3. The associated diradical, composed of two radical units linked *meta* through a benzene, is expected to be a ground-state triplet.

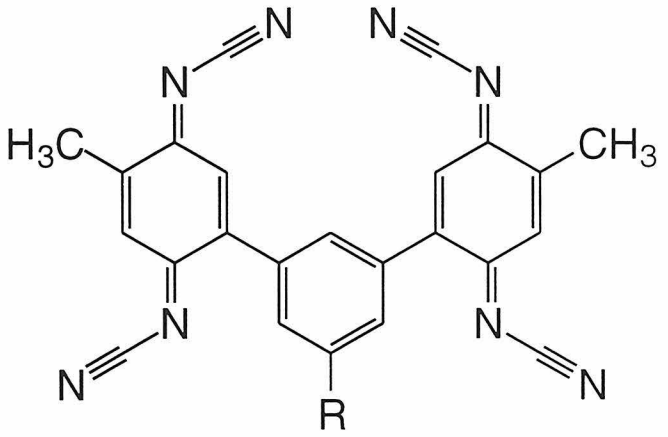

R=H, t-Bu

Figure 3.3 - *m*-Bis(dicyanoquinonediimine) benzene (MBDCNQI)

Synthesis of MBDCNQI

The synthesis of MBDCNQI is shown in Scheme 3.1. The quinone groups are introduced protected as the dimethylhydroquinone. Direct coupling of the brominated protected hydroquinone (**1**) to a boric acid

proceeds in poor yield because of the electron-rich character of the ring. The bromide is instead converted to a boric acid **(3)**, which is labile to aqueous base. Coupling of **(3)** to 1,3-dibromo-5-*tert*-butylbenzene **(2)** in anhydrous DMF gives product **(4)** in an acceptable yield. The *tert*-butyl group in the 5-position is necessary for the stability of the final (unreduced) product. With H in the 3-position, the MBDCNQI would decompose rapidly upon concentration in a rotory evaporator.

The protected hydroquininone is easily oxidized by ceric ammonium nitrate, with pyridine-2,6-bis(carboxylic acid)-N-oxide added to protect against side reactions, to produce **(6)**.[13] The final MBDCNQI is made using conventional conditions[5] and recrystallized from benzene or benzene/cyclohexane. The dark red, crystalline product can be made on the multi-gram scale and is stable indefinitely when stored in a dark, dry environment. Crystals form as a benzene solvate and will fragment upon drying. Elemental analysis of the material gives inconsistant results as it is difficult to remove of all the benzene from the crystals.

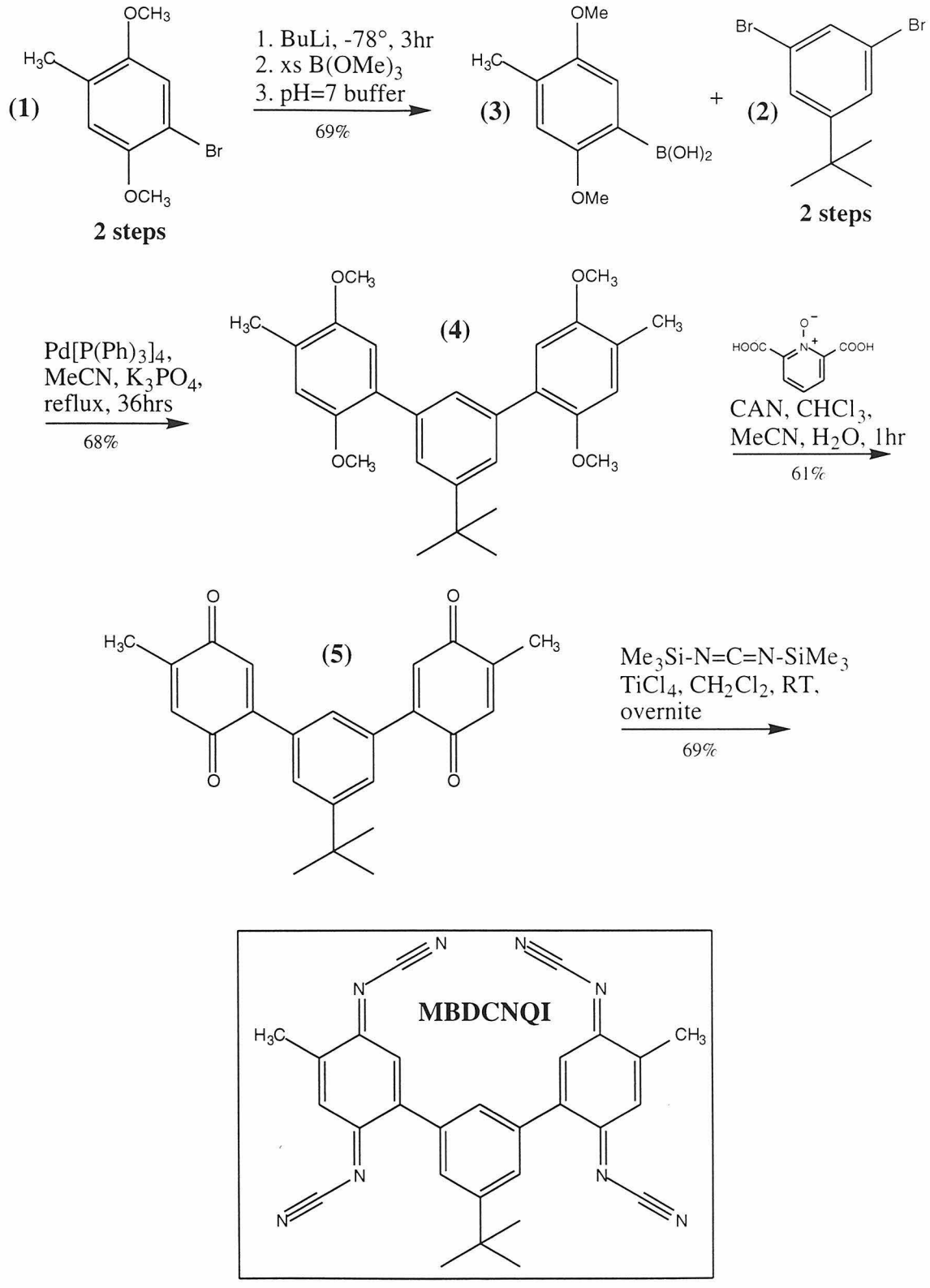

Scheme 3.1 - Synthesis of MBDCNQI

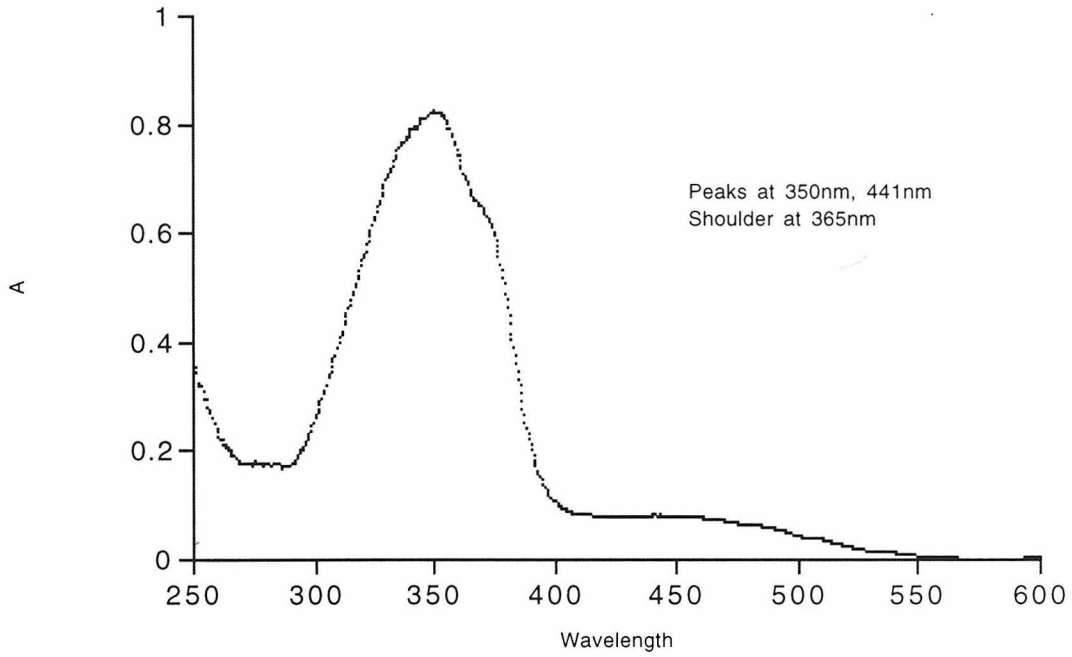

Figure 3.4 - UV/VIS of MBDCNQI in dichloromethane. ε_{350} **= 52000.**

MBDCNQI is unstable to nucleophiles and only very clean, preferably distilled solvents should be used to make solutions. Solutions of the ligand in benzene, dichloromethane or tetrahydrofuran are a pure red/orange color, and the UV-VIS is shown in

Figure 3.4. In acetonitrile, solutions may have a brown tinge that results from reduction of a small amount of the ligand to the blue anion radical by trace nucleophiles present in the solvent. Even distilled acetonitrile can give this effect, and care must be maintained to start the distillation with maximally clean acetonitrile in order to eliminate it. MBDCNQI will decompose when

heated in methanol or other protic solvents, though heating under ambient conditions in non-nucleophillic solvents, such as benzene, does not damage the material. MBDCNQI should not be recrystallized from polar solvents.

The ^{1}H NMR of MBDCNQI in chloroform can be slightly broadened due to anion radical impurities resulting from reaction of the ligand with trace nucleophiles in the solvent or the NMR tube. The FAB mass spectrum of the material gives a molecular peak of M+5, corresponding to the protonated, tetrareduced species. A control mass spectrum of 2,5-dimethyl(DCNQI) purchased from Aldrich Chemical company gave a mass peak of M+3, as expected for its protonated, direduced form.

MBDCNQI dianion diradical is a triplet

The cyclic voltammagram (Figure 3.5) of MBDCNQI shows two chemically reversible reduction waves at +0.33 and -0.26 vs Ag/AgCl. Each wave is assumed to represent a $2e^-$ reduction, simultaneously performing the same step on both quinone groups. The second wave, corresponding to the formation of the diamagnetic tetraanion, is kinetically very slow and poorly resolved even at sweep rates as low as 20mv/sec. The first wave is wider than 56mV, but no conclusions about electrochemical reversibility can be drawn from this, since the two reductions may not center on exactly the same potential. The potentials of the two reductions are only slightly shifted from those of dimethyl-DCNQI (0.21V, -0.38V).[5]

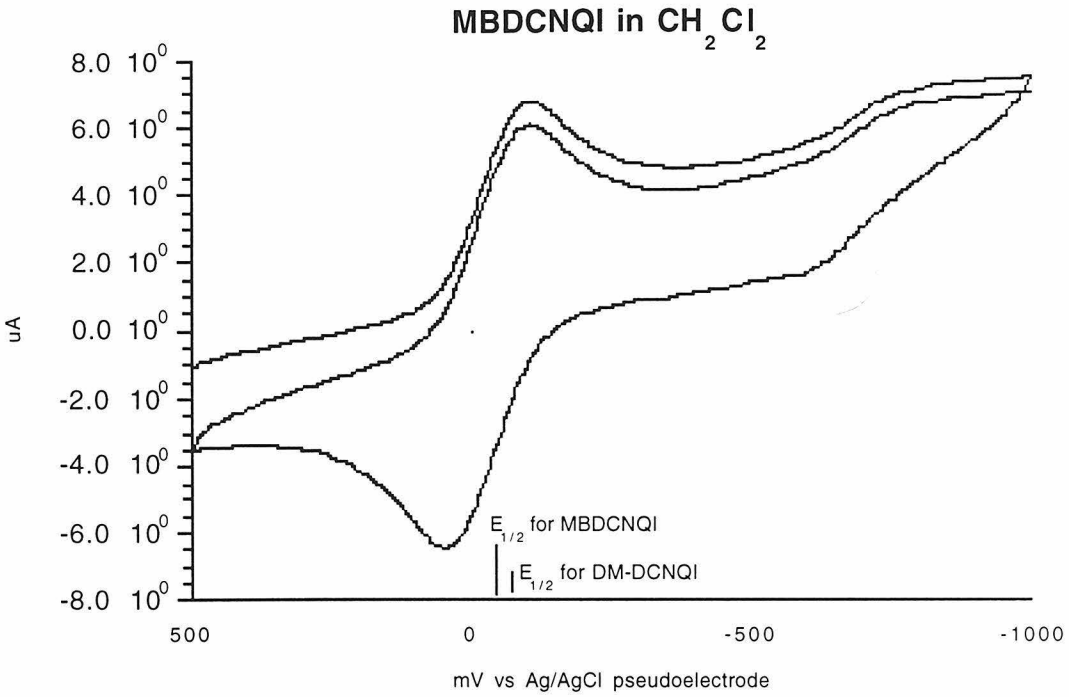

Figure 3.5 - CV of MBDCNQI in methylene chloride with 0.1M tetrabutylammonium perchlorate at 200mv/s.

Direduction of MBDCNQI with two equivalents of cobaltocene gives a blue material that can be magnetically characterized. Cobaltocene is a paramagnetic material that, when oxidized, becomes a diamagnet, so its contribution to a saturation plot should be minimal. The saturation behavior of the MBDCNQI diradical dianion at 1.9K gives a curve that corresponds to a spin state of S≈1, or a triplet. This is the most chemically stable triplet made of anion spin-containing units.

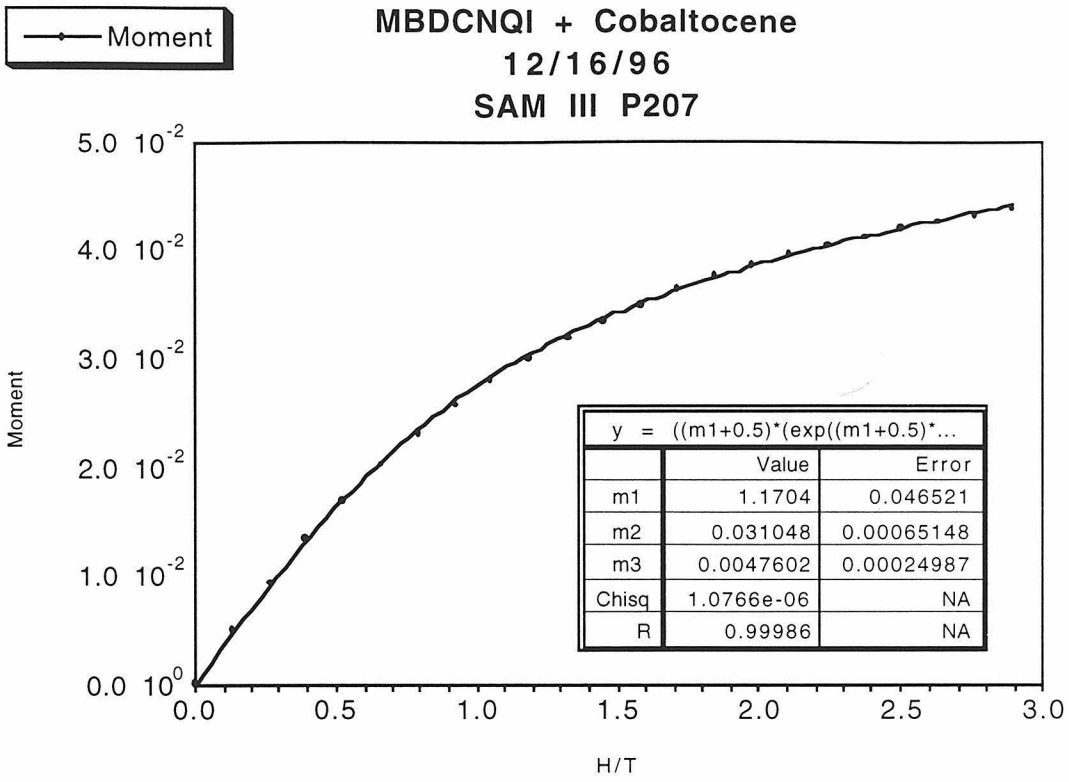

Figure 3.6 - Saturation curve for the salt $MBDCNQI^{2-} \bullet 2\ Co(Cp)_2^+$ shows S≈1 behavior.

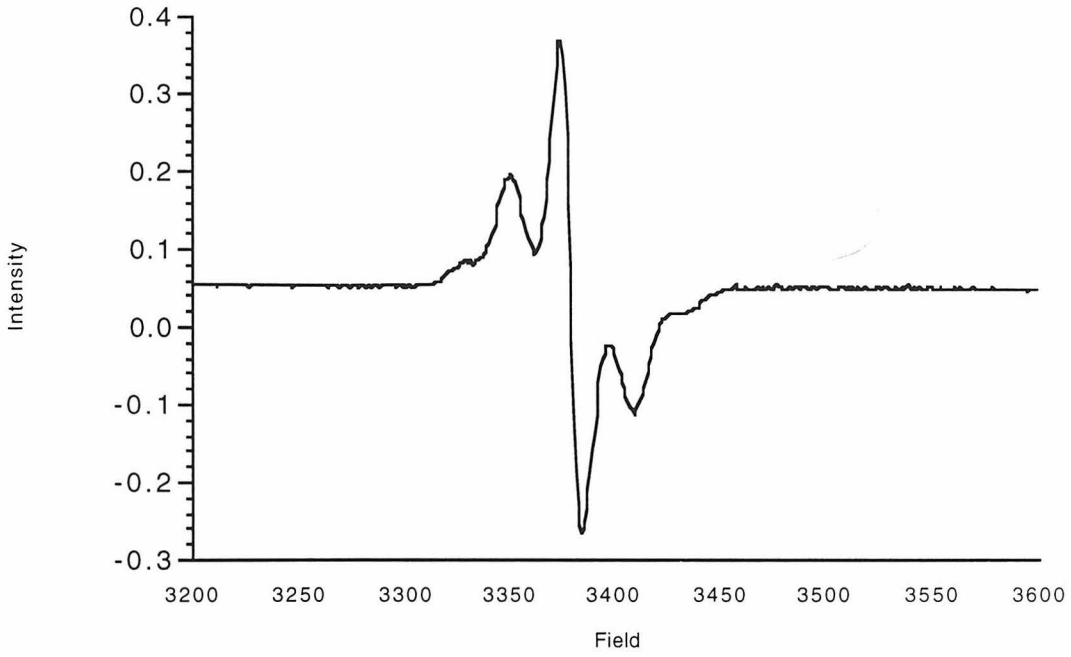

Figure 3.7 - EPR of 1μM MBDCNQI doped with 1.1 equiv $Co(Cp)_2$ in benzene at 77K. The modulation was 4 gauss, 0.128 time constant, 2500 gain, and frequency=9.281 GHz. D=0.0047cm^{-1}, E=0.0025cm^{-1}, and g=1.96.

The EPR of MBDNCQI doped with a slight excess of cobaltocene and frozen in benzene matrix at 77K reveals a triplet with a singlet impurity (Figure 3.7). The D value of the triplet is consistent with the approximate physical separation of the two quinone moieties. No half-field transition

could be seen; this is not unexpected, given the small value of D.

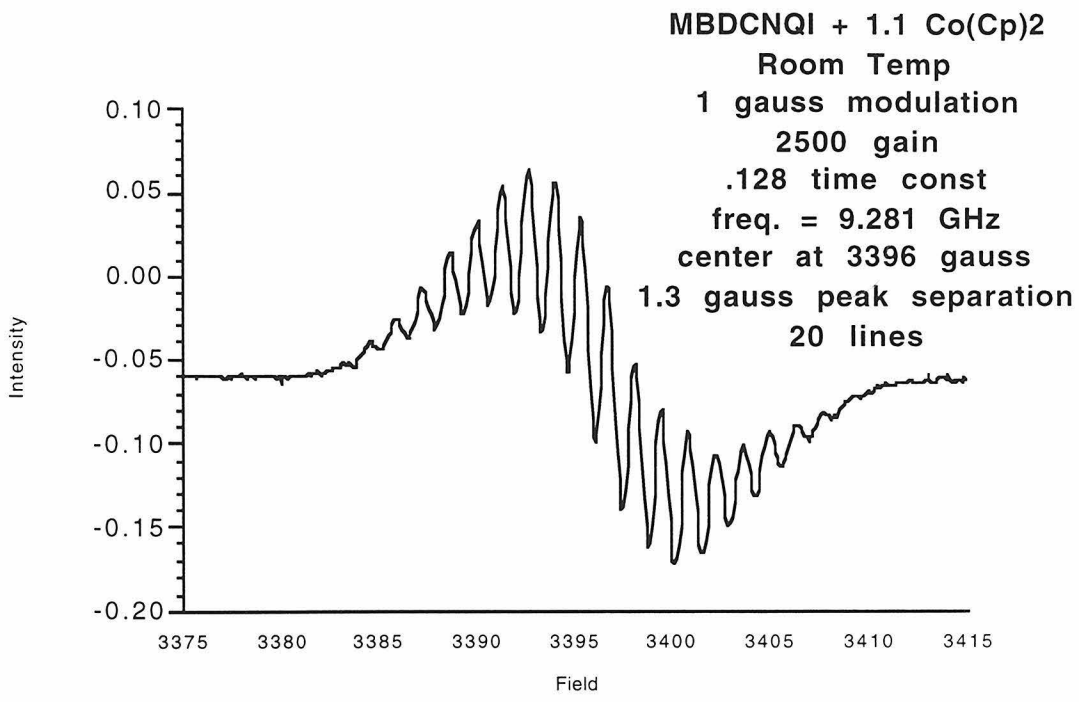

The room temperature EPR of MBDCNQI dianion in benzene gives a complex, 20 line spectrum. The literature spectra of DNCQIs give extremely narrow lines; these lines broadened considerably for larger molecules, and would be expected for MBDCNQI.[14] No attempt was made to fit this data to a computational model.

Complexes of MBDCNQI with Metal Iodides

Like DCNQI, MBDCNQI can ligate to metals through its cyano groups. The geometry of MBDCNQI should allow the ligand to bind in a bidentate fashion. Two cyano groups may bind to a metal both at the molecule's "top" in Figure 3.8, and potentially at its "bottom", where the phenyl ring may twist out of plane to allow ligation. Studies of CPK models confirm that this binding is not unreasonable for a metal with small auxilliary ligands completing its ligand sphere.

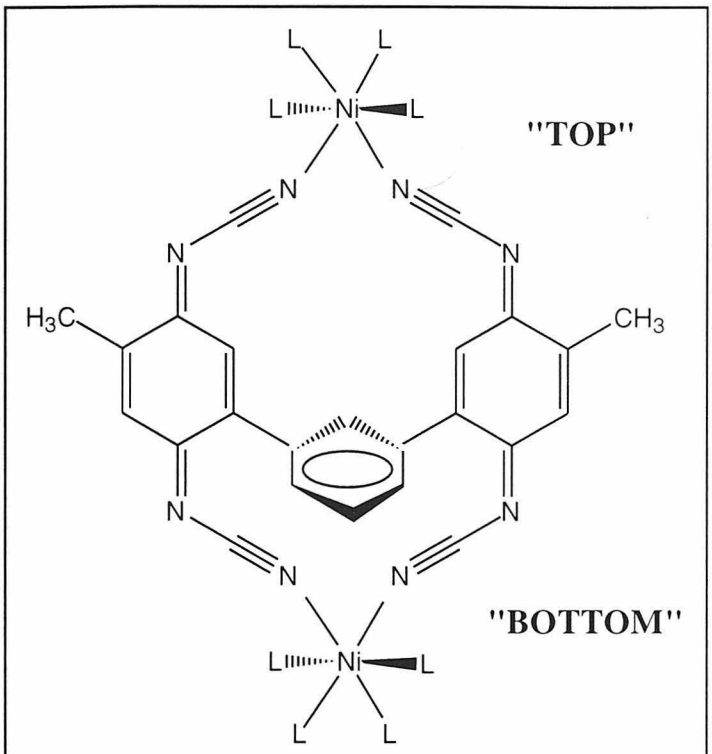

Figure 3.8 - Potential chelation of MBDCNQI to metals via all four nitriles.

MBDCNQI reacts with a variety of metal iodides, being reduced either by the metal atom itself and/or an iodide ligand (forming I_2). A two-fold or greater excess of metal iodide is dissolved in acetonitrile and mixed with an acetonitrile solution of MBDCNQI at room temperature; a blue solid immediately precipitates. This solid is insoluble in refluxing THF, DMF, and

DMSO, as would be expected for a network solid formed by MBDCNQI binding multiple metals. Complexes of V, Cr, Mn, Fe, Co, Ni, and Cu have been synthesized and characterized by IR and SQUID.

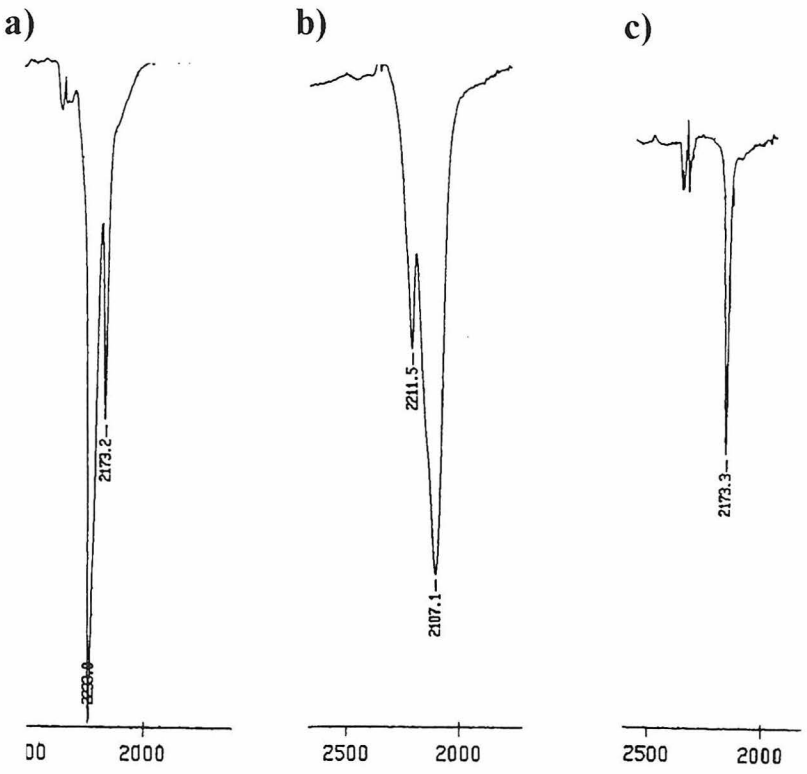

Figure 3.9 - IR spectra of MBDCNQI complexes: a) unreduced MBDNCQI bound to vanadium. b) reduced MBDCNQI bound to manganese (broadness suggests multiple environments. c) neutral, metal-free MBDCNQI.

IR spectroscopy is particularly informative for these cyano-containing ligands, as the cyano group is well-resolved from other parts of the spectrum. The unbound, neutral ligand has a sharp cyano stretch at 2173cm^{-1}, which shifts to 2103 cm^{-1} after forming an uncoordinating dianion diradical with $Co(Cp)_2^+$ (Figure 3.9). Both of these peaks are narrow, as the cyano groups

should be in only two minimally different environments (corresponding to those at the "top" vs "bottom" of the molecule, as shown in Figure 3.8).

The reaction between MBDCNQI and CuI or copper metal in acetonitrile[11] produced an insoluble black solid. Elemental analyses indicate empirical formulas of Cu(MBDCNQI) and Cu_2(MBDCNQI) respectively. A nitrile IR stretch at 2129 cm^{-1} indicates that reduction of the ligand occurs in both systems, and its broadness hints at multiple ligand environments rather than a single, pure compound. At high temperatures there is a magnetic signal, although it is difficult to interpret its meaning because the molecular weight and oxidation states of the material are not known, and it cannot be purified. Both materials exhibited strong antiferromagnetic downturns at low temperatures, and there is about 10% of the anticipated signal left at at a magnetic field of 5.5T at 1.9K, when a paramagnet would be nearly saturated.

MBDCNQI does react with silver metal in acetonitrile to yield a black solid. This material is similar to the above copper metal complex but was not extensively persued because of its insolubility and silver's diamagnetism.

Magnetic characterization of MI_2 complexes

The metal solids were magnetically characterized with a SQUID. Variable temperature behavior from 1.8K to 300K was taken at 2000 gauss, and variable field data was collected from 0 to 5.5T at 1.9K.

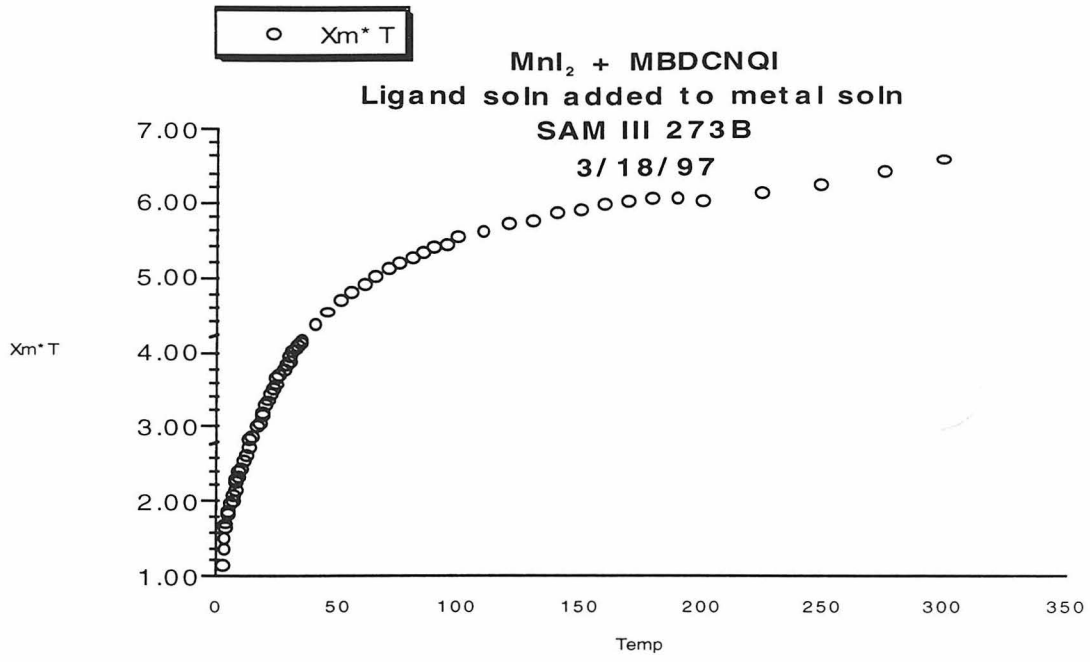

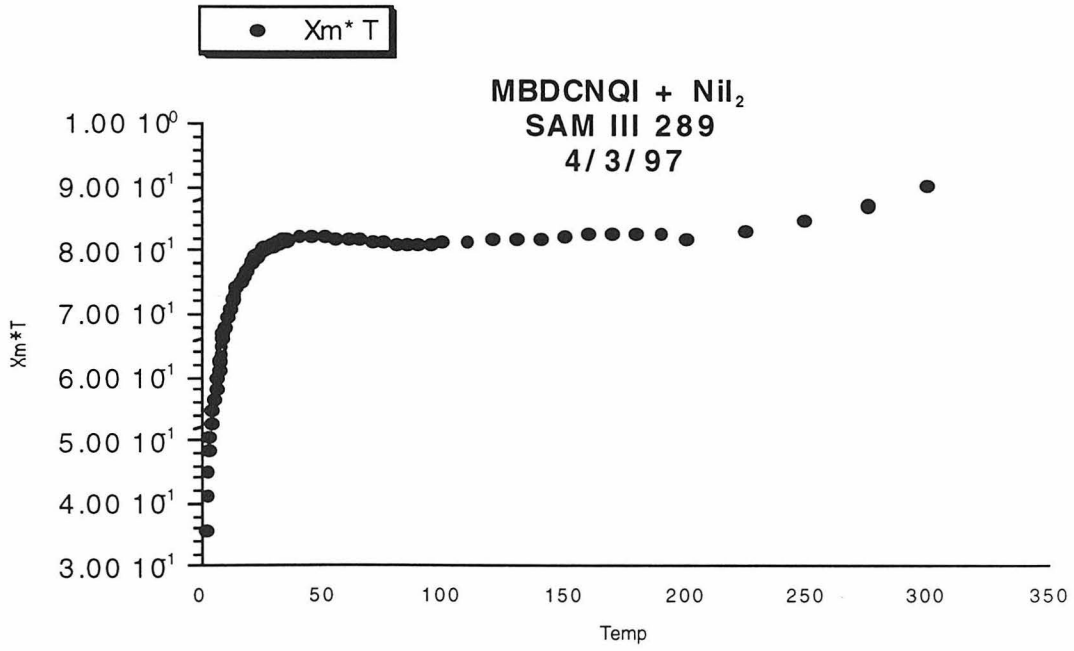

Figure 3.10 -a) The variable temperature data for the product of the reaction between MnI_2 and MBDCNQI is qualitatively very similar to the data for complexes with other metals. b) The variable temperature data for the product of the reaction of NiI_2 and MBDCNQI shows a small but real upturn below 100K.

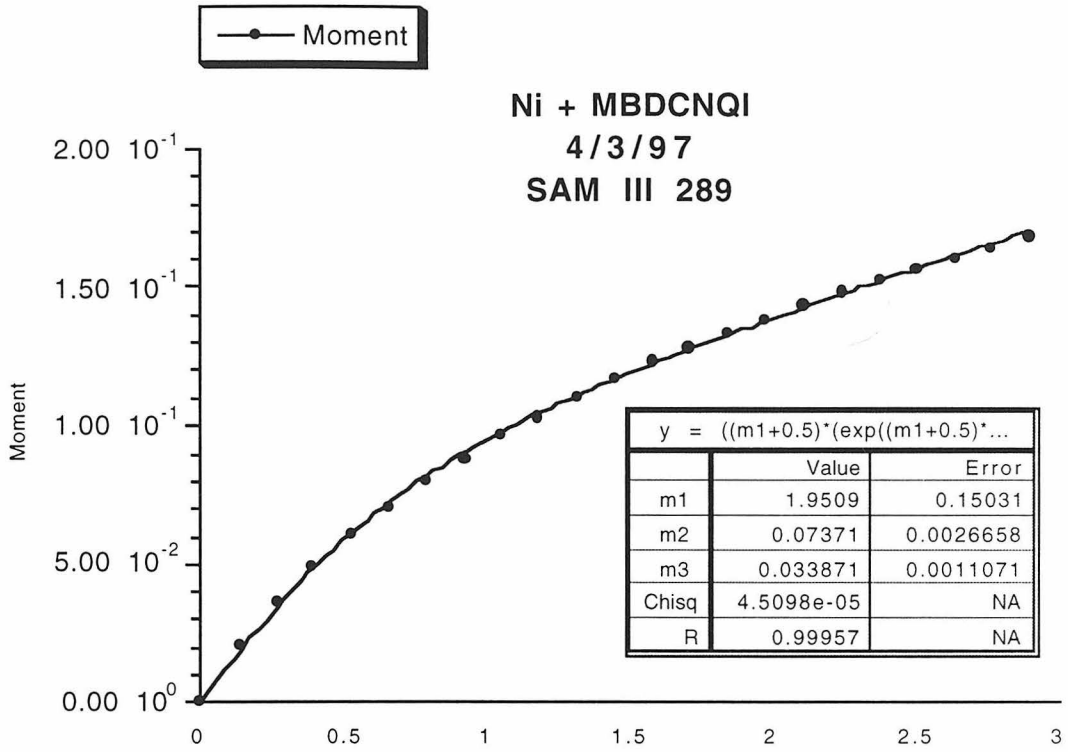

Figure 3.11 - The saturation behavior of the complex between NiI_2 and MBDCNQI fits to S=2, with a large linear component. A saturation plot at 4.5K (not shown) fits to S=3.3.

The radical electrons on the reduced ligand reside in π molecular orbitals and are expected to interact antiferromagnetically with metals containing unpaired electrons in d_π orbitals, as discussed in chapter 1. First-row transition metals expected to behave this way include: V(II), V(III), Cr(III), Mn(II), Mn(III), Fe(II), Fe(III), and Co(II). If the metal has unpaired electrons in d_σ orbitals only, the ligand is expected to interact ferromagnetically with the metal; this should be the case for octahedral or square planar Ni(II) and Cu(II).

The most interesting material was the product of the reaction of MBDCNQI with NiI_2. This material shows a small but real upturn starting at 90K and peaking near 50K in the variable termperature data (Figure 3.10b). In addition, the variable field data shows S≈2 behavior, characteristic of a ferromagnetic complex between a ligand and a nickel atom (Figure 3.11). This behavior is an unambigous identification of the magnetic interaction between the metal and the ligand.

One complicating factor in this variable field data should be noted, and that is the large linear component to the Brillouin fit, which is too large to correspond to the diamagnetic correction in the Brillouin equation. A linear response to variable field under conditions where one might expect saturation is characteristic of a linear Heisenberg antiferromagnet. This is not uncommon for antiferromagnetically coupled materials, including many of the MI_2 starting materials and several organic nitronylnitroxides discussed in Chapter 2. Many pure materials also display a minimal curvature in addition to this large linear component, sometimes fitting to S<0.5, a condition which is not physically possible. In this research such curvatures have never overestimated the spin state of the material as determined by variable temperature methods. In these cases the assumption of noninteracting paramagnets that underlies the Brillouin plot is false, but the fit to the spin state is often nearly what one would expect for ideal materials. As such, the S=2 spin state is not irrefutably representative of the material, but it can be

argued with a high degree of certainty that S>1, and that the spin state of the material is raised by ferromagnetic interactions between the ligand and metal.

Soluble complexes of metals and MBDCNQI

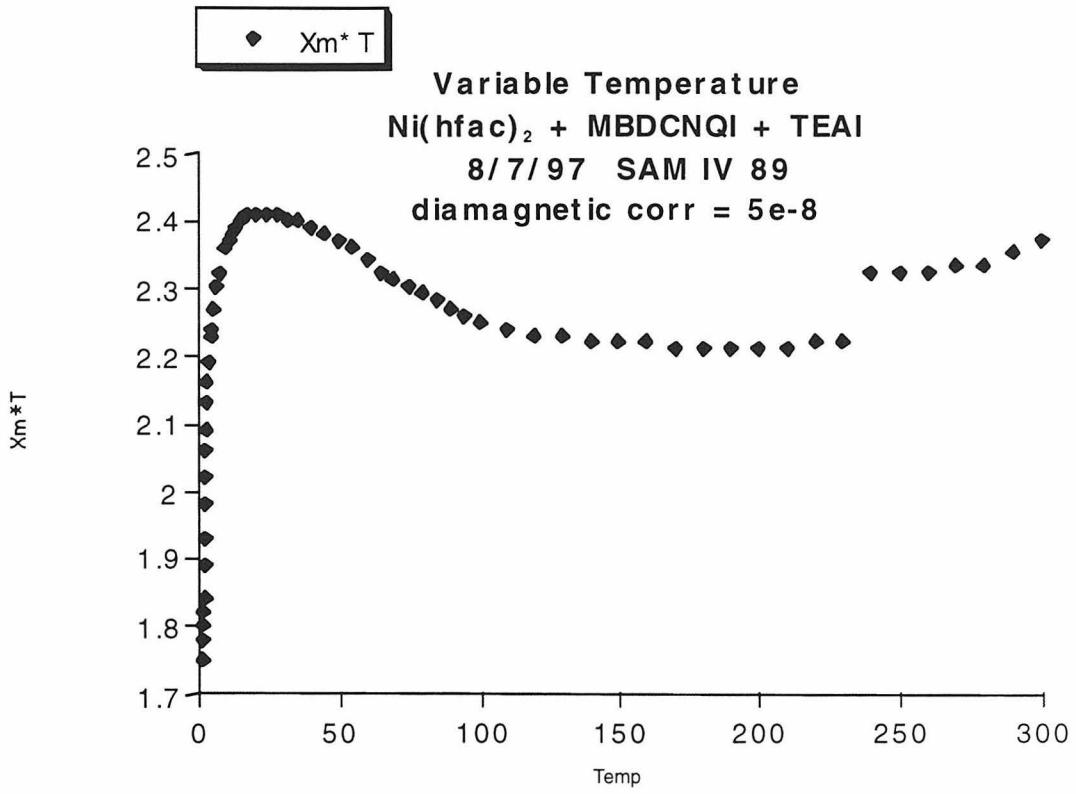

Figure 3.12 - The reaction between $Ni(hfac)_2$ and $MBDCNQI^{2-}$ • 2 $TEAI^{+}$ yields an insoluble solid with a significant upturn. A control experiment using DCNQI as the ligand yielded qualitatively similar results. The discontinuity of the data at 240K is an error of the instrument seen in other experiements and is not real.

Several attempts were made to create a soluble system of Ni and MBDCNQI that could be better characterized. MBDCNQI reduced with

tetraethylammonium iodide (TEAI) in acetonitrile was reacted with Mn and $Ni(acac)_2$ and $Ni(hfac)_2$ to yield insoluble compounds with magnetic data similar to the reaction if NiI_2 with MBDCNQI (Figure 3.12). This is likely the result of dissociation of the acac or hfac ligand from the metal, followed by irreversible formation of an insoluble Ni-MBDCNQI network. Other metal acac and hfac derivatives gave similar results.

Manganese porphyrin complexes were also reacted with reduced MBDCNQI to yield interesting materials, analagous to the TCNE-Mn(porph) ferromagnet characterized by Miller's group.[15] These materials were also insoluble, and thus impossible to completely characterize. There was extremely weak evidence of an upturn near 70K, but because of the difficulty of working with this material, the product was not pursued.

In order to create a more stable compound, a metal complex had to be created with a capping ligand that could inhibit network formation by being drastically less likely to dissociate than acac or hfac. The purple complex of nickel nitrate with tris(2-aminoethyl)amine (N4), shown in Figure 3.13, was crystallized from hot ethanol/THF as the hydrate, and subsequently used for further studies.

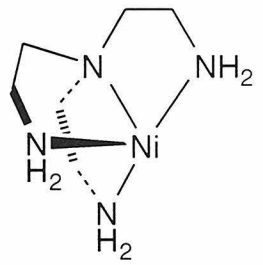

Figure 3.13 - Nickel capped by tris(2-aminoethyl)amine. The solid is crystallized as the hydrate.

Complexes with Ni(N4) and attempts at crystallization

Ni(N4) can be dissolved in methanol and mixed with the MBDCNQI dianion (from a reaction with TEAI) in a variety of solvents to form a blue solution that is stable at low concentrations.

Several attempts have been made at crystallization, including: slow cooling, slow evaporation under argon, vapor-phase diffusion of hexanes into a solution of the complex, and layering hexanes above a solution of complex at room temperature. The samples have been too soluble for cooling to successfully crash them out of solution from the reaction mixture. Removing the solvent, redissolving the material in a minimum of solvent, and cooling causes the precipitation of a fine blue/black powder in all conditions tried. Crystals of a colorless tetraethylammonium salt were isolated, but never crystals of the desired product.

Though the solutions are stable when cold, slow concentration at room temperature yields an amorphous powder that will not redissolve. This decomposition may result from an inherent instability of the material or from dissociation of the N4 capping ligand to allow network formation. All attempts at slowly crashing out material by evaporation or diffusion of a poor solvent (hexanes) into a solution of product at room temperature have resulted in this insoluble powder.

The iodide salt of Ni(N4) can also be made by dissolving the nitrate in methanol and adding a methanolic solution of excess LiI, then crashing the

product out with ether. This salt is preferred because it eliminates the need for tetraethylammonium salts, which can precipitate out before the product in low dielectric solvents. The resulting blue solid is shown by elemental analysis (C 15.98, H 4.05, N 12.19, expected C 15.71, H 3.95, N12.21) to have completely lost its nitrate counterions.

Reactions with the iodide salt yield very similar results to those from the nitrate salt. Reaction of MBDCNQI with NiN4 iodide at -78°C yields a fine blue powder.

Conclusion

The MBDCNQI dianion diradical is a triplet as determined by EPR and SQUID. The molecule easily forms complexes with many transition metals to form insoluble network solids. Its interactions with nickel complexes are ferromagnetic, as predicted. Complexes with a nickel capped by a tetradentate ligand are more stable towards decomposition into a network solid, but this still may occur at room temperature. This material did not display any tendancy to from crystals.

Experimentals

1,3-Dibromo-5-*t*-butylbenzene (2) 2-*t*-Butylaniline (50g. 0.34 mol) is dissolved in 500ml DMF and cooled in an ice bath. NBS (120g, 0.68 mol) is added over

15 minutes and the reation turns dark. The system is stirred for 90 minutes at room temperature then heated to 70°C. t-Butyl nitrite (67 ml, 0.75 mmol) is dissolved in 100ml DMF and added dropwise over 30 minutes to the aniline solution, evolving nitrogen gas. The system is allowed to cool to room temperature and stirred overnight. Column chromatography followed by distillation affords 30g (31% overall yield) of the colorless, crystalline product. 300 MHz ^{1}H NMR, $CDCl_3$, δ = 1.31, s, 9H; 7.45, d, 2H; 7.50, t, 1H. 75 MHz ^{13}C, $CDCl_3$, δ = 31.1, 35.2, 122.9, 127.7, 131.2, 155.3.

2,5-Dimethoxy-4-methylbenzeneboronic acid (3) A solution of 2,5-dimethoxy-4-methyl-1-bromobenzene **(1)** (67.5g, 0.292 mol) under argon in 500ml of freshly distilled THF is cooled to -78°C. 200ml of 1.6M butyllithium in hexanes is canulaed in slowly, and the solution is stirred at -78°C for 4 hrs. Care must be taken to ensure that the system continues to stir throughout the butyllithium addition. 150ml of freshly distilled trimethylborate is dissolved in 300ml THF in a 2L roundbottom flask and this system is cooled to -78°C under argon. The lithiated solution is canulaed into the trimethyl borate solution over 25 minutes. This mixture is stirred for 3 hours at -78°C then allowed to warm to room temperature overnight. The product solution is quenched with pH=7 buffer, then extracted with ether and brine. The organic layer is dried with $MgSO_4$ and evaporated. The resulting solid is recrystallized from hexanes. 30g of pure product (52% yield) is recovered. The mother liquor can be evaporated down and 9.2g of less pure material (total 69% yield)

can be recovered upon recrystallizing from hexanes. 300 MHz ^{1}H NMR, $CDCl_3$, δ = 2.28, s, 3H; 3.86, s, 3H; 3.89, s, 3H; 6.61, s, 2H (boric acid hydrogens - shift is variable); 6.77, s, 1H; 7.30, s, 1H. 75 MHz ^{13}C, $CDCl_3$, δ = 17.0, 55.9, 56.1, 113.3, 117.2, 131.8, 152.1, 158.7 (boric acid carbon is not visible).

Bis-1,3-(2,5-dimethoxy-4methylphenyl)-5-*t*-butylbenzene (4) **2** (10.5g, 36.0 mmol) and **3** (15.0g, 76.5 mmol) are combined in a 500ml flask and the system is flushed with argon. The solids are dissolved in 125ml of freshly distilled and degassed acetonitrile, and powdered K_3PO_4 (73.8g, 348 mmol) and $Pd[P(Ph)_3]_4$ (1.0g, 0.87 mmol, 2.4%) are added. The system is refluxed 9 hrs. Diethyl ether is added and the organic layer is washed 3 times with water then dried with $MgSO_4$. The organic solvent is evaporated and the product is recrystallized from methanol to isolate 9.5g of a beige solid. 1.3g more is isolated this way from the mother liquor. The total yield is 68%. 300 MHz ^{1}H NMR, $CDCl_3$, δ = 1.43, s, 9H; 3.81, s, 6H; 3.84, s, 6H; 6.93, s, 2H; 6.99, s, 2H; 7.60, t, 1H; 7.65, d, 2H. 75 MHz ^{13}C, $CDCl_3$, δ = 16.5, 31.7, 35.0, 56.1, 56.5, 113.6, 114.9, 125.6, 126.5, 127.8, 129.1, 138.1, 150.2, 150.3, 151.9. GC/MS m/z 434 (M^+, 100), 419 (17), 348 (25), 217 (10), 57 (25).

MBQ (5) **4** (9.5g, 21.7 mmol) is dissolved in 100mL of chloroform and 100 mL of 50% acetonitrile in water, then cooled in an ice bath. Ceric ammonium

nitrate (50g, 91.2 mmol) is dissolved in 150 ml of 50% acetonitrile. Solid pyridine-2,6-dicarboxylic acid-N-oxide[13] is added to the solution of **4**, the ceric ammonium nitrate solution is added quickly thereafter, and the mixture is stirred for 2 hours. The chloroform later is washed 4 times with water, dried with $MgSO_4$, and evaporated. 3.95g of **5** are recoverred by recrystallizing the residue from methanol. 1g more may be recovered by recrystallizing the mother liquor. Total yield is 61%. 300 MHz ^{1}H NMR, $CDCl_3$, δ =1.36, s, 9H; 2.11, s, 6H; 6.72, q, 2H; 6.90, s, 2H; 7.40, t, 1H; 7.55, d, 2H. 75 MHz ^{13}C, $CDCl_3$, δ = 15.6, 31.3, 35.1, 127.8, 128.0, 132.7, 133.1, 133.9, 145.7, 145.9, 151.8, 186.8, 188.1. FTIR 2966 (m), 1660 (vs), 1602 (m), 1236 (m), 1178 (m), 913 (m), 898 (m).

MBDCNQI 5 (3.95g, 10.45 mmol) and bis(trimethylsilyl)carbodiimide (16g, 86 mmol) are dissolved in 200ml freshly distilled dichloromethane and cooled to ice. $TiCl_4$ (16g, 84 mmol) is added over 5 minutes. The dark solution is allowed to warm to room temperature and stirred overnight, then cooled to ice and carefully quenched with water. The biphasic solution containing suspended TiO_2 is filtered through celite and the dichloromethane layer is dried with $MgSO_4$ and evaporated. The product is recrystallized from benzene to yield 2.7g (55%). Mp = 146 (dec). 300 MHz ^{1}H NMR, $CDCl_3$, δ = 1.40, s, 9H; 2.39, 2, 6H; 7.35, t, 1H; 7.49, s, 2H; 7.52, d, 2H; 7.60, d, 2H. 75 MHz ^{13}C, CD_2Cl_2, δ = 16.8. 30.9, 35.0, 128.2, 128.3, 128.9, 129.1, 132.8, 146.8, 146.9, 152.2, 175.4, 175.6, cyano carbons not visible. GC/MS m/z 475.2 (M^++5, 36), 451.2 (35),

433.2 (20), 417.1 (20), 391.2 (20), 307.1 (100), 289.1 (65), 291.1 (33). FTIR 2964 (m), 2174 (s), 1546 (vs), 1385 (vs), 1262 (m), 1112 (m, broad), 802 (m, broad), 668 (s).

MBDCNQI dianion diradical. MBDCNQI is dissolved in dichloromethane. An acetonitrile solution of excess tetraethylammonium iodide or 2 equivalents cobaltocene is added to the MDCNQI, and the solvent is removed in vacuo. The nitrile stretch of this material is 2103 cm^{-1}, charcteristic of an unbound reduced DCNQI system.

General procedure for the synthesis of MI_2 and other insoluble metal complexes of MBDCNQI. MBDCBQI (35mg, 0.75mmol) is dissolved in acetonitrile with heating. In a separate flask, the metal iodide (excess) is dissolved in acetonitrile with heating. Upon cooling, the MBDCNQI solution is added to the metal iodide solution and a blue product precipitates. This product is insoluble in all organic solvents. The FTIR of the product does not depend on the order or rate of addition or the solvent used. Elemental analysis of the products shows one half to one equivalent of unreacted iodide per equivalent of MBDCNQI. The materials were characterized by the position of the nitrile stretch in the IR: unreacted MBDCNQI: 2173 cm^{-1} (sharp); Cu salt: 2138 cm^{-1} (broad); Mn salt: 2116 cm^{-1} (broad), 2236 cm^{-1} (weak); Fe salt: 2084 cm^{-1} (broad), 2236 cm^{-1}; Ni salt: 2100 cm^{-1} (broad); Cr salt: 2085 (broad), 2227 cm^{-1} (broad, weak); Co salt: 2122 cm^{-1}; 2172 cm^{-1}; 2236 cm^{-1} (shoulder); V salt: 2173 cm^{-1} (sharp), 2233 cm^{-1} (sharp). Other metal complexes

follow the same procedure, replacing the MI_2 with, for example, tetraethylammonium iodide (TEAI) plus $Mn(hfac)_2$. These materials had nitrile stretches in the area of 2110 cm^{-1} and 2221 cm^{-1}.

Ni[tris(2-aminoethyl)amine] nitrate, monohydrate (NiN4 nitrate). Nickel nitrate hexahydrate (5.45g, 18.7mmol) is dissolved in 20mL water, and tris(2-aminoethyl)amine is added, causing the reaction to change color from green to purple. After 1 hour 20mL ethanol is added, and THF is added until the product precipitates. Heating the system and slow cooling allows purple crystals to form, elemental analysis C 20.82, H 5.84, N 24.29 (theoretical C 20.77, H 5.81, N 24.22).

Ni[tris(2-aminoethyl)amine] iodide. (NiN4 iodide). NiN4 nitrate and excess lithium iodide are dissolved in 25mL distilled methanol under argon and combined. The product solution is canulaed into 300mL of distilled diethyl ether and filtered. The resulting blue powder has elemental analysis C15.98, H 4.05, N12.19 (theoretical C15.71, H3.95, N12.21).

NiN4 complexes of MBDCNQI. a) 1 equivalent NiN4 nitrate is dissolved in methanol; 1 equivalent MBDCNQI is dissolved in acetonitrile; 3 equivalents TEAI is dissolved in acetonitrile. The TEAI solution is added to the MBDCNQI, turning it blue. The MBDCNQI is then added to the NiN4 nitrate solution to form a blue/black solution. The product has a broad IR stretch at

about 2120 cm^{-1}. The product can also be reduced with LiI, dried in vacuo, and washed with ether to remove excess lithium salts, though this is incomplete based on elemental analysis. Attempts at crystallization were unsuccessful. b) 1 equivalent of NiN4 iodide is dissolved in methanol; MBDCNQI is added from an acetonitrile or THF solution and the solution turns blue/black. All attempts at recrystallizing this solution by cooling yielded only a fine precipitate.

---

[1] Ferraris, J.; Cowan, D.O.; Walatka Jr., V.; Perlstein, J.H.; *Journal of the American Chemical Society*, **1973**, *95*, 948

[2]Williams, J.M.; Schultz, A.J.; Geiser, U.; Carlson, K.D.; Kini, A.M.; Wang, H.H.; Kwok, W-K.; Whangbo, M-H.; Schirber, J.E.; *Science*, **1991**, *252*, 1501

[3] Miller, J.S.; Epstein, A.J.; *Angewante Chemie, International Edition*, **1994**, *33*, 385

[4] Aumüller, A.; Hünig, S.; *Liebigs Ann. Chem.*; **1986**, *1986*, 165

[5] Aumüller, A.; Hünig, S.; *Liebigs Ann. Chem.*; **1986**, *1986*, 142

[6]Hünig, S.; *Journal of Materials Chemistry*, **1995**, *5*, 1469

[7] Manriquez, J.M.; Yee, G.T.; Mclean, R.S.; Epstein, A.J.; Miller, J.S.; *Science*, **1991**, *252*, 1415

[8] Campana, C.; Dunbar, K.R.; Ouyang, X.; *Chemical Communications*, **1996**, *1996*, 2427

[9] Xiang, O.Y.; Campana, C.; Dunbar, K.R.; *Inorganic Chemistry*, **1996**, *35*, 7188

[10]Zhao, H.H.; Heintz, R.A.; Dunbar, K.R.; Rogers, R.D.; *Journal of the American Chemical Society*, **1996**, *118* , 12844

[11] Hünig, S.; Aumüller, A.; Erk, P.; Meixner, H.; *Synthetic Metals*, **1988**, *27*, B181

[12] a) Martin, N.; Navarro, J.A.; Seoane, C.; Albert, A.; Cano, F.H.; Becker, J.Y.; Khodorkovsky, V.; Harlev, E.; Hanack, N.; *Journal of Organic Chemistry*, **1992**, *57*, 5726. b) Czekanski, T.; Hanack, M.; Becker, J.Y.; Bernstein, J.; Bittner, S.; Kaufman-Orenstein, L.; Peleg, D.; *Journal of Organic Chemistry*, **1991**, *56*, 1569

[13] Syper, L.; Kloc, K.; Mlochowski, J.; Szulc, A.; *Synthesis* , **1979**, *1979*, 521

[14] Gerson, F.; Gescheidt, G.; Möckel, R.; Aumüller, A.; Erl, P.; Hünig, S.; *Helvetica Chemica Acta*, **1988**, *7*, 1665

[15]Miller, J.S.; Calabrese, J.C.; McLean, R.S.; Epstein, A.J.; *Advanced Materials*, **1992**, *4*, , 498

Chapter Four : Investigations of Derivatives of Poly(arenemethide)

Of all the conducting polymers synthesized, poly(acetylene) has stood out as the subject of the most intense investigations. This is for several reasons, including its primacy (it was the first conducting polymer discovered) and its simplicity[1] (its straightforward structure is well-accomodated to theoretical modeling).

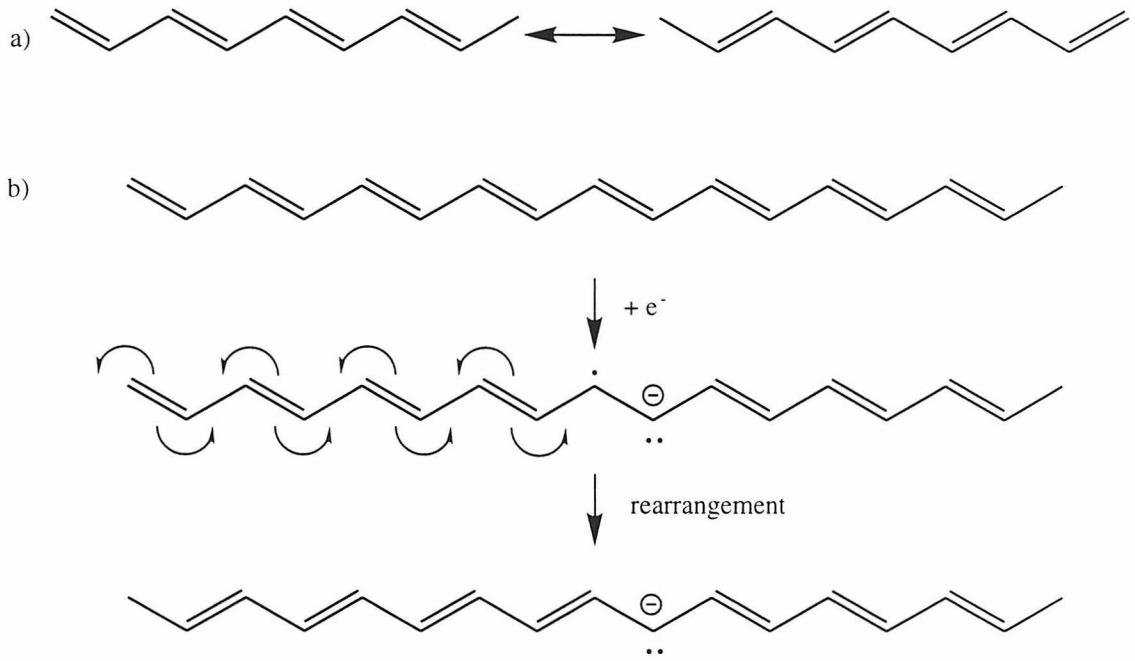

Figure 4.1 - a) The degenerate ground states of polyacetylene. b) Doping the polymer initially creates a radical anion, which can rearrange into a spinless state called a soliton.

Poly(acetylene) is unusual among the conducting polymers because its simple structure is degenerate - there are two energetically identical but

physically different possible ground states, as shown in Figure 4.1a. This degeneracy has physical ramifications: when doped, the polarons formed can rearrange to form spinless solitons (Figure 4.1b). This effect has been confirmed by magnetic studies on the doped polymer.[2]

Solitons have been of considerable interest to physicists, but polyacetylene, along with a less-studied form of polyaniline[3], are the only conducting polymers that have been synthesized with a true degenerate structure. The understanding of solitons in organic polymers would be greatly increased by the addition of a third member to the family.

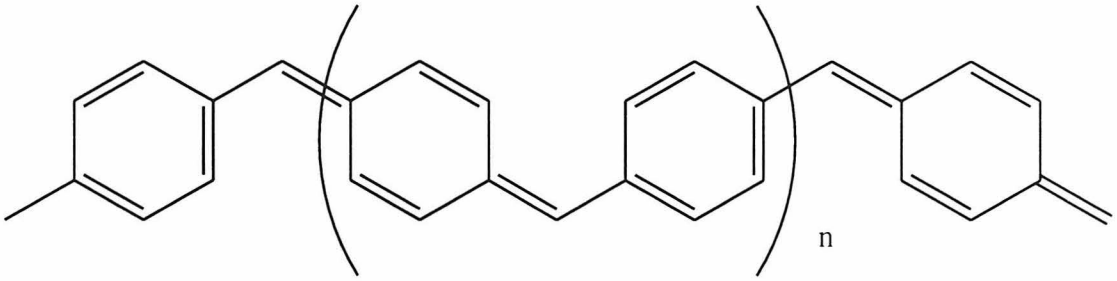

Figure 4.2 - Poly(arenemethide)

One such possible member is the theoretical polymer, poly(arenemethide), shown in Figure 4.2. Conceptually, the alternating double and single bonds of poly(acetylene) have been replaced with alternating quinones and benzene rings, respectively. This material is predicted to carry solitons and have an exteremely low bandgap.[4] Unfortunately, quinonemethides are known to be extremely unstable, and this exact material is unlikely to ever be synthesized.

Derivatives of the parent poly(arenemethide) are possible. Scherf et al. have attempted to synthesize a ladder polymer, but the product was poorly characterized.[5] No other attempts at poly(arenemethide) synthesis have appeared in the literature.

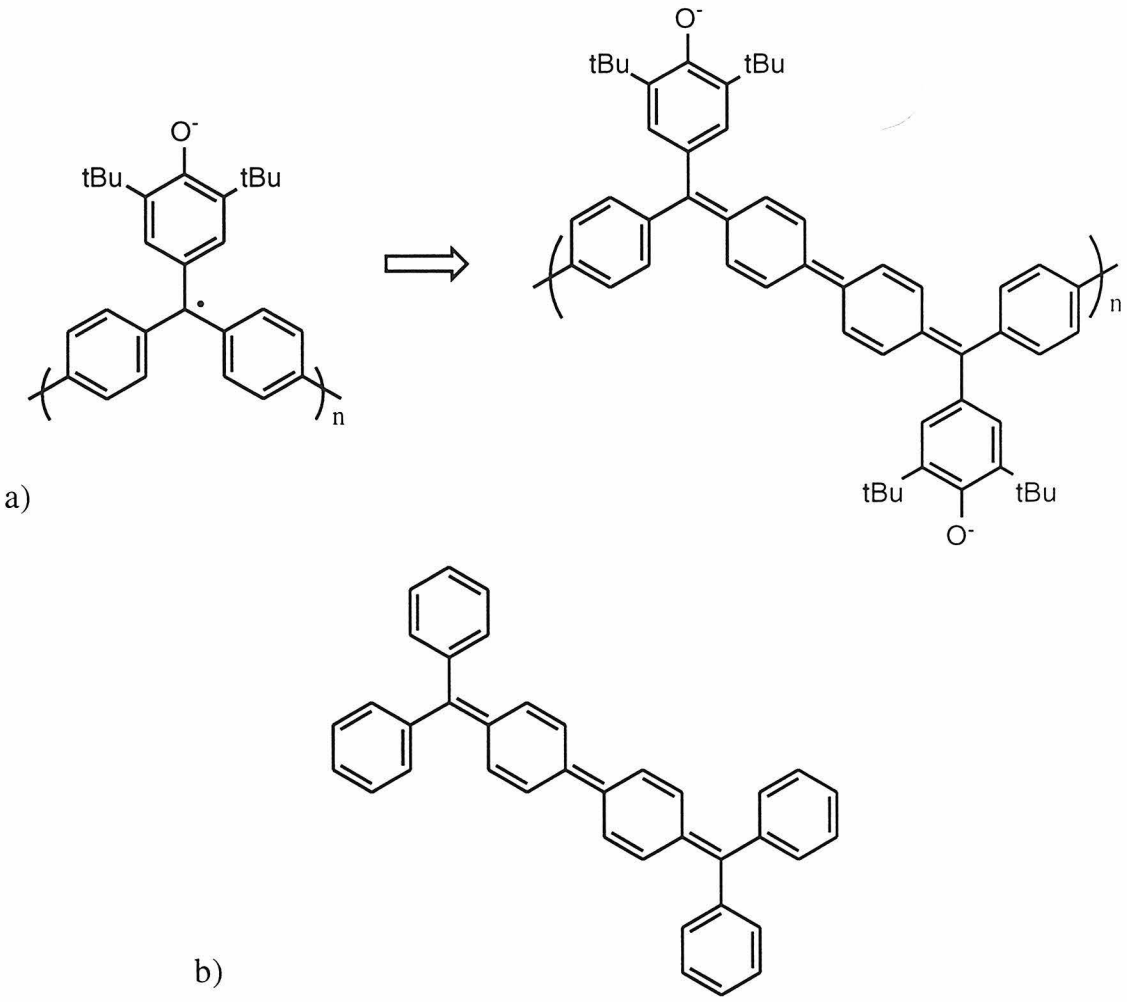

Figure 4.3 - Synthetically accessible derivatives of PAM, such as the poly(fuchsone) polyanion (a) can be conceptuallized as derivatives of Chichibabin's hydrocabon (b).

Our strategy towards poly(arenemethide) uses the α-phenyl derivative such as that shown in Figure 4.3a. The concenptual monomers of these

polymers are derivatives of Chichibabin's hydrocarbon (Figure 4.3b), which is well-known and has been crystallized.[6] By allowing delocalization of any radical character along the α-phenyl group, these derivatives are expected to be electronically more stable than the parent. Any twisting of the phenyl groups will decrease the resonance stability but add steric protection to the α carbon. Finally, the addition of solubilizing groups to the α-phenyl ring should allow these polymers to be completely characterized in both the solid state and in solution.

Synthesis and characterization of Polymers

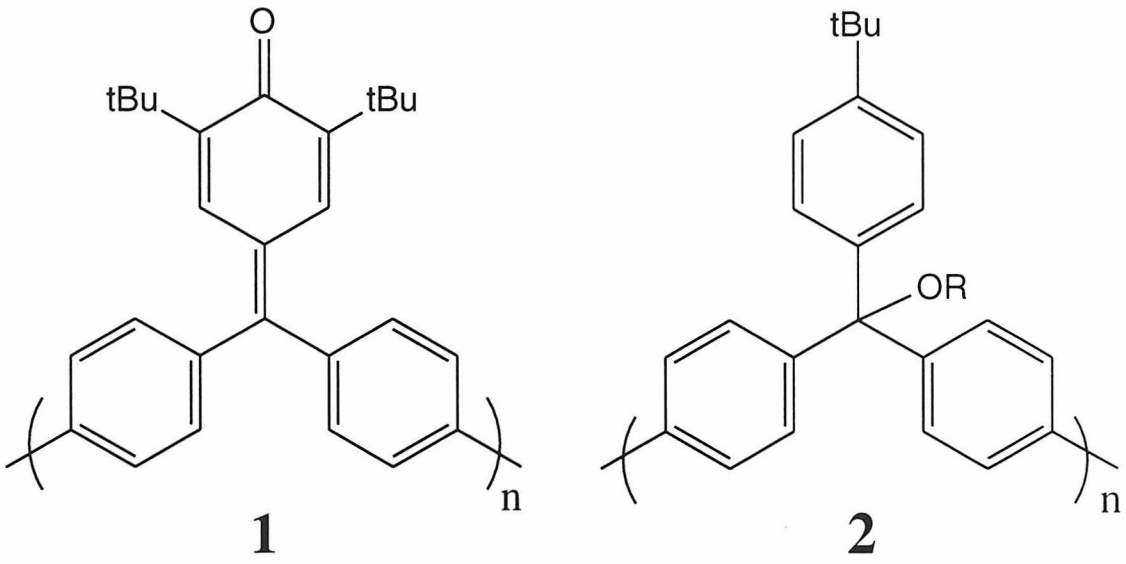

Figure 4.4 - Target polymers (1) and (2). These polymers will assume the PAM backbone when doped.

Polyfuchsone

Polyfuchsone (**1**) was synthesized by both an asymmetric Suzuki coupling and a symmetric nickel-catalyzed condensation.

The Suzuki path is outlined in Scheme 4.1. The asymmetric benzhydrol (**3**) is prepated using standard alkyllithium chemistry. The condensation of **3** with 2,6-di(*tert*-butyl)phenol must be done with some care: the trimethylsilyl group is labile under the condensation conditions. Nitric acid is added to a solution of the starting materials in a minimum of nitromethane at ice temperature, and the solution is stirred for only 10 minutes before the reaction is quenched with brine and extracted with ether. Yields for this procedure are about 40%.

Next, **4** is oxidized to the fuchsone **5** with DDQ in nearly quantitative yield and recrystallized. The TMS can then be exchanged for a boric acid by using 3 equivalents of BBr_3 and 2 equivalents of triethylsilane. The first equivalent of BBr_3 chelates the fuchsone oxygen and lends a significant amount of cationic character to the system, inhibiting cleavage of the TMS. Under these conditions, the triethylsilane reduces the fuchsone in situ and a second equivalent of BBr_3 cleaves the TMS. Quenching the reaction with pinacol yields **6**.

Polymerization of **6** with $Pd(PPh_3)_4$ in toluene/2.0M Na_2CO_3 for 7 days yields the polymer **7**. The polymer is quantitatively oxidized to **1** with DDQ. Alternatively, the precursor **6** can be oxidized with DDQ to a fuchsone monomer, and polymerization goes forward under the same conditions. **1** is

purified from the catalyst and low-molecular weight oligomers by dissolving in THF and crashing twice from methanol and once from hexanes. GPC analysis of the material shows M_n=7200, M_w=12500, PDI=1.74, where M_n is the equivalent of a twenty-mer. This length was confirmed by vapor-phase osmometry.

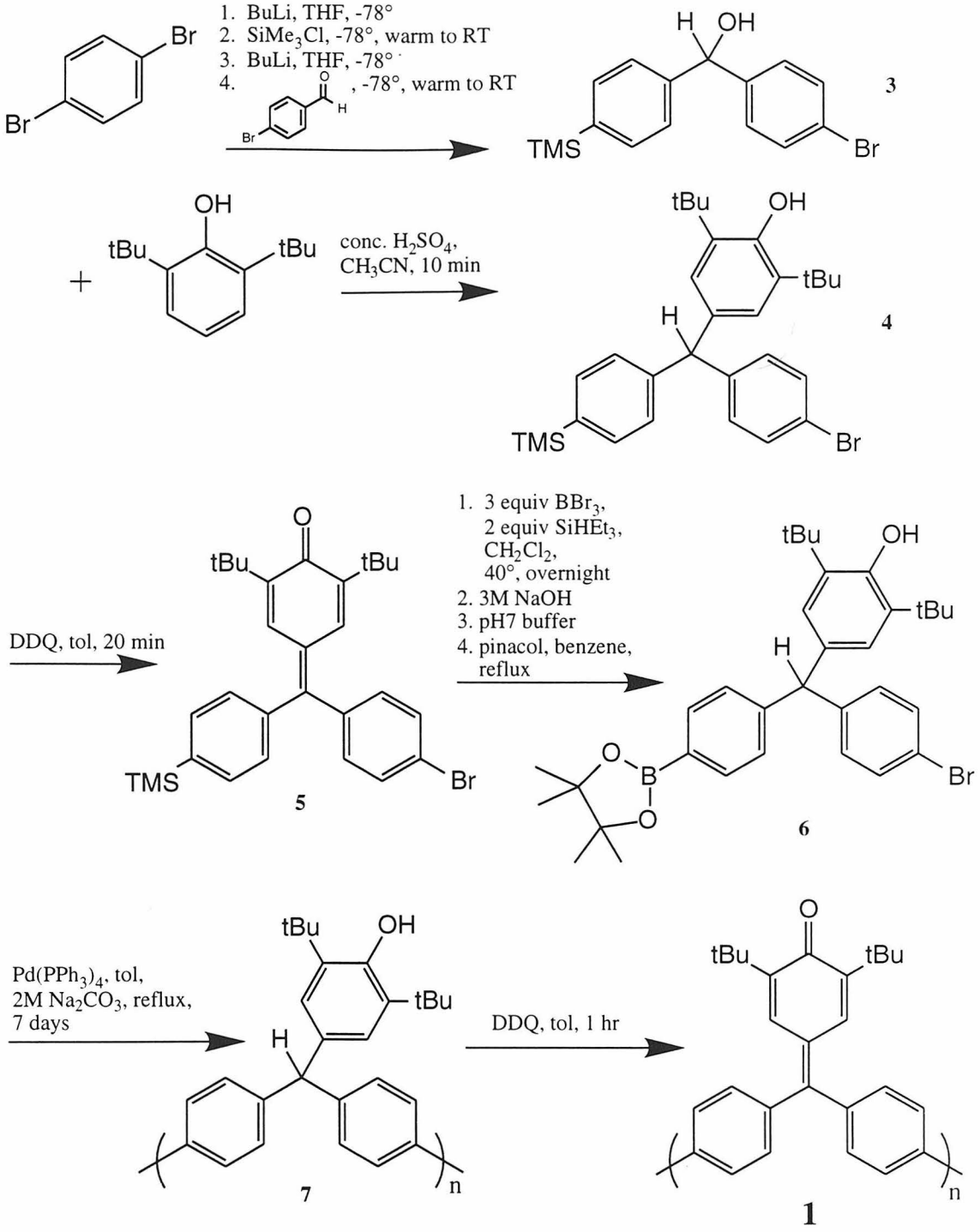

Scheme 4.1 - A synthesis of poly(fuchsone) via Suzuki chemistry

An improved method was developed based on direct coupling of dibromofuchsone[7] promoted by nickel, shown in Scheme 4.2. Nickel homocouplings generally proceed in high yield only in polar solvents, such as DMF, in which the polyfuchsone is insoluble. Modification of the procedures of Percec[8] and DeSimone[9] gives a system where 5% $Ni(PPh_3)Cl_2$ in the presence of 1 equivalent of Zn and 1 equivalent of tetraethylammonium iodide in THF polymerizes dibromofuchsone and dichlorofuchsone with excellent yield. The product was partially reduced under the polymerization conditions but could be oxidized quantitatively back to the fuchsone with DDQ. GPC analysis shows M_n=16000, M_w=26900, and PDI=1.69, which corresponds to an average length of about 40-45 units, and this was confirmed by vapor phase osmometry. This material is barely soluble in any solvent and must be refluxed in hot THF to be dissolved; the solubility was probably the limiting factor in the polymerization length. Crashing dissolved polymer out from THF twice with methanol follwed by once with hexanes yields pure product. This polymer was used for all fuchsone experiments listed below.

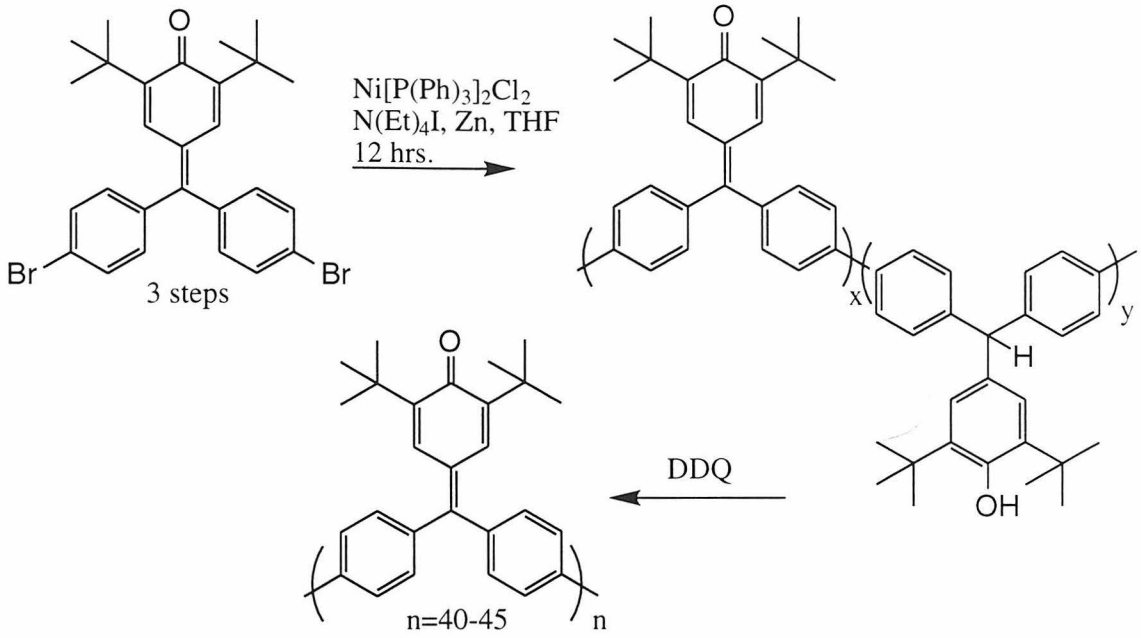

Scheme 4.2 - Improved synthesis of poly(fuchsone) via nickel chemistry

The ^{1}H NMR for **1** is unusually sharp for a polymer, indicating it may behave as a rigid rod in solution. ^{13}C NMR data could not be collected: the material gels in THF or chloroform at high concentrations, adding to the difficulty of obtaining a ^{13}C spectrum for any polymer. The CV of the polymer (Figure 4.4) is slightly shifted from that of the monomer, with a chemically reversible first wave followed by an irreversible second wave. The separation between the two waves is approximately 500 meV.

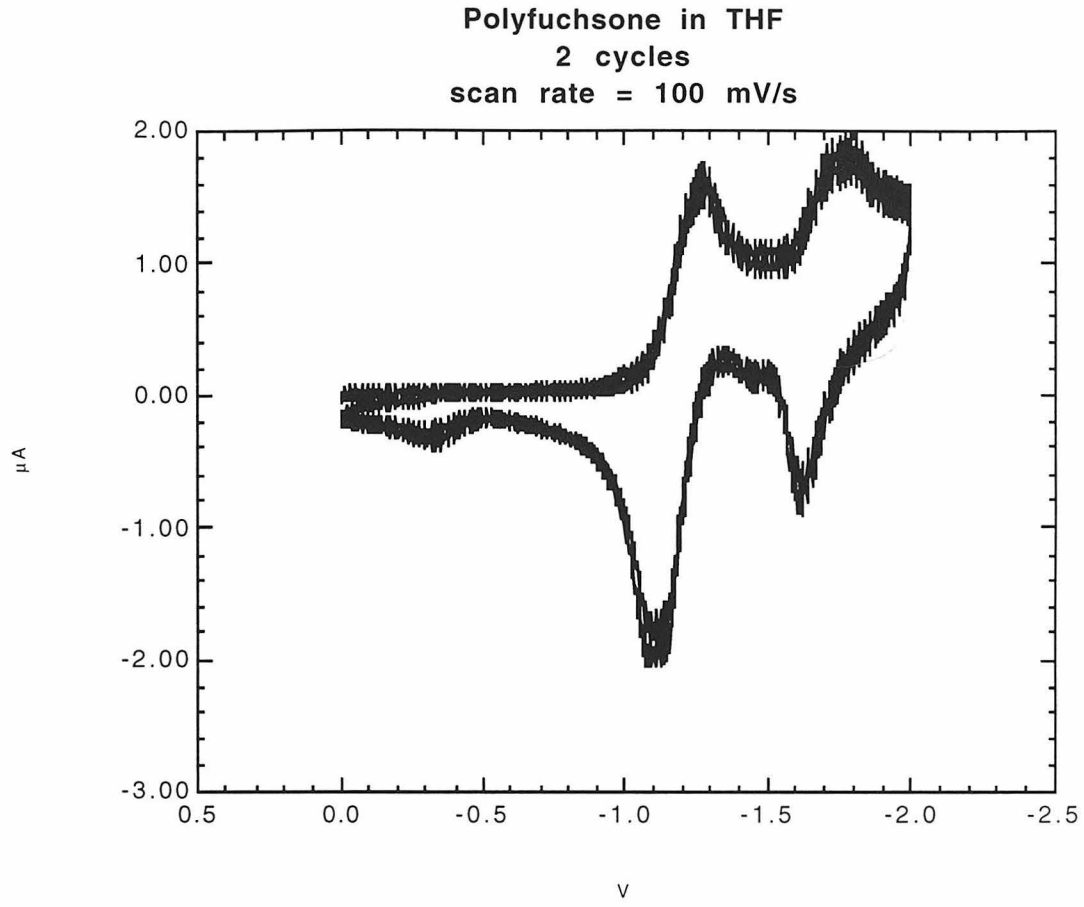

Figure 4.5 - CV of poly(fuchsone) in THF with 0.1M $LiClO_4$ vs an Ag/AgCl pseudoelectrode. The first reduction wave at $E_{1/2}$=-0.87V vs NHE is chemically reversible; the second is not, and results in the growth of a new oxidation wave at -0.3V that is not inherent to the material. The fuzziness of the data is due to electronic feedback in the instrument and does not affect the results.

Polytrityl precursor polymer (PTP)

The polytrityl precursor **2a** (PTP) was synthsized via standard Suzuki conditions, shown in Scheme 4.3. 4-*tert*-Butylphenylmagnesium bromide was reacted with dibromobenzophenone and quenched with methyl iodide to

yield the methoxy ether. Alternatively, the alcohol formed when the system is quenched with water can be dissolved in trifluoroacetic acid and quenched with methanol to yield the methoxy ether. Lithiation with one equivalent of butyllithium followed by quenching with trimethylborate then ethylene glycol yields the polymerization monomer. Polymerization using 5% $Pd(PPh_3)_4$ in toluene/2.0M Na_2CO_3 for 7 days, followed by purification by dissolving in THF and crashing out three times with methanol, gives the polymer **2a**. VPO analysis shows M_n of about 2000, corresponding to hexamer.

PTP **2a** can also be prepared from **8** above using the nickel catalyst system developed for the fuchsones. GPC analysis shows this polymer is a decamer, with M_n=3450, M_w=4600, and PDI=1.33.

Treatment of **2a** with trifluoroacetic acid (TFA) generates a purple cation in solution. Removal of the TFA in vacuo leaves the trifluoroacetate **2b**. This product contains a covalent bond between the trityl unit and the trifluoroacetate, and the purple color is the result of a small amount of cation created by excess TFA that cannot be removed. This TFA can interfere with attempts to dope the material and can be eliminated by dissolving the polymer in dichloromethane and neutralizing the acid with a drop of distilled lutidine. After removing the solvent, the resulting polymer **2b** is colorless.

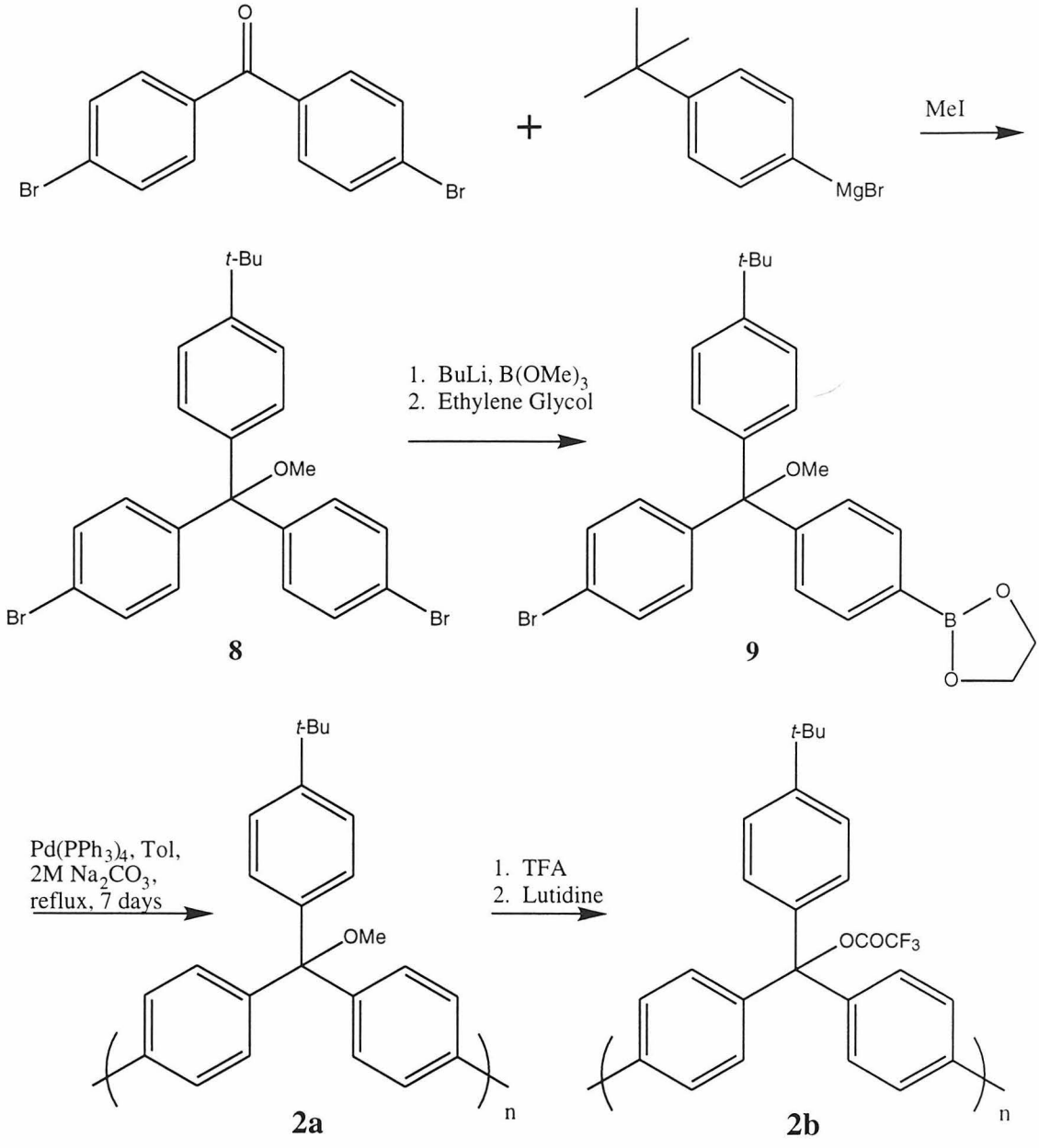

Scheme 4.3 - Synthesis of poly(trityl) precursors (PTPs) 2a and 2b.

Doping of polymers

Polyfuchsone

Attempts at chemically doping polyfuchsone were unsuccessful. Dissolving the polymer and stirring with solid sodium or sodium naphthalide lead to degradation of the material, as did attempts to expose a thin film of **2** to potassium vapor.

Electrochemical doping was performed in THF with 0.3M $LiClO_4$ and is described elsewhere.[10] All solvents used were purified by distillation or passing through an activated alumina column and were freeze-pump-thawed three times. Doping was performed in a drybox under nitrogen atomosphere.

The polymer itself could not be dissolved in the solution with electrolyte and was instead dissolved in pure THF and added to the cell after pre-electrolysis. Reduction was performed at -1.1V vs Ag/AgCl, which should incompletely dope the material. The green reduced polymer stays in solution during the entire process. The electrolysis solution is poured into a flask and evacuated to leave a residue of polymer and electrolyte. Addition of ether to this flasks dissolves the electrolyte but not the polymer, and the residue is collected by filtration. Addition of THF dissolves the polymer, but the resulting solution is the original orange color, characteristic of undoped fuchsone, not green. These solutions have been cast as thin films onto glass plates and have shown no conductivity by four-point probe measurements.

Further experiments have shown that the polymer will slowly lose its color over hours when left standing in solution in the drybox.

The polymer was also cast as a thin film (about 100nm) on an ITO-coated slide. This slide was used as the working electrode in a cell containing acetonitrile and 0.1M tetrabutylammonium perchlorate, in which the undoped polymer is insoluble. Electrolysis of the slide results in dissolution of the material, which could not be recovered.

Attempts at electrolysis in a 0.1 mm UV cell also failed. The molar absorbtivity of the material is high enough that 10μM solutions of polymer were required, increasing complications due to very low-level contaminants in the solvent.

Poly(trityl) precursor (PTP)

The original attempts to dope PTP focused on reduction of the poly(trifluoroacetate) derivative **2b**. Addition of cobaltocene to a chloroform solution of **2b** oxidizes cobaltocene to coboltocenium and reduces the polymer to the blue PAM oligomer. The blue color is persistent for weeks in the absence of air or water. The reduced polymer could not be separated from the cobaltocenium trifluoroacetate salt for conductivity measurements.

Another series of attempts were made to dope **2a** directly using lithium powder, as has been done by Racja with similar materials.[11] PTP is stirred with Li powder in THF for one week, after which it has an intense blue color. This color may last for months in a sealed tube. The NMR of the product

from a reaction in d_8-THF, however, shows no change after exposure to air, and it is unclear that it represents the PAM.

Attempts were made to dope PAM polymers from both procedures towards the preparation of a conducting polymer. Blue solutions of PAM in dichloromethane were mixed with 0.1 to 0.5 equivalents of $AgBF_4$ or $AgNO_3$. This produced a slight purple color in the solution, characteristic of the trityl cation. Thin films of these doped polymers, cast either by spin coating or slow evaporation, did not show any signs of conductivity.

Discussion and Conclusions

This project failed to yield any conducting polymers. There are two possible reasons for this failure: the materials are highly twisted, and perhaps too unstable. These explanations apply to both poly(fuchsone) and poly(trityl) and will be discussed for both systems.

Twisting as a barrier to conductivity

As discussed in Chapter 1, twisting of the conjugated backbone of polyacetylene destroys conductivity in the material. These materials are based on the trityl unit, in which the phenyl rings are known to be significantly twisted out of planarity. Polymers based on fluorene, such as that shown in Figure 4.6, might have had less (though not zero) backbone twisting. Attempts at synthesizing monomers with the proper topology and based on fluorene were unsuccessful. It is also unclear whether such a rigid system would still be soluble. In retrospect, because substituted poly(*p*-phenylene)s are poor conductors[12], it seems unlikely that the systems studied here would be any better.

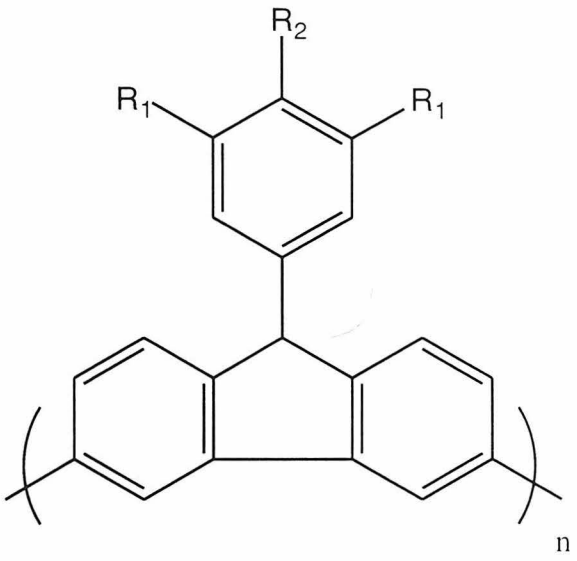

Figure 4.6 - PAM precursors based on fluorene might eliminate some twisting.

Instability of the materials

As discussed in the introduction, the target PAM derivatives are conceptually based on Chichibabin's hydrocarbon as the monomer. Chichibabin's hydrocarbon has a long and controversial history[6], in part because of the instability of the material. NMR of the crystals used for the

known crystal structure[13] gives a very broad signal, likely due to radical impurities. The hydrocarbon is also known to be extremely sensitive to oxygen and moisture.

Polymers based on such a material must overcome not only the inherent instability of the monomer, but also the presence of defects at the end of the polymer chain. These defects may allow crosslinking through unreacted terminal bromides or unblocked phenyl rings. Any chains with an odd number of monomers will be highly delocalized radicals, and such a system might be expected to be even more reactive than the closed-shell Chichibabin's hydrocarbon.

These systems are different than Chichibabin's hydrocarbon and were designed with bulky groups on the α-phenyl rings to maximize their stability. It is unclear that the poly(fuchsone) polyanion in particular would be expected to behave at all like Chichibabin's hydrocarbon. This system does have an irreversible reduction wave 500mV from the polyanion, though, and in practice has been on the edge of stability. In retrospect, this instability is not suprising and likely contributed significantly to the failure to find conductivity in these systems. For this reason it is unclear that the polymer listed in Figure 4.6 would make a good target, even if a path to its synthesis could be found.

Experimentals

4-Bromo-4'-trimethylsilylbenzhydrol (3) *p*-Dibromobenzene (11.8g, 50 mmol) dissolved in 75mL freshly distilled THF under argon, is cooled to -78°C, and 20mL 2.5M butylithium (50 mmol) in hexanes is added dropwise. The solution is stirred for 45 minutes and trimethylsilylchloride is added dropwise. The solution is allowed to warm to room temperature and stirred for 2 hours, then cooled to -78°C. 20mL 2.5M butyllithium (50 mmol) is then added dropwise and the solution is stirred for 30 minutes. 4-Bromobenzaldehyde (9.25g, 50 mmol) in 7 mL THF is then added dropwise, and the solution is allowed to warm to room temperature and stirred overnight. After a standard workup the crude material is recrystallized twice from hexanes. 9.0g of colorless crystals are obtained (54%). Mp=92-94°C. 2.5g more can be obtained by 4x recrystallization of the mother liquor from hexanes. The total yield is 69%. 300 MHz ^{1}H NMR, $CDCl_3$, δ = 0.27, s, 9H; 5.80, s, 1H; 7.32, 2 overlaying d, 4H. 75 MHz ^{13}C, CD_2Cl_2, δ = GCMS m/z: 336 (M^+, 10), 334 (M^+, 10), 321 (90), 319 (100), 177 (30), 151 (10), 73 (20).

(3,5-di-*t*-butyl-4-hydroxyphenyl)-(4-trimethylsilylphenyl)-(4-bromophenyl)methane (4) The asymmetric benhydrol **3** (1.68g, 5 mmol) is dissolved in 20ml nitromethane. Concentrated sulfuric acid (0.15mL) is added and the solution and it is immediately cooled in an ice bath and stirred 10 minutes. Water and diethyl ether are added and the system is extracted

and washed twice with a sodium bicarbonate solution, then dried with $MgSO_4$ and evaporated. The material is not further purified.

2,6-di-*t*-butyl-4′-bromo-4″-trimethylsilylfuchsone (5) Crude **4** (5 mmol theoretical, from above) is dissolved in 10ml toluene and DDQ (1.13g, 5 mmol) is added as a solid, and the system is stirred for 20 minutes. 10mL of hexanes are added to the solution and it is chromatographed in a column packed in hexanes, ramping the solvent from hexanes to 10% ethyl acetate in hexanes. The orange product is recrystallized from ethanol. 1.1g yield (42% over 2 steps). 300 MHz ^{1}H NMR, $CDCl_3$, δ = 0.34, s, 9H; 1.29, s, 18H; 7.11. s. 1H; 7.16, d, 2H; 7.19, s, 1H; 7.21, d, 2H; 7.55, d, 2H; 7.58, d, 2H. 75 MHz ^{13}C, CD_2Cl_2, δ = GCMS m/z: 522 (M^+, 30). 520 (M^+, 30), 507 (75), 505 (75), 465 (100), 463 (90), 73 (90).

4-[(3,5-di-*t*-butyl-4-hydroxyphenyl)-(4-bromophenyl)methyl]phenylboric acid, catechol ester (6) Fuchsone **5** (497 mg, 0.95 mmol) and triethylsilane (226mg, 2mmol) are added to a dry flask under argon, which is then cooled to -78°C. 3mL 1.0M BBr_3 in CH_2Cl_2 (3 mmol) is added and the system is stirred for 3 hours cold, then affixed with a condenser and refluxed overnight. The system is allowed to cool and quenched with 10% NaOH solution, then pH=7 buffer. The organic layer is worked up in the usual way and the resulting solid is columned in 30% ethyl acetate in hexanes and pumped dry. 382mg of the boric acid is isolated (81%). The catechol ester can be made by refluxing

the boric acid in a dean-stark trap with catechol in benzene, then subliming away the excess catechol. 300 MHz ^{1}H NMR, $CDCl_3$, δ = 1.38, s, 18H; 5.15, s, 1H; 5.47, s, 1H; 6.90, s, 2H; 7.02, d, 2H; 7.14, dd, 2H; 7.23, d, 2H; 7.32, dd, 2H; 7.43, d, 2H; 8.01, d, 2H.

2,6-di-*t*-butyl-4′-bromo-fuchsone, 4″-boric acid, catechol ester The acid form of **6** (382mg, 0.77 mmol) is dissolved in toluene and DDQ (176 mg, 0.77 mmol) is added. The solution is stirred in toluene for 2 hours, hexanes are added to the solution and it is columned in 0 to 50% ethyl acetate in hexanes. The orange solid is recrystallized from acetonitrile. 224mg product (82%) collected as orange needles. 300 MHz ^{1}H NMR, $CDCl_3$, δ = 1.14, s, 9H; 1.16, s, 9H; 7.17, m, 6H; 7.37, m, 4H; 7.59, d, 2H; 8.15, d, 2H.

Poly 4′,4″-((3,5-di-*t*-butyl-4-hydroxyphenyl)-diphenyl)methane (7) Into 3mL of degassed toluene is added **6** (350 mg, 0.62 mmol) and tetrakistriphenylphosphine palladium (0) (small scoop). 2mL 2.0M Na_2CO_3 solution is degassed and added and the system is refluxed for 7 days. The product is precipitated three times with ethanol to yield a beige powder, 109mg (0.30mmol, 48%). GPC in THF shows M_n=6400, M_w=7700, PDI=1.21, corresponding to approximately 18-mer; this is confirmed by vapor phase osmometry. 300 MHz ^{1}H NMR, $CDCl_3$, δ = 1.37, broad s, 18H; 5.11, broad s, 1H; 5.50, broad s, 1H; 6.98, broad s, 2H; 7.21, broad d, 4H; 7.52, broad d, 4H.

Poly 4',4"-(2,6-di-*t*-butylfuchsone) (1) a) **7** is dissolved in toluene, excess DDQ is added, and the solution stirred for 2 hours. The polymer is precipitated three times with ethanol, and NMR confirms that the oxidation has gone to completion. The GPC of the material remains unchanged, indicating no degradation. b) 2,6-di-*t*-butyl-4'-bromo-fuchsone, 4"-boric acid, catechol ester (895mg, 1.56 mmol) is polymerized using the same conditions listed above for **7**. The polymer is crashed out once with ethanol and twice with methanol. 566mg of orange powder (99%) is collected. GPC in THF shows M_n=7200, M_w=12500, PDI=1.74, indicating at least 20mer. c) Nickel bis(triphenylphosphine)dichloride (46.9mg, 0.87mmol. 3.2%), tetraethylammonium iodide (690mg, 2.68mmol), and Zn dust (1.5g, 23.1mmol) are stirred in 2mL freshly distilled THF under argon for 2 hours to form a red-brown solution. 2,6-Di-*t*-butyl-4,4"-dibromofuchsone (1.43g, 2.71mmol) in 4mL THF is added and the system is refluxed 18 hours, then poured into methanol and filtered. The remaining solid, a combination of polymer and Zn dust, is stirred in 20mL boiling THF and filtered hot. Once the filtrate is cooled, excess DDQ is added and the system stirred for three hours. The solution is precipitated from THF twice with methanol and once with hexanes. GPC/viscometry gives M_n=13800, M_w=28800, PDI = 2.1, corresponding to 38-mer; VPO indicates approximately 40-mer. Elemental analysis shows less than 0.5% bromide, with 86.9% C and 7.51% H (theoretical 88.0%C, 7.66%H). 948mg product (95% yield) is collected.

300 MHz ^{1}H NMR, $CDCl_3$, δ = 1.26, s, 18H; 7.24, s, 2H; 7.39, d, 4H; 7.75, d, 4H.

4-*t*-butylphenyl-di(4'-bromophenyl)methyl methyl ether (8) 4,4'-Dibromobenzophenone (6.8g, 20mmol) is dissolved in 100mL THF, and 10mL 2.0M *t*-butylphenylmagnesium bromide (20 mmol) is added and the system is stirred at room temperature for one hour. After a standard workup, the crude material is dissolved in trifluoroacetic acid and added quickly to 50mL of freshly distilled methanol, then worked up again in ether/water and chromatographed in 10% ethyl acetate in hexanes. Chromatography yields a white powder (6.0g, 61%). 300 MHz ^{1}H NMR, $CDCl_3$, δ = 1.36, s, 9H; 3.08, s, 3H; 7.34, m, 8H; 7.57, d, 4H.

PTP (2a) Nickel bis(triphenylphosphine)dichloride (69mg, 0.1mmol. 2.6%), tetraethylammonium iodide (1.01g, 3.9mmol), and Zn dust (2.5g, 38mmol) are stirred in 4mL freshly distilled THF under argon for 30 minutes. **8** (2.00g, 4.1mmol) in 4mL THF is added and the system refluxed for 20 hours. The polymer solution is precipitated with methanol and filtered to give a powder containing zinc and polymer. The polymer is dissolved in THF, precipitated with methanol and filtered through celite, then redissolved in THF, precipitated with hexanes, and collected. When left exposed to air the solid yellows slightly, though its NMR remains unchanged. GPC/viscometry measurements in THF show M_n=3450, M_w=4600, PDI=1.33, which corresponds

to decamer. Total yield is 350mg polymer (25%). 300 MHz ^{1}H NMR, $CDCl_3$, δ = 1.32, s, 9H; 3.11, s, 3H; 7.35, m, 4H; 7.54, bs, 8H.

PTP (2b) PTP **2a** is dissolved in trifluoroacetic acid, which is immediately pumped off into a cold trap. The purple residue is dissolved in distilled dichloromethane, and one drop of lutidine is added, causing the solution to immediately become colorless. The solvent is again pumped into a cold trap to leave a colorless residue. The 300 MHz ^{1}H NMR spectrum is extremely broad but shows no peak corresponding to methanol or the methyl ether of **2a**.

Reduction of 1 Bulk electrolysis of **1** is performed in a glove box and is described elsewhere.[10] Electrolysis yielded a green solution which could be isolated and pumped dry inside a glove box. The electrolyte can be dissolved in distilled, degassed diethyl ether and the polymer is collected by filtration. The polymer can be redissolved in THF, but all the green color is lost and it regains its original orange color.

Reduction of 2a PTP **2a** is dissolved in THF and an excess of powdered lithium metal is added. The system is stirred for one week and turns a deep blue. The ^{1}H NMR of the material (with the reaction performed in d_8-THF) is very broad and shows no change upon exposure to air (despite loss of color). The blue solution can be cast as a thin film, but displays no conductivity. A

solution of reduced **2a** can be treated with a small amount (10-50%) of silver tetrafluoroborate, and the resulting blue/purple solution cast as a film, but it too shows no conductivity.

Reduction of 2b PTP **2b** can be reduced with cobaltocene to yield a blue polymer than shows no conductivity. This material can be oxidized with silver salts as described above to yield a purple solution that also does no conduct.

---

[1]Etemad, S.; Heeger, A.J.; MacDiamid, A.G.; *Annual Reviews in Physical Chemistry*,**1982**, *33*, 443

[2] Heeger, A.J.; Kivelson, S.; Schrieffer, J.R.; *Reviews of Modern Physics*, **1988**, *60*, 781

[3]Epstein, A.J.; MacDiarmid, A.G.; *Synthetic Metals*, **1995**, *69*, 179

[4]Bredas, J.L.; Boudreaux, D.S.; Chance, R.R.; Silbey, R.; *Molecular Crystals and Liquid Crystals*, **1985**, *118*, 323

[5]a) Scherf, U.; Müllen, K.; *Polymer Communications*, **1992**, *33*, 2443. b) Chmil, K.; Scherf, U.; *Makrmol. Chem., Rapid Communications*, **1993**, *14*, 217

[6] Montgomery, L.K.; Huffman, J.C.; Jurczak, E.A.; Grendze, M.P.; *Journal of the American Chemical Society*, **1986**, *108*, 6004

[7] Anderson, K.K.; Thesis, California Institute of Technology, Pasadena, CA, 1996, p.67

[8] Percec; Okita; *Jourrnal of Polymer Science A*, **1993**, *31*, 877

[9] Phillips; Shears; Samulski; DeSimone; *Macromolecules*, **1994**, *27*, 2354 and from DeSimone, personal communication.

[10] Anderson, K.K.; Thesis, California Institute of Technology, Pasadena, CA, 1996, p.25

[11]Rajca-A.; *Molecular Crystals and Liquid Crystals A*, **1997** , *305* , 567

[12] Kovacic, P.; Jomes, M.B.; *Chemical Reviews*, **1987**, *87*, 357

[13] crystals used in reference 6 kindly provided by L.K. Montgomery.

Appendix I: Crystal data for nitronylnitroxides and imino nitroxides

All solutions except **10** were performed by Larry Henley and Dr. Michael Day at the Beckman Institute x-ray crystallography lab. Data was collected using a CAD-4 diffractometer in ω scanning mode at 0.71073Å MoKα radiation. Nitronylnitroxide **10** was solved by Dr. Joseph Ziller at the University of California, Irvine x-ray crystallography lab using a Seimens D3 diffractometer. Direct methods were the primary solution method for all structures (SHELXS-86). Refinement of the structures was by full matrix least-squares on F^2 (SHELXL-93). The data was unrestrained. Hydrogen placement was done by a difference Fourier map. Crystals were grown by slow cooling or evaporation.

	1	**3**	**7**
Chemical Formula	$C_{19}H_{17}F_4N_2O_2$	$C_{21}H_{17}F_4N_2O_2$	$C_{15}H_{14}F_5N_2O_2$
Crystallization solvent	Benzene	Methanol	Methylcyclo-hexane
Collection Temperature	85 K	85 K	85 K
M W	381.35	405.37	349.28
Crystal shape	Blade	Concave blades	Tabular
Crystal color	Deep purple	Purple/Gray	Forest green
Crystal size / mm^3	0.28 x 0.30 x 0.56	0.44 x 0.26 x 0.22	0.34 x 0.26 x 0.14
Space group	$P2_1/n$	$P2_1n$	$P2_1/n$
a/Å	9.980(2)	6.218(2)	6.296(3)
b/Å	11.858(2)	28.025(14)	11.016(7)
c/Å	14.688(3)	10.669(5)	22.26(3)
α/°	90	90	90
β/°	94.40(3)	90.68(3)	91.32(6)
γ/°	90	90	90
U/$Å^3$	1733.1(6)	1859.0(14)	1544(2)
Z	4	4	4
D_c/g cm^{-1}	1.462	1.448	1.503
μ/mm^{-1}	0.124	0.121	0.141
F(000)	788	836	716
Index ranges	$0 \le h \le 17$, $0 \le k \le 20$, $-25 \le l \le 25$	$0 \le h \le 8$, $-36 \le k \le 36$, $-13 \le l \le 13$	$0 \le h \le 7$, $0 \le k \le 13$, $-26 \le l \le 26$
Reflections Collected	19395	9491	6478
R_{merge}	0.034	0.039	0.023
GOF_{merge}	1.03	1.19	0.96
Ind. Reflections	9097	4244	2636
Data/ parameters	9094 / 312	4240 / 330	2636 / 273
R1	0.0461	0.0607	0.0361
wR2	0.0882	0.1030	0.0703
θ range/°	2.2 to 37.5	2.0 to 27.5	1.8 to 25.0
GOF_{F^2}	1.762	2.138	1.811
Largest diff. peak and hole e$Å^{-3}$	0.655 and -0.284	0.421 and -0.606	0.371 and -0.269

	6+7	**8**	**9a**
Chemical Formula	62% $C_{15}H_{14}F_5N_2O_2$ 38% $C_{15}H_{19}N_2O_2$	$C_{21}H_{19}F_4N_2O_2$	$C_{17}H_8F_4O$
Crystallization solvent	Methylcyclohexane	Methanol	Methanol
Collection Temperature	85K	85K	85K
M W	349.28 and 259.32	407.38	304.23
Crystal shape	Blade	Blades	Blade
Crystal color	Green	Emerald	Colorless
Crystal size / mm^3	0.44 x 0.37 x 0.18	0.45 x 0.19 x 0.09	0.45 x 0.26 x 0.16
Space group	C2/c	$P2_1/n$	$P2_1/c$
a/Å	19.292(7)	14.029(3)	12.447(2)
b/Å	11.830(3)	7.299(10)	6.8270(10)
c/Å	13.479(7)	18.124(5)	16.483(6)
α/°	90	90	90
β/°	108.24(4)	100.45	106.69(2)
γ/°	90	90	90
U/$Å^3$	2920(2)	1825.1(7)	1341.6(6)
Z	8	4	4
D_c/g cm^{-1}	1.441	1.483	1.506
μ/mm^{-1}	0.124	0.124	0.131
F(000)	1316	844	616
Index ranges	$-22 \le h \le 21$, $-14 \le k \le 14$, $-15 \le l \le 0$	$0 \le h \le 16$, $-8 \le k \le 8$ $-21 \le l \le 21$	$0 \le h \le 14$, $-8 \le k \le 8$, $-19 \le l \le 19$
Reflections Collected	6070	7123	5468
R_{merge}	0.027	0.034	0.018
GOF_{merge}	1.06	1.07	
Ind. Reflections	2556	3217	2352
Data/ parameters	2556 / 274	3217 / 338	2352 / 231
R1	0.0481	0.0385	0.0342
wR2	0.0838	0.0678	0.0710
θ range/°	2.05 to 25.00	1.7 to 25.0	1.7 to 25.0
GOF_{F^2}	2.133	1.484	2.016
Largest diff. peak and hole e$Å^{-3}$	0.392 and -0.246	0.234 and -0.231	0.171 and -0.261

Appendix II: Thermal Elipsoids and Snapshots of Crystals

Nitronylnitroxide 1

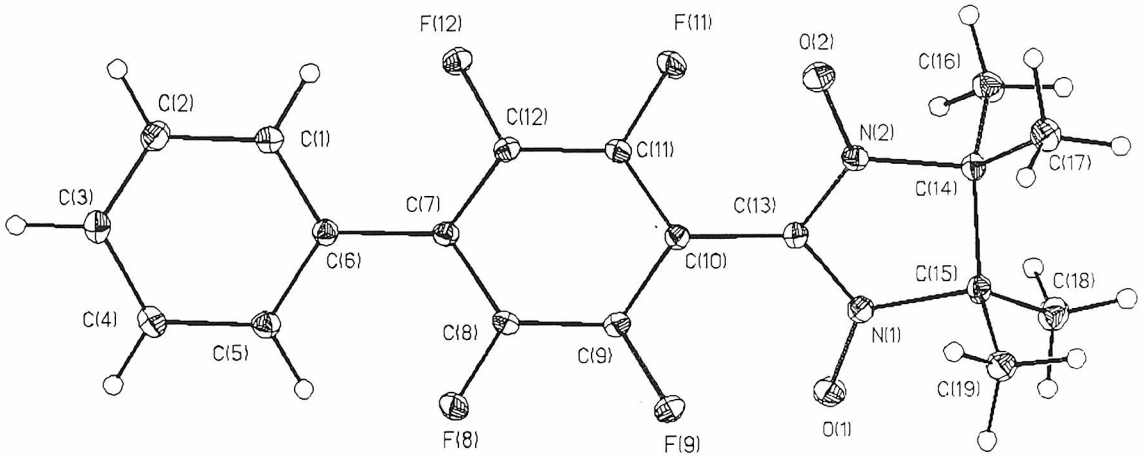

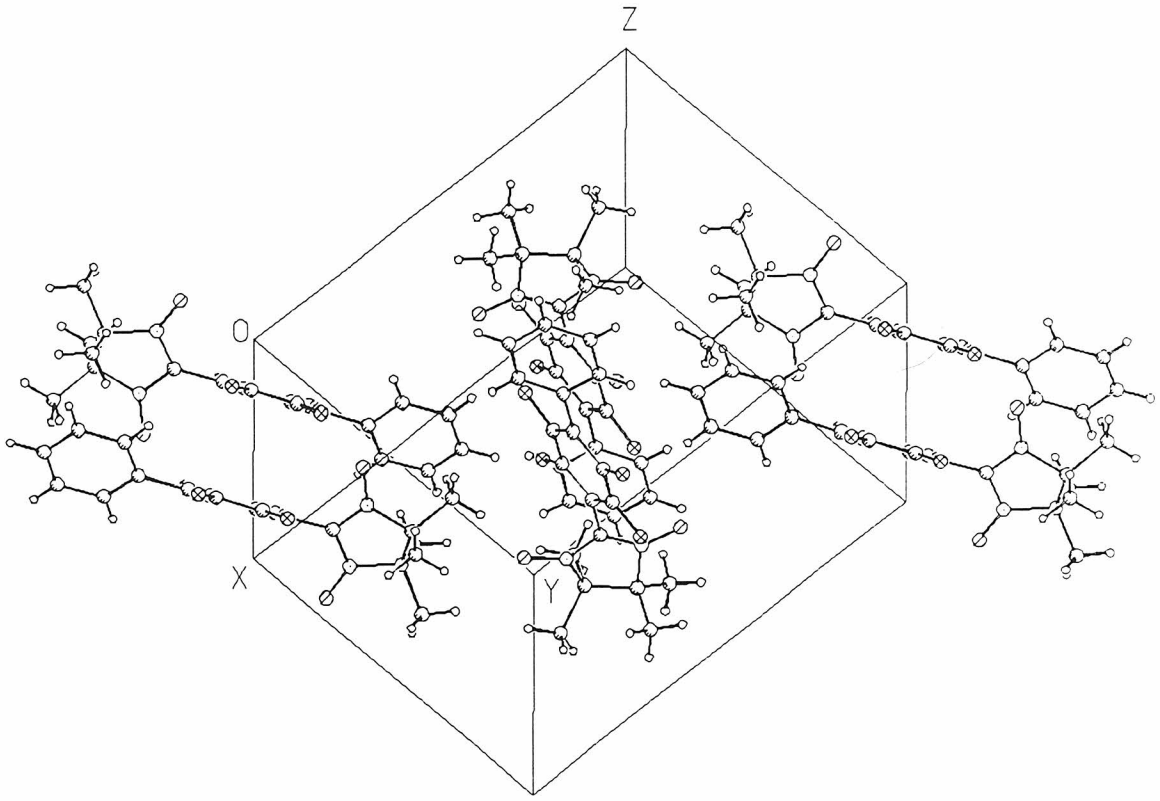
Z
O
X
Y

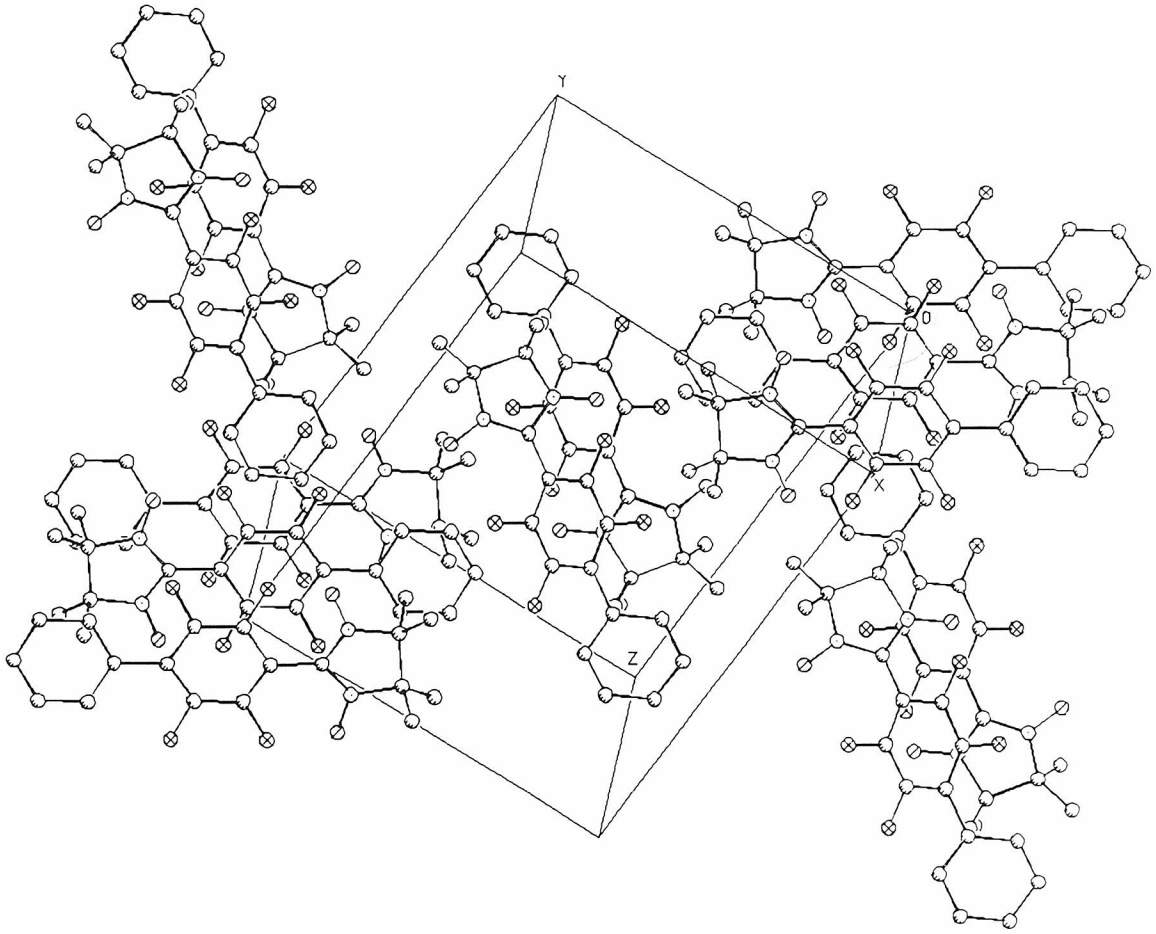
Y
X
Z

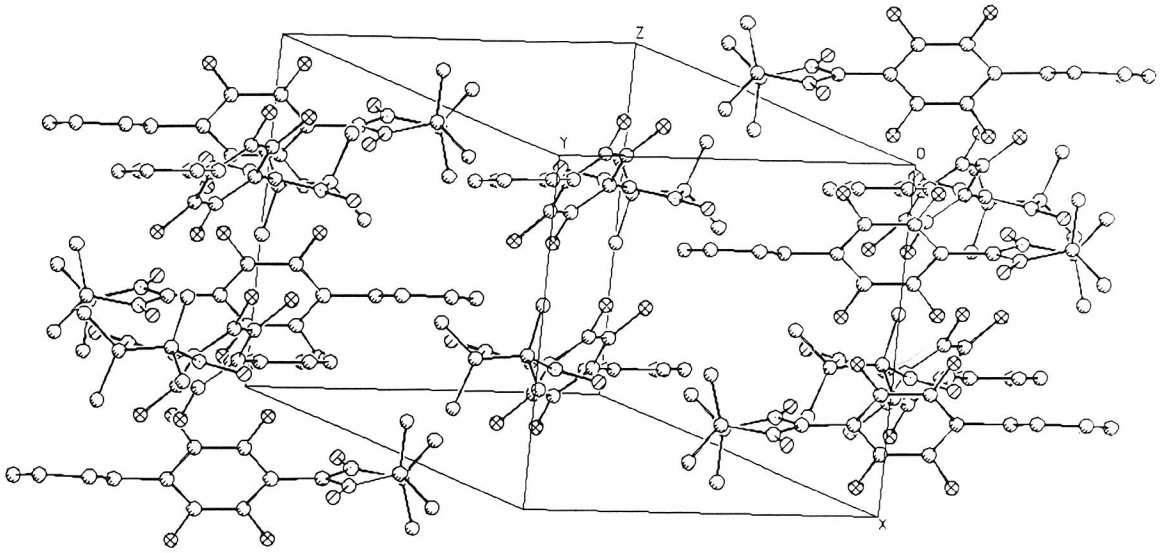
Z
Y
O
X

Nitronylnitroxdie 3

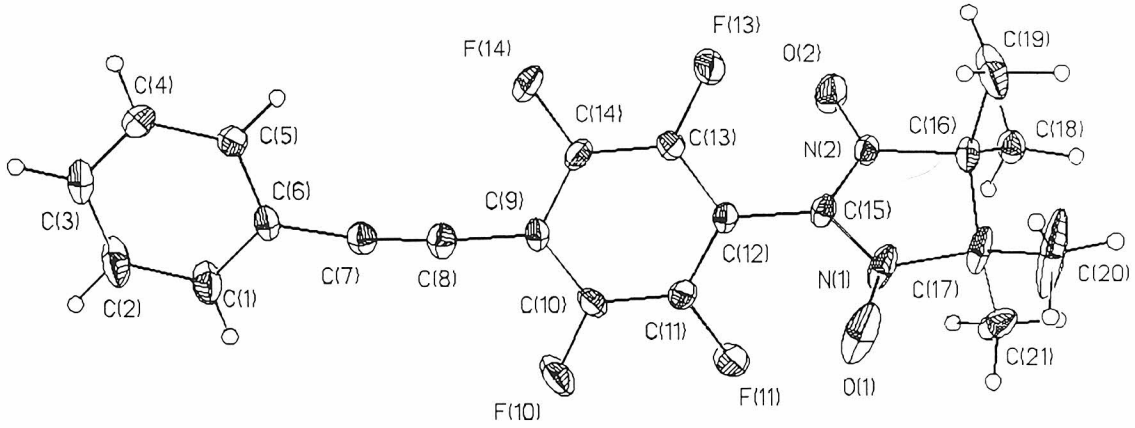

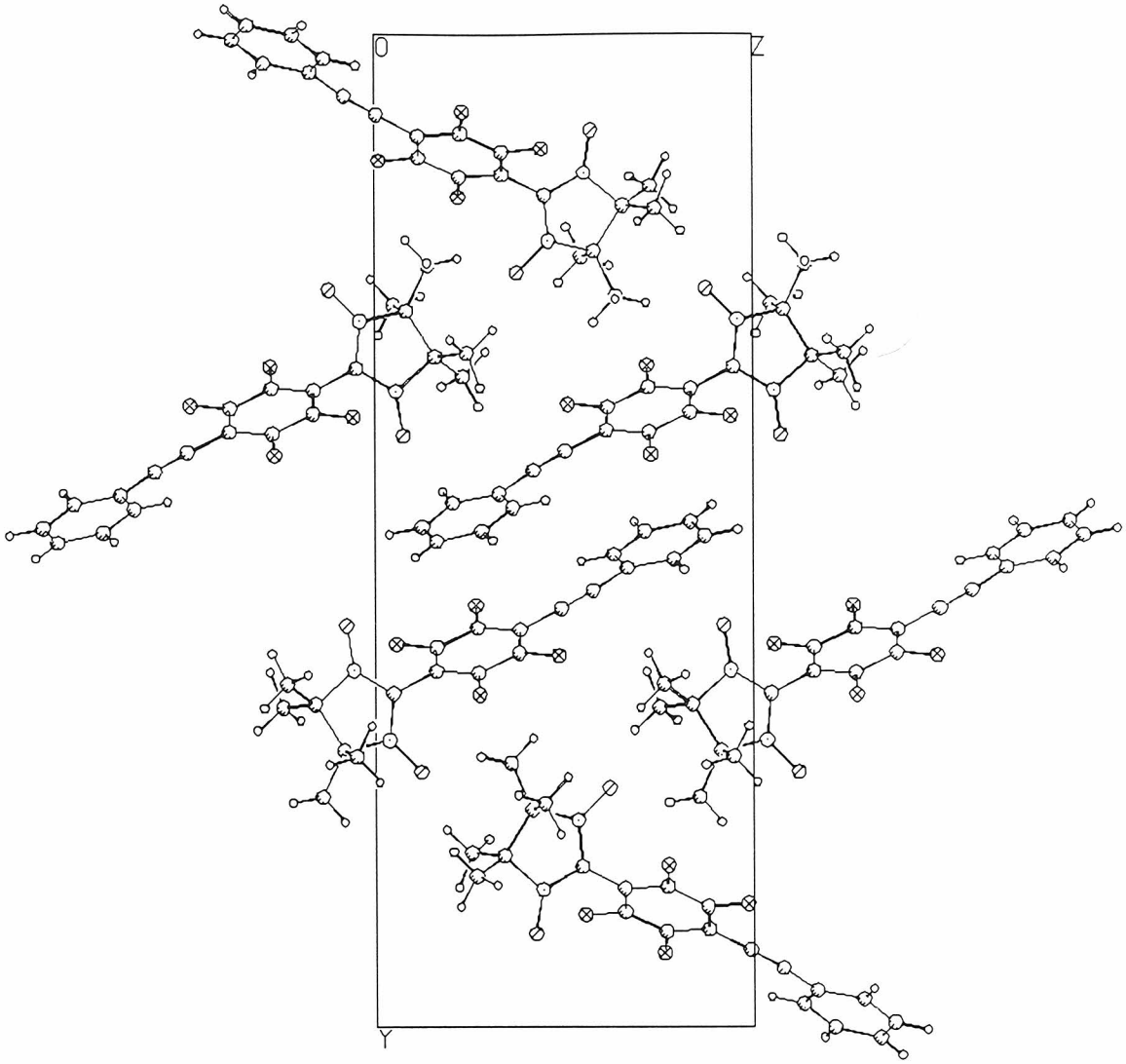
O
Z
Y

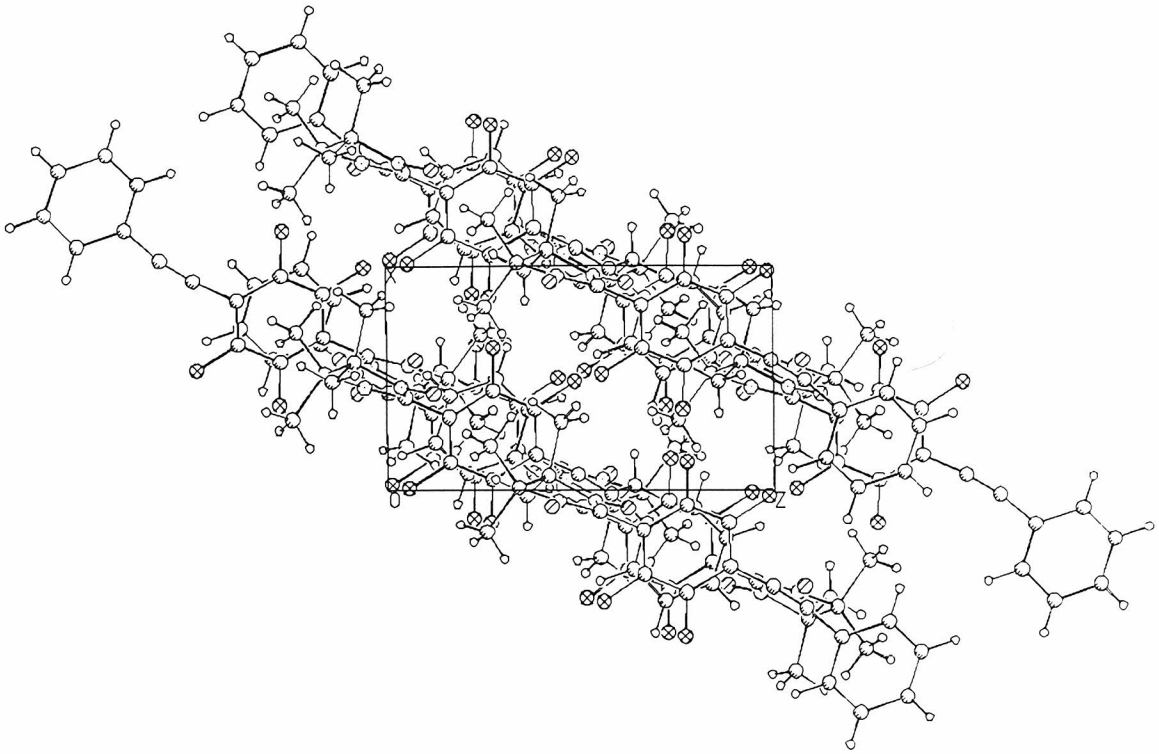
X
Z

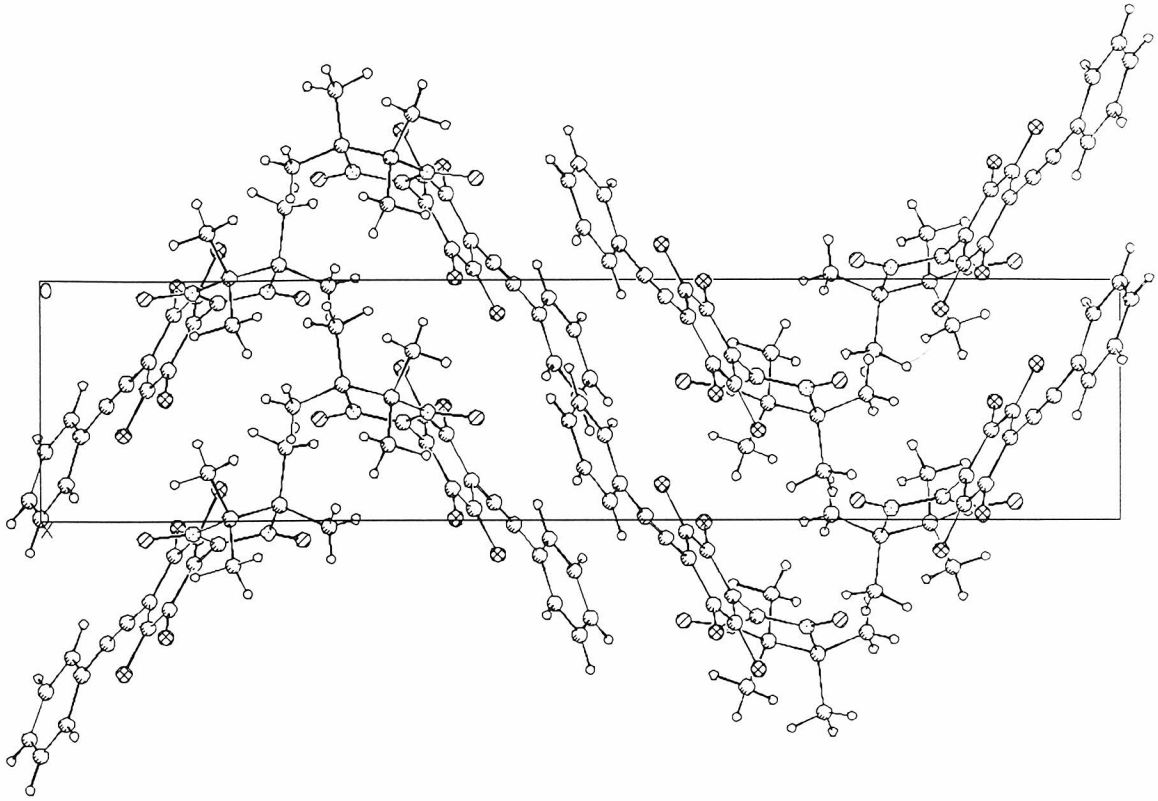

Nitronylnitroxide 7

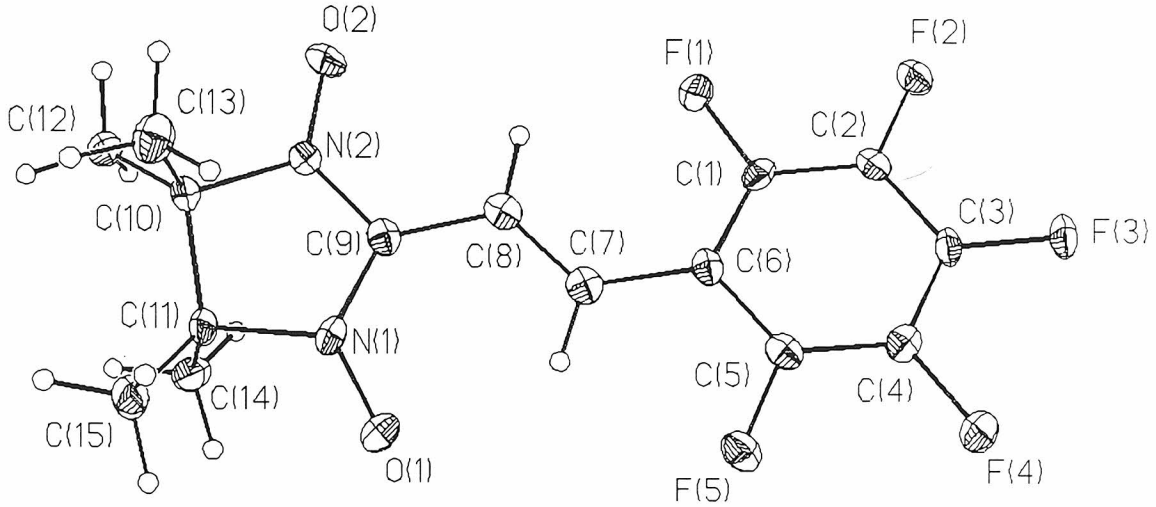

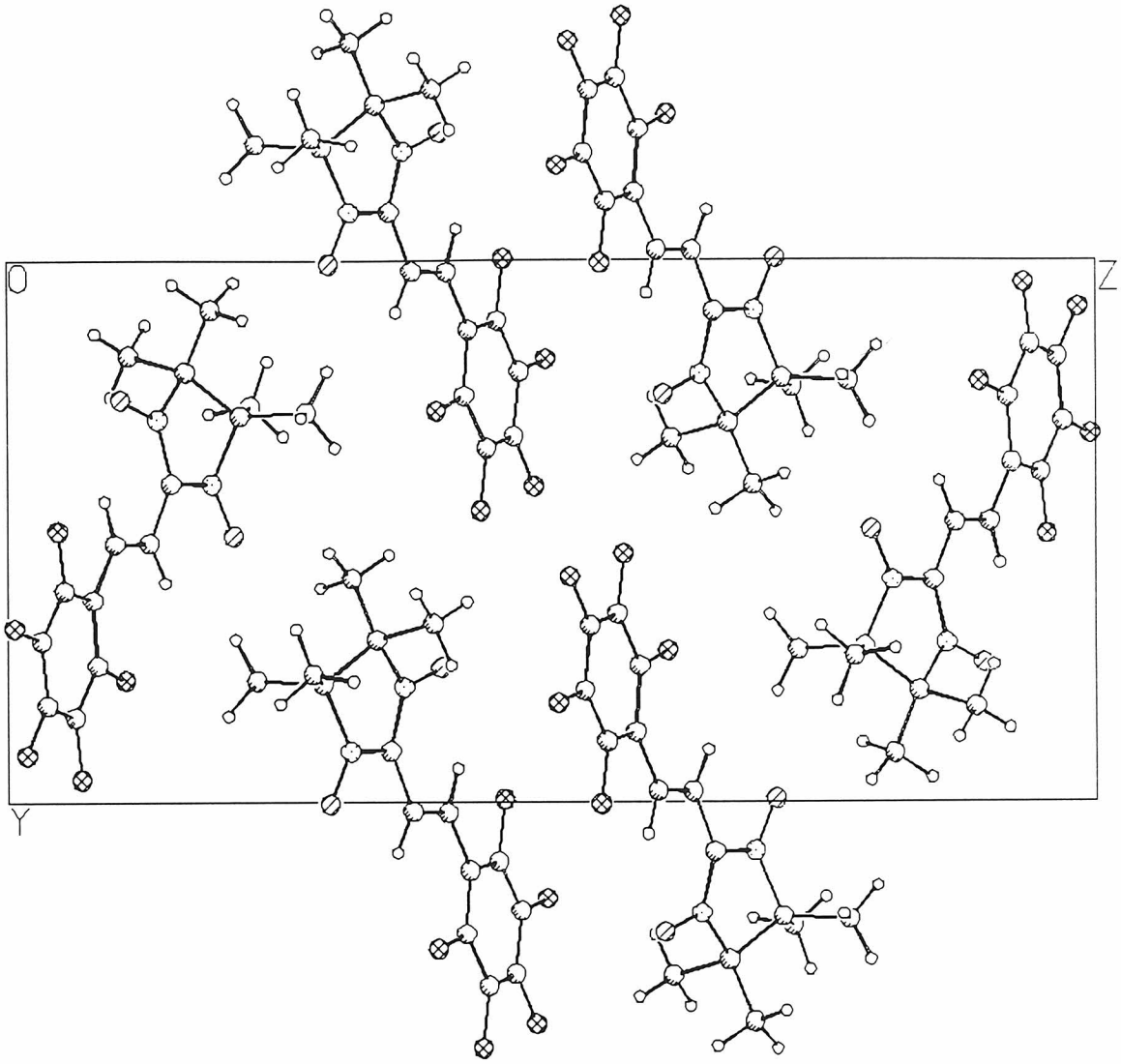
O
Z
Y

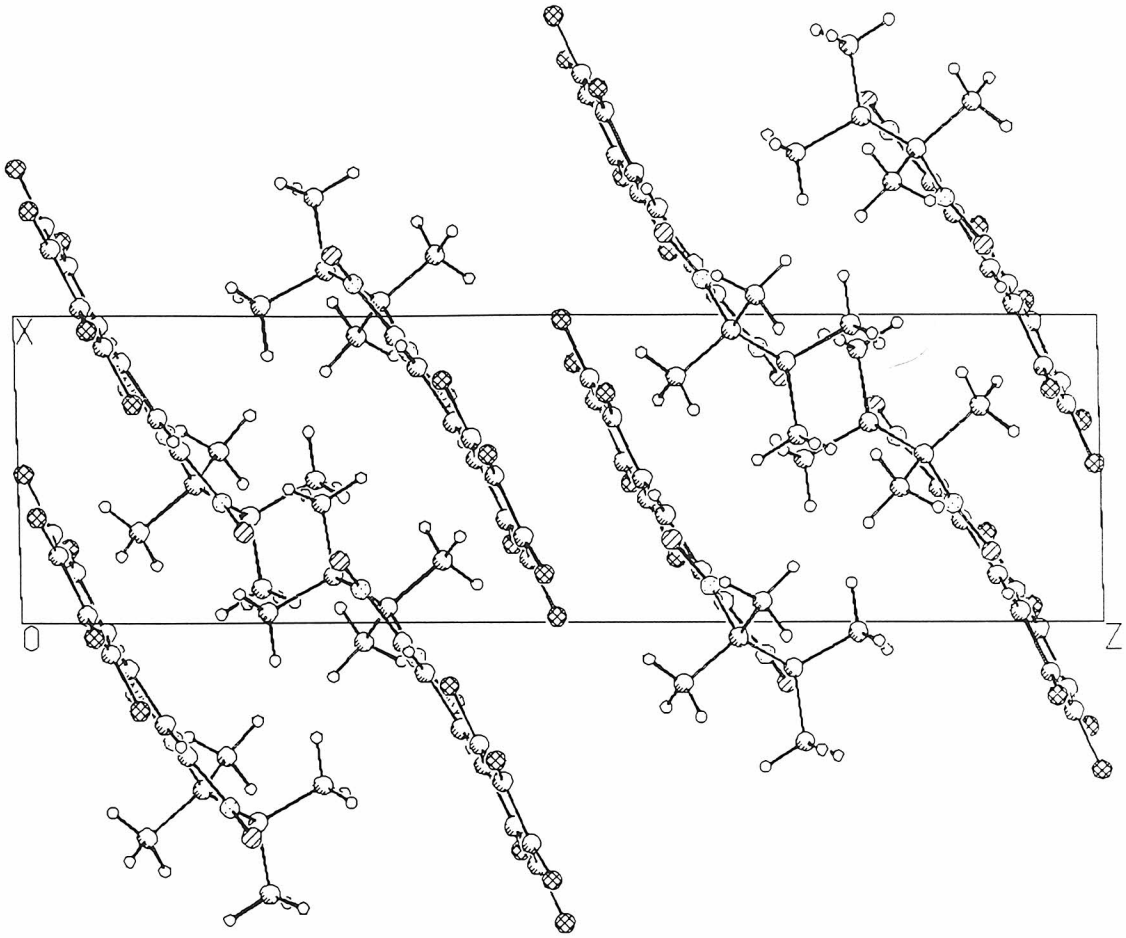
X
O
Z

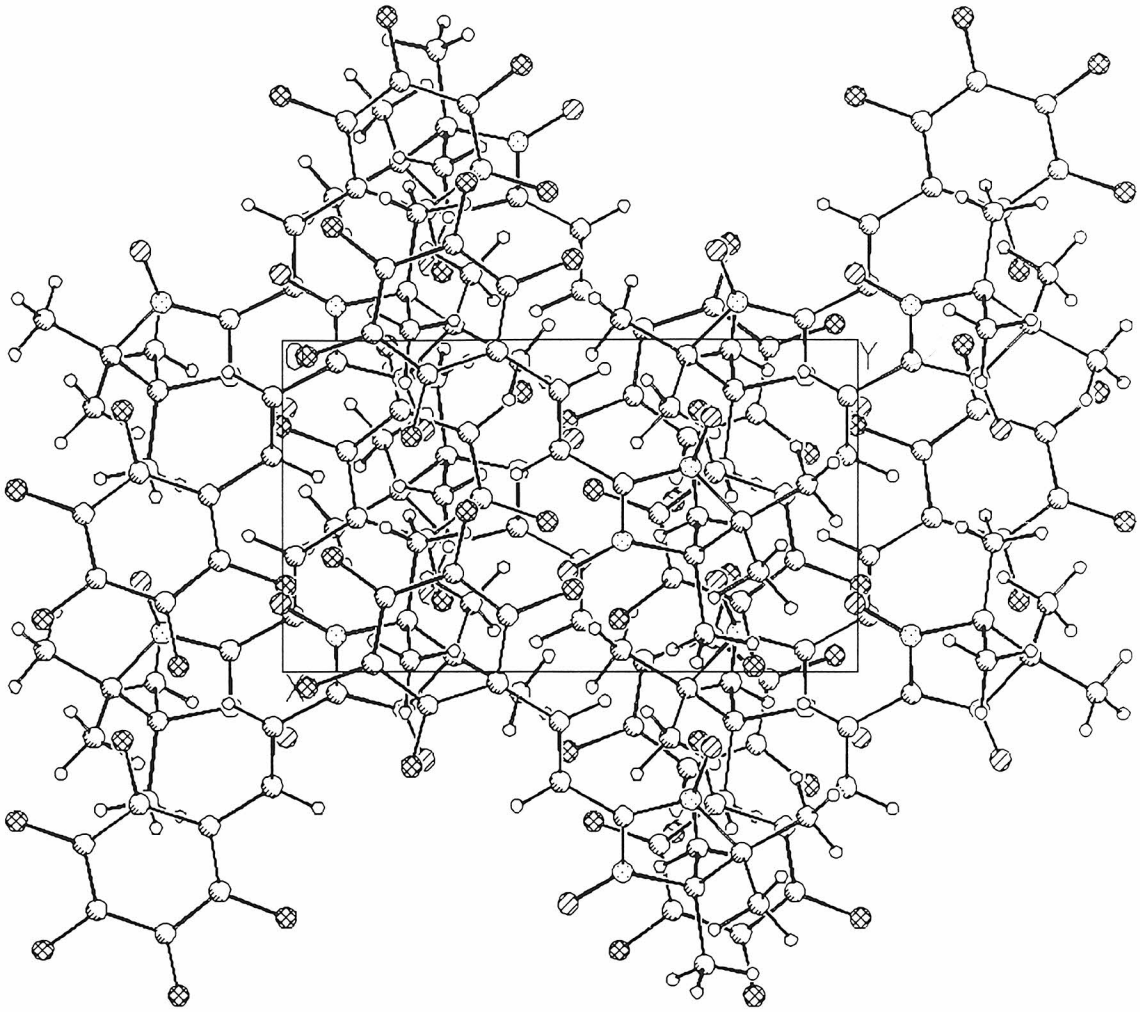
Y

Mix of Nitrnylnitroxides 6 and 7

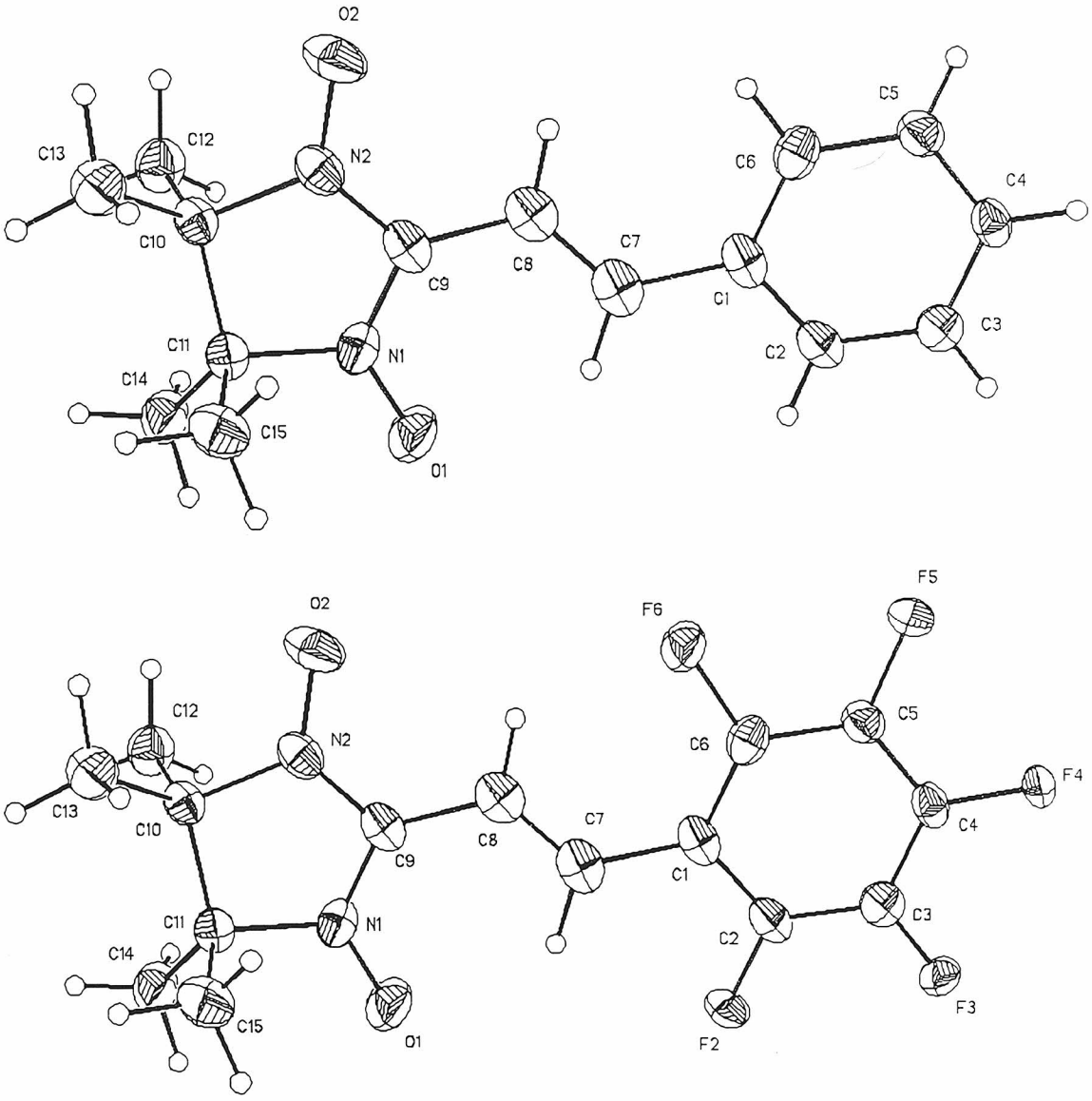

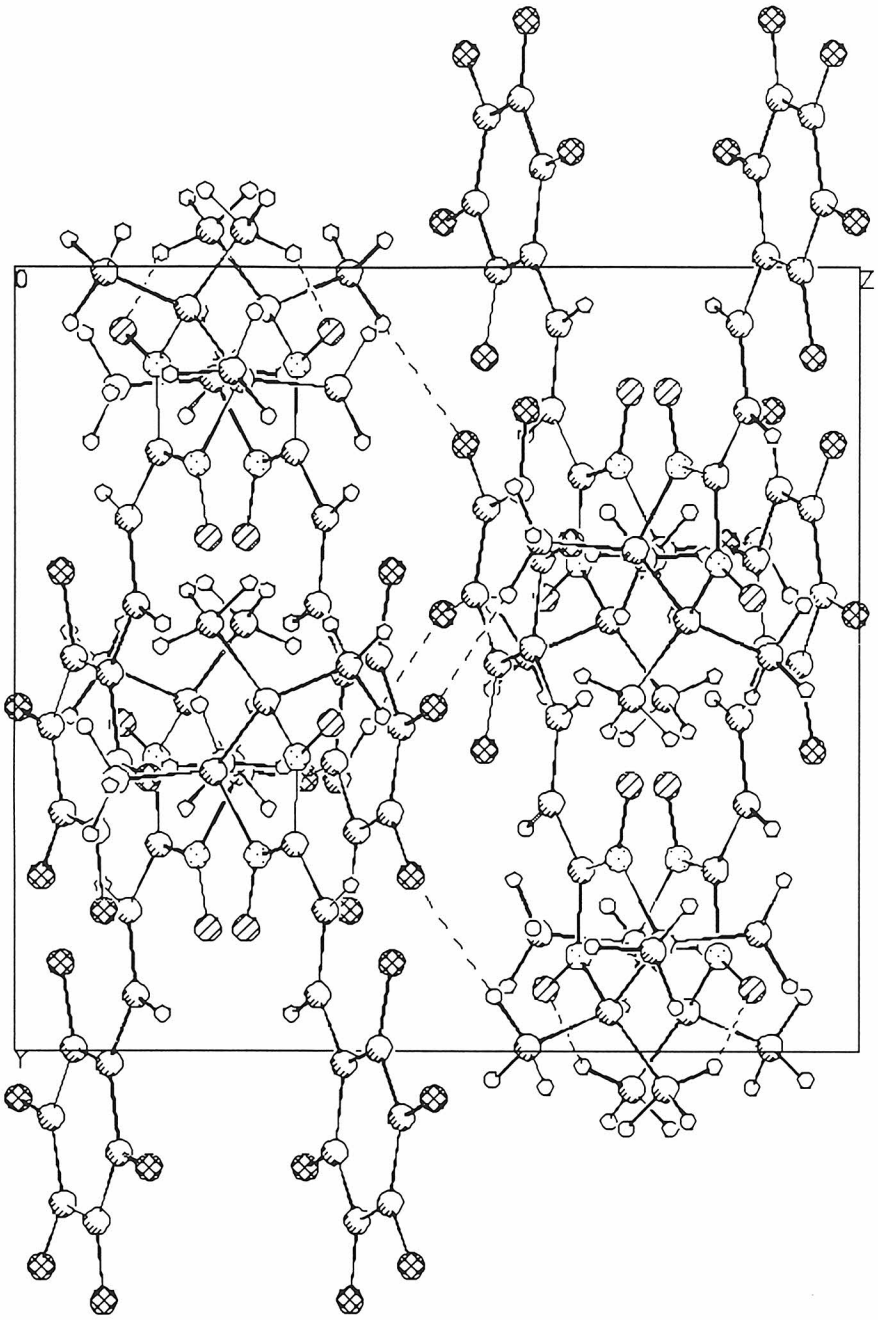
0
Z
Y

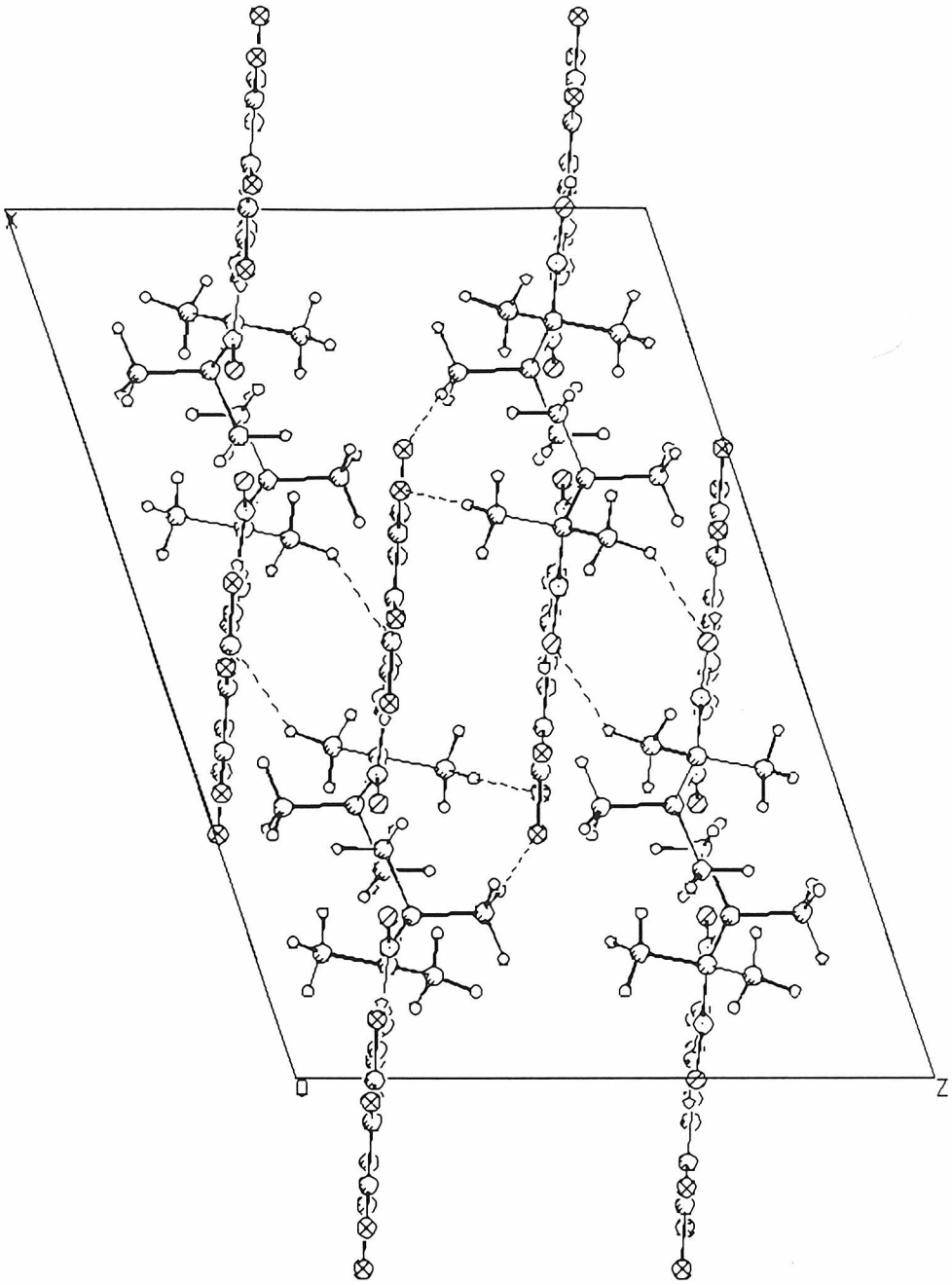
X
Z

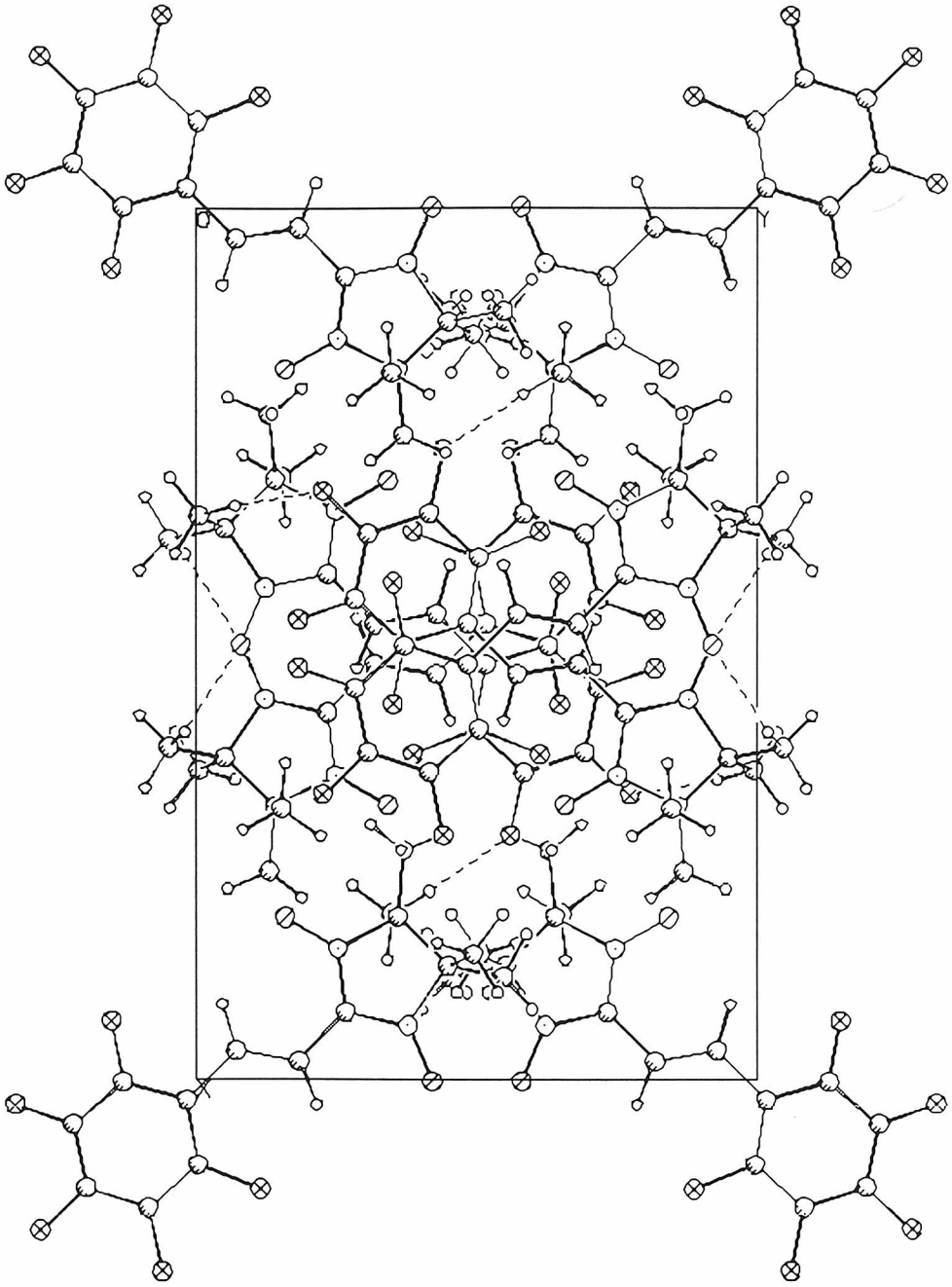

Nitronylnitroxide 8

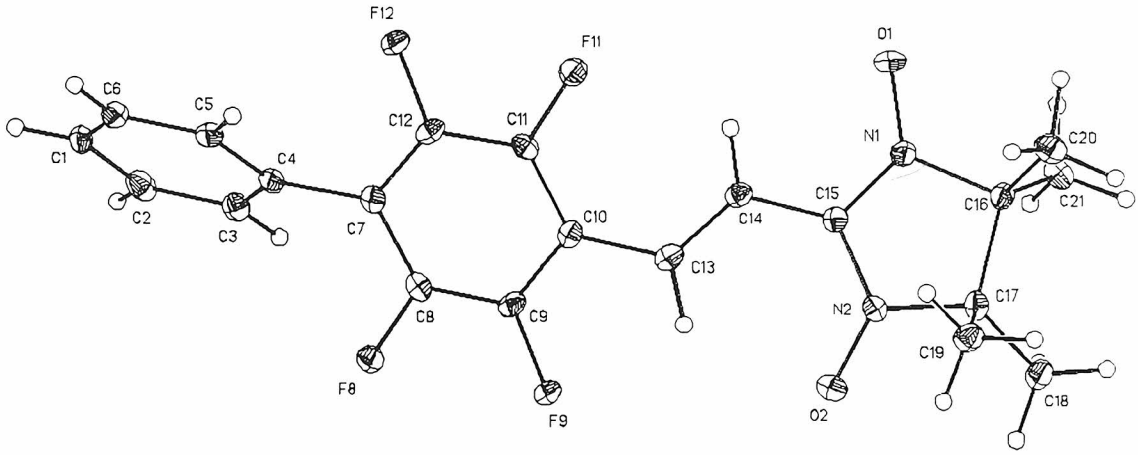

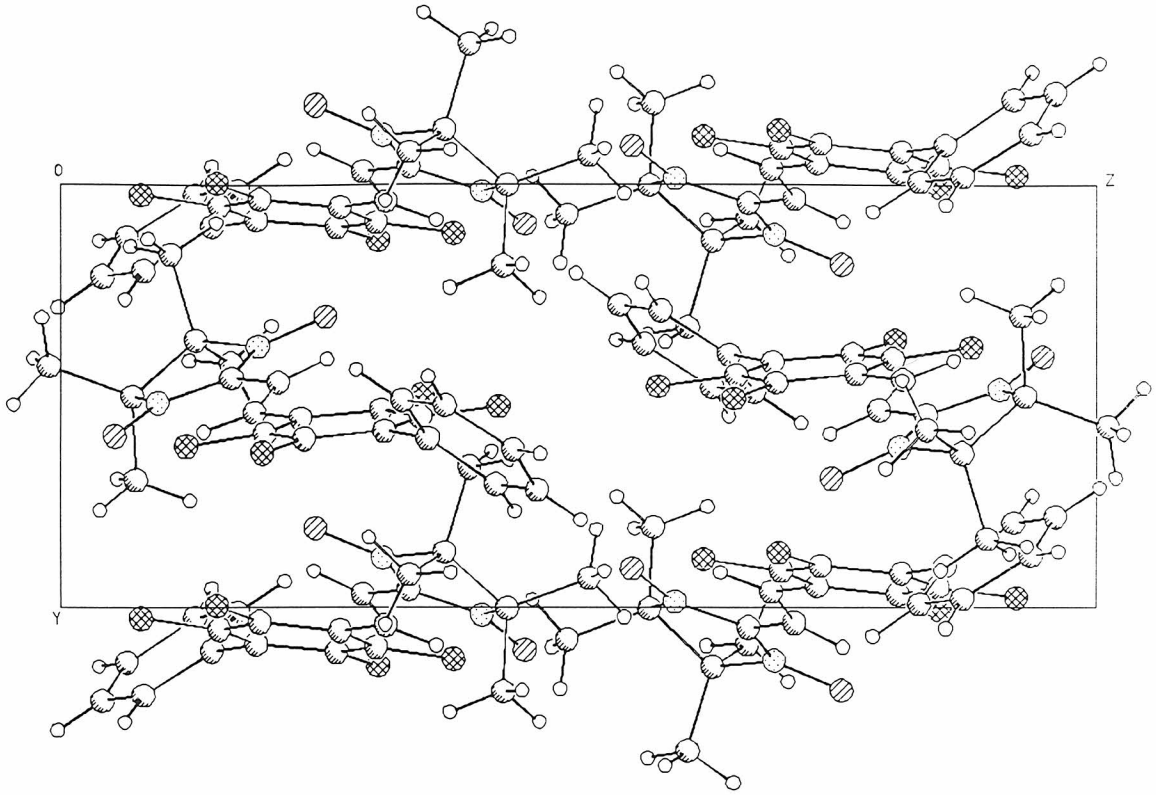
0
Z
Y

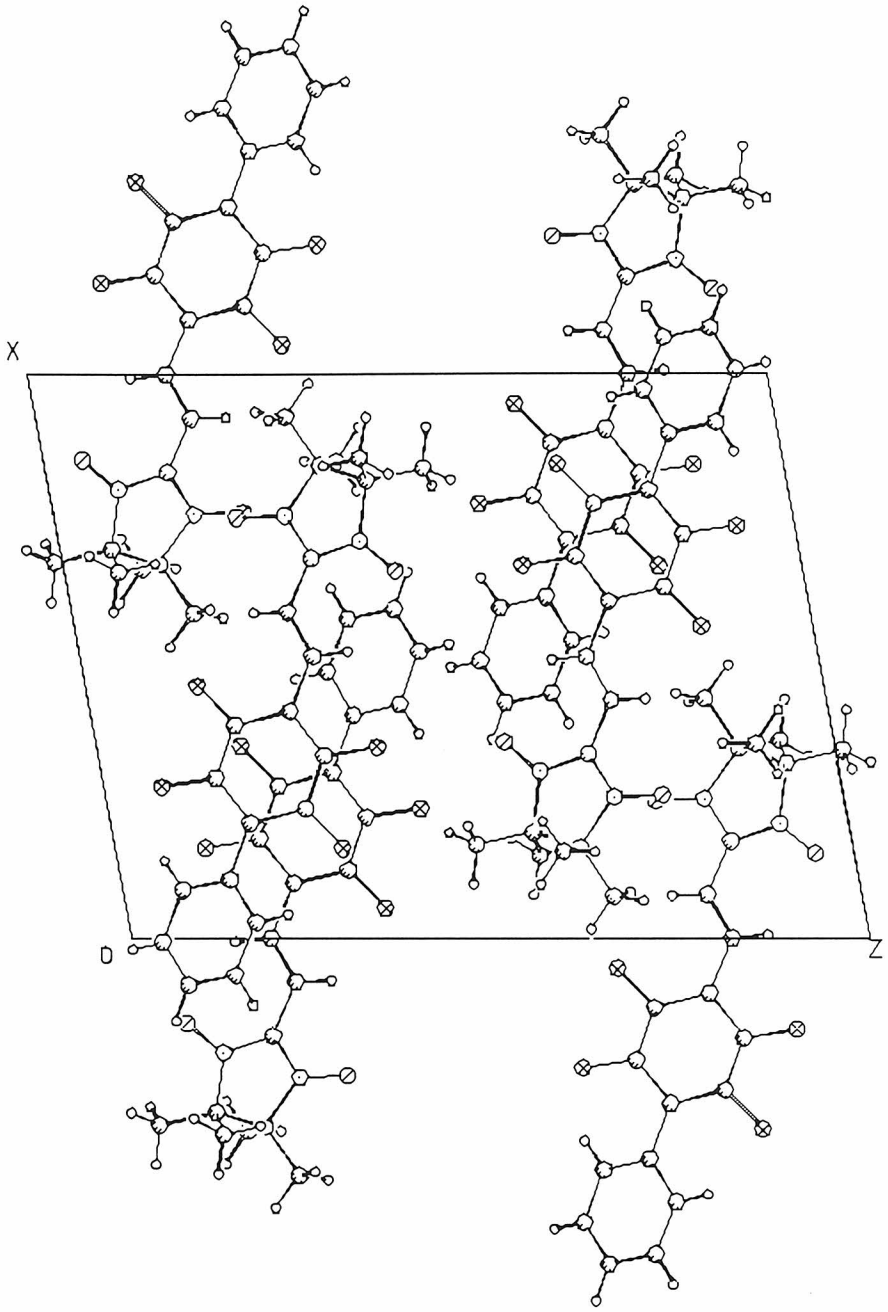
X
O
Z

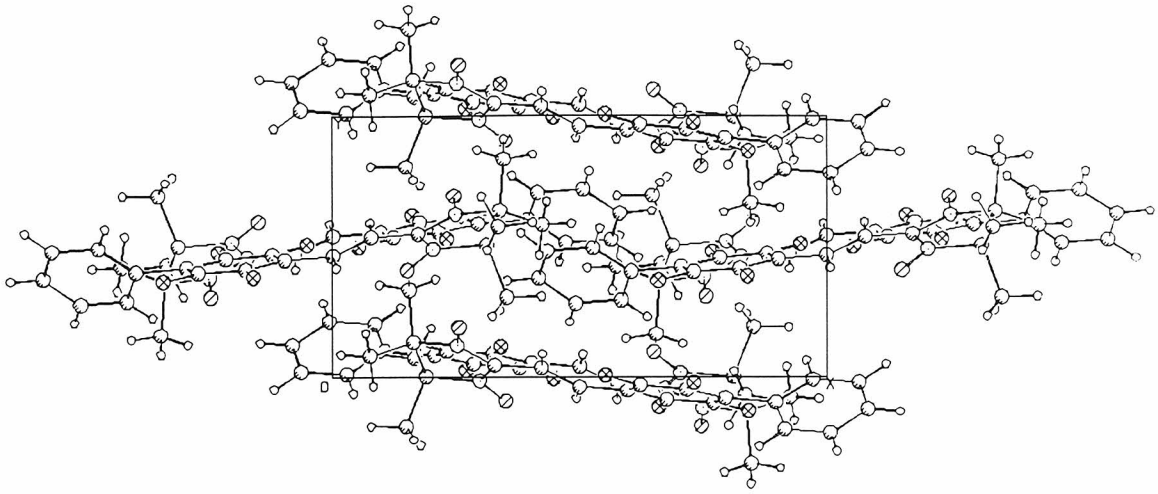

Cinnemaldehyde 9a

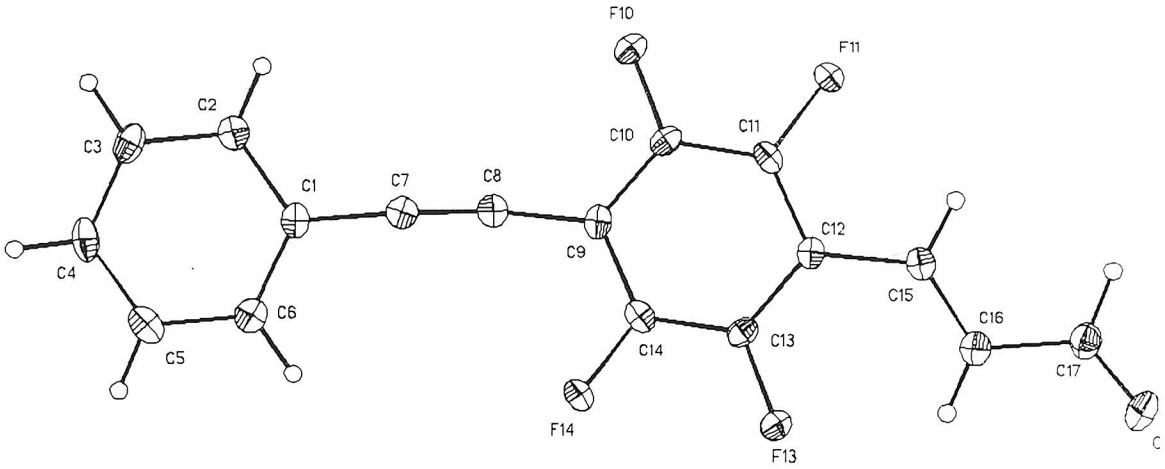

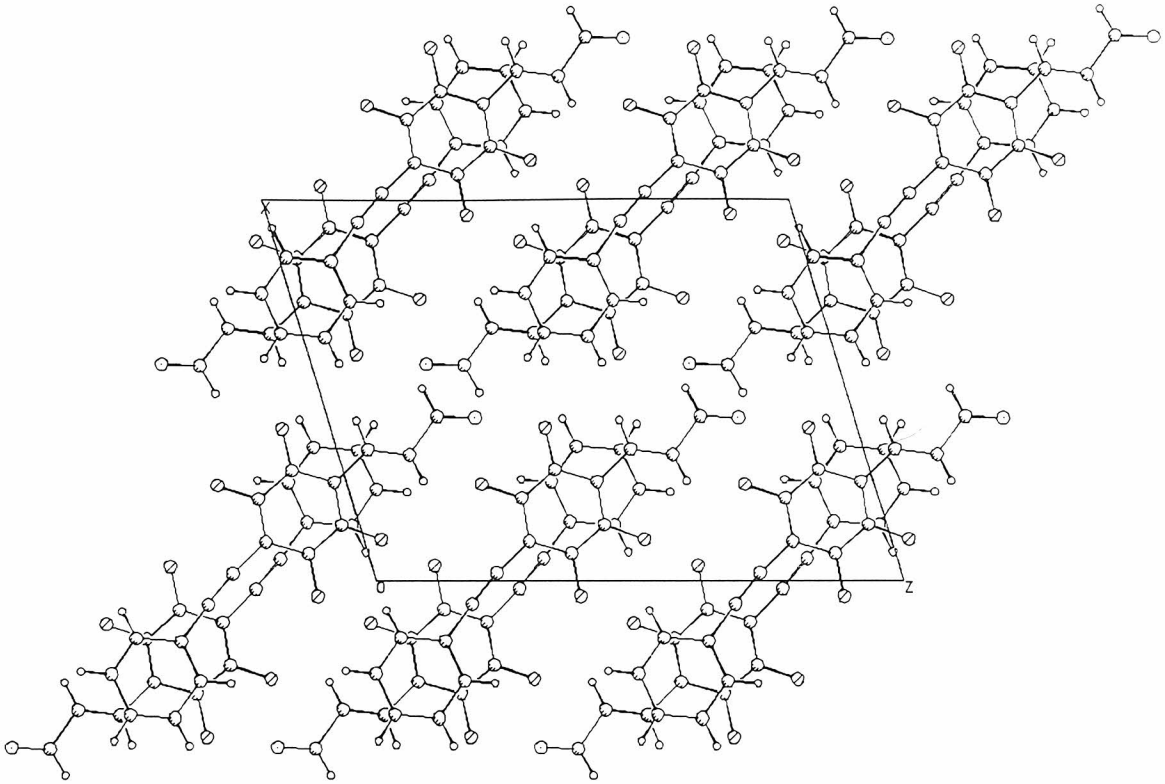
z

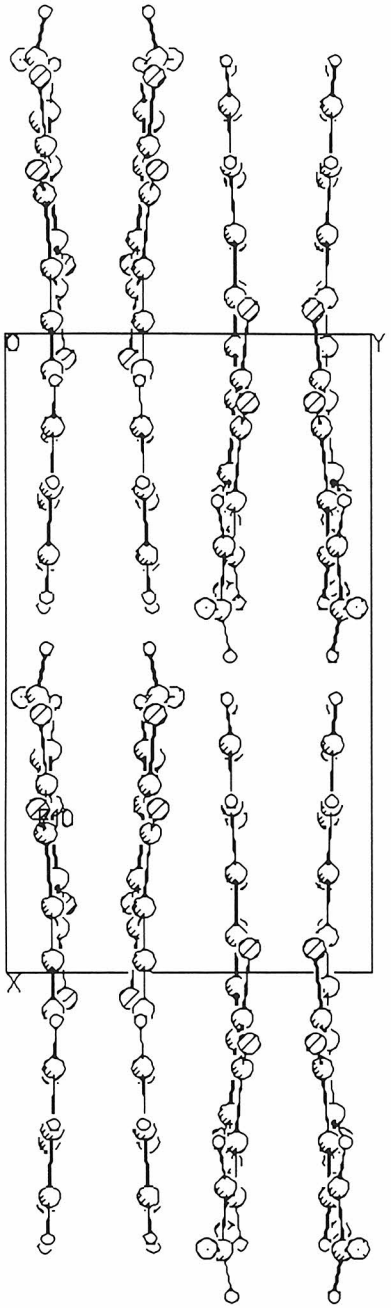
O
Y
X

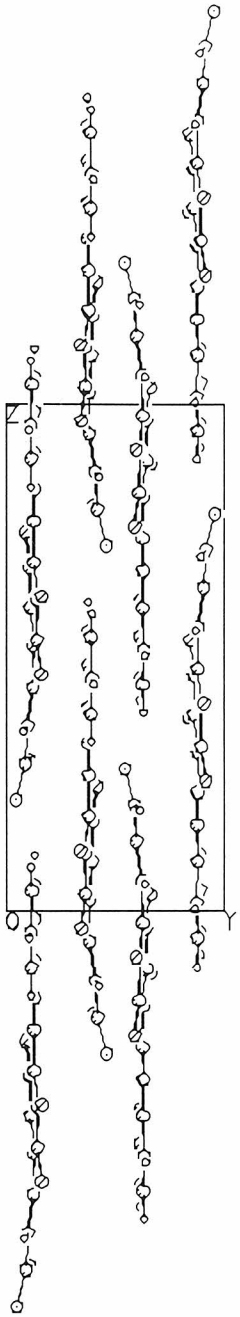
Z
O
Y

Nitronylnitroxide 9

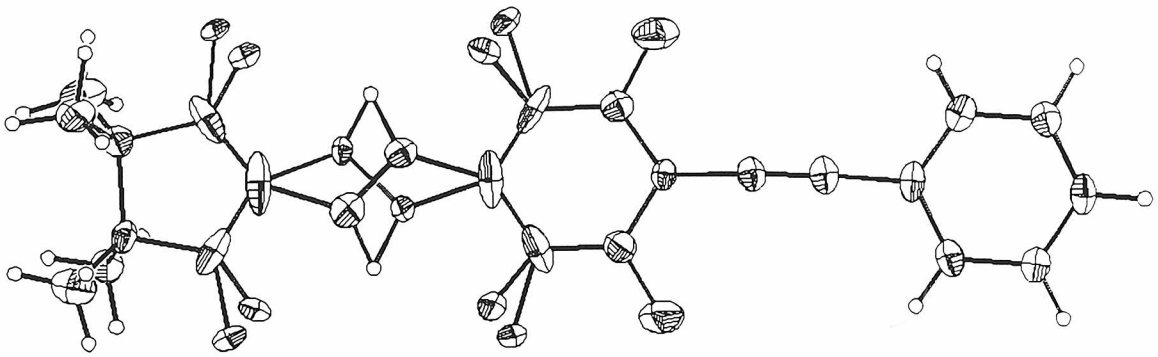

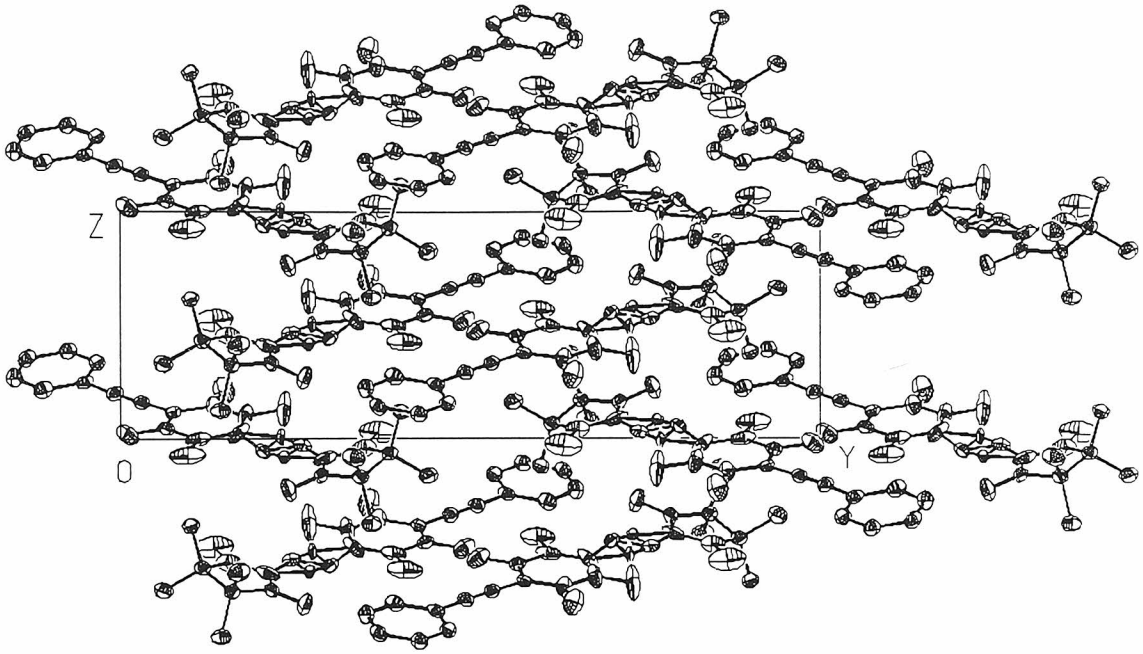
Z
O
Y

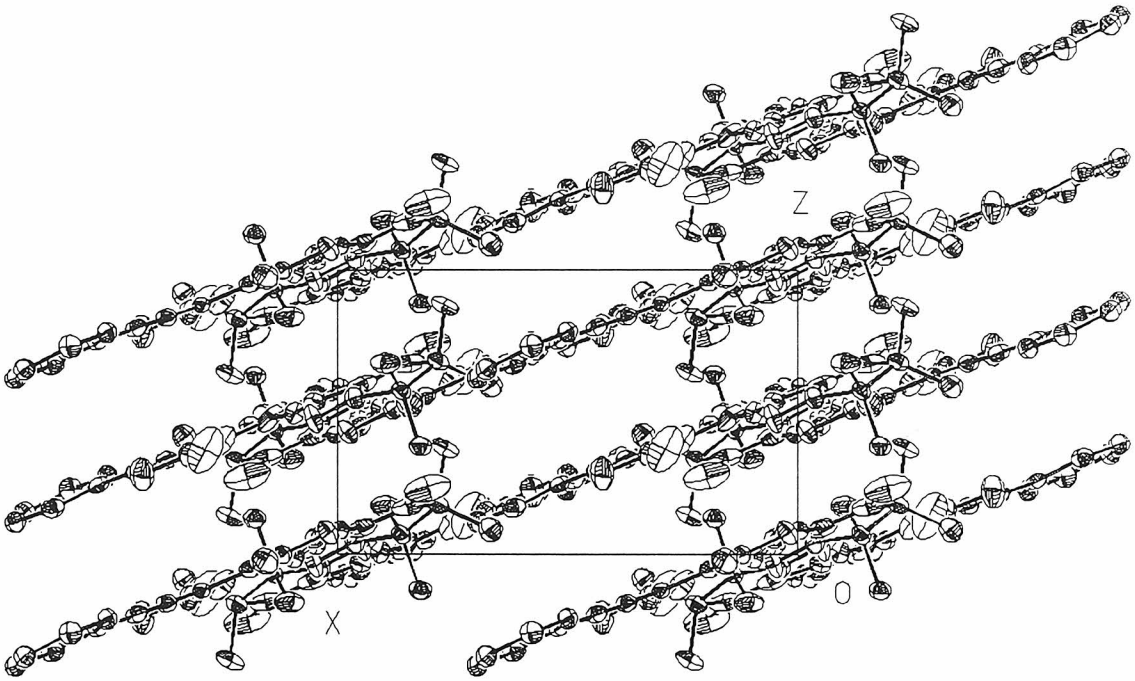
Z
X
O

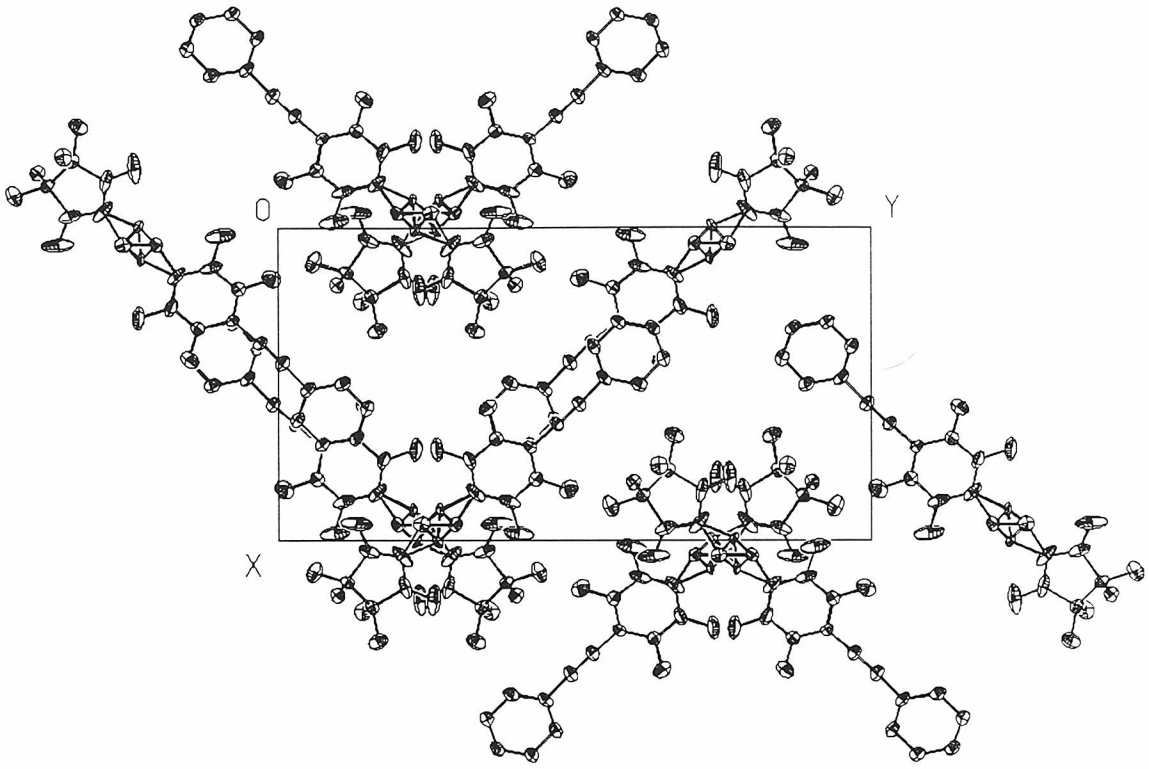
O
Y
X

Imino nitroxide 11

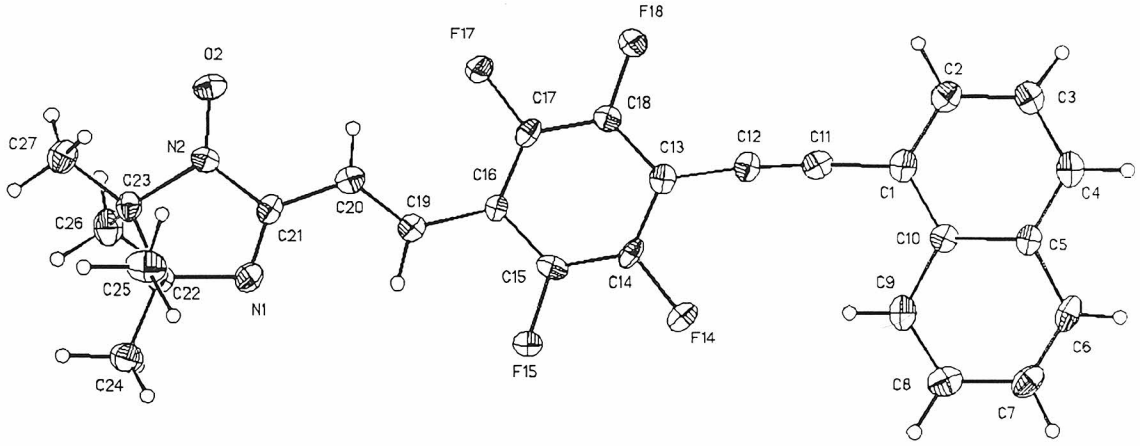

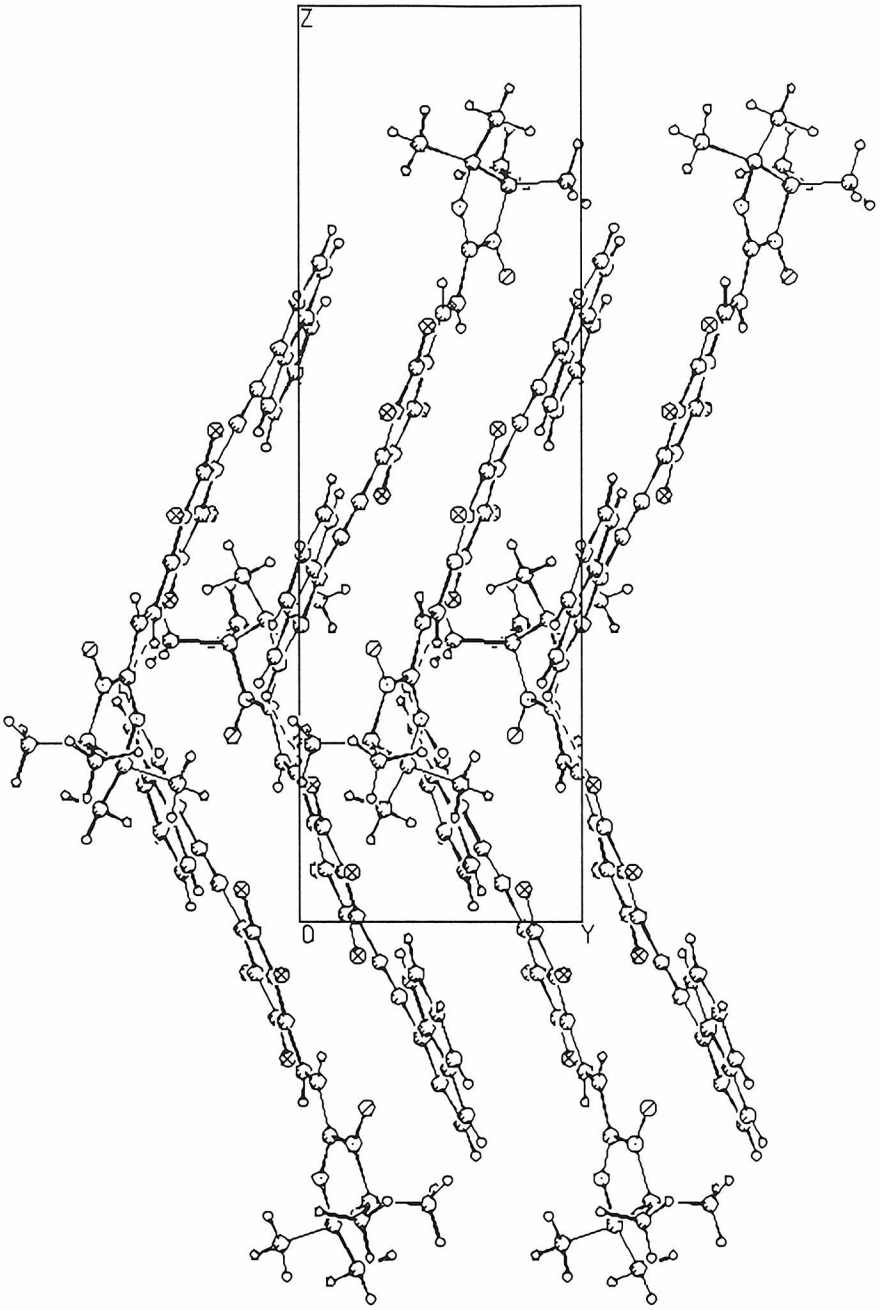
Z
O
Y

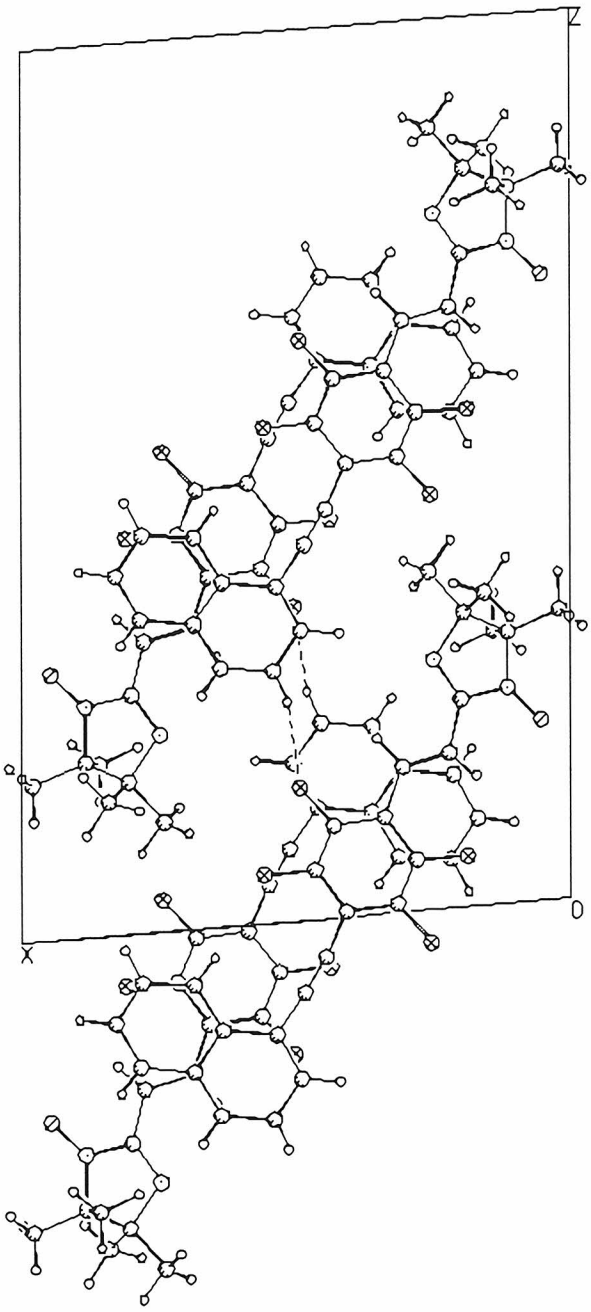
Z
O
X

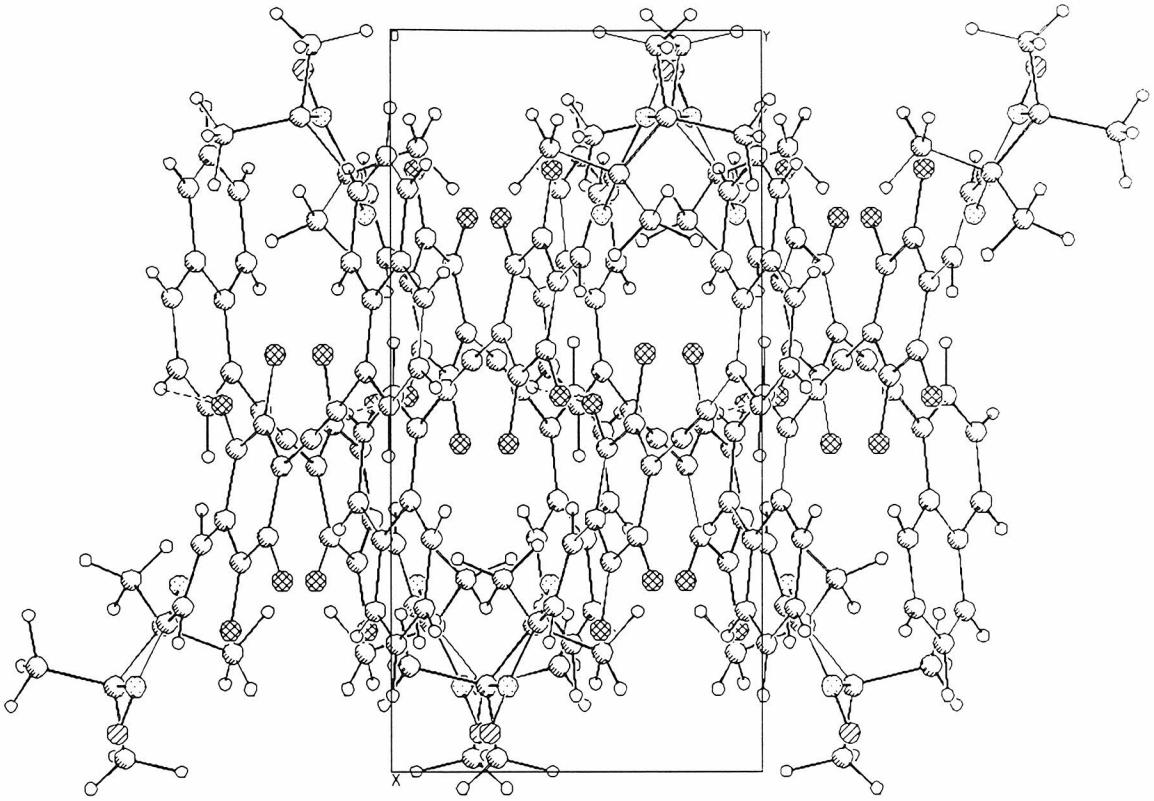
Y
X

Exit persued by a bear.

-William Shakespeare, *A Winter's Tale*